Electrical Engineering and Automation

Industrial

System performance analysis of an isolated microgrid with renewable energy sources and a battery and hydrogen storage system

An evaluation of different storage system configurations

Pauline Ahlgren
Ellen Handberg

Division of Industrial Electrical Engineering and Automation
Faculty of Engineering, Lund University

Master thesis

System performance analysis of an isolated microgrid with renewable energy sources and a battery and hydrogen storage system

- An evaluation of different storage system configurations -

Authors
Pauline Ahlgren
Ellen Handberg

Supervisors
Ingmar Leisse, E.ON
Olof Samuelsson, IEA

Examiner
Jörgen Svensson, IEA

Faculty of engineering LTH

Division of Industrial Electrical Engineering and Automation, IEA

March 19, 2018

Abstract

As more renewable and intermittent power sources are incorporated into the grid, the need for energy storage solutions increases. Implementation of hybrid energy storage solutions (HESS) could enhance system flexibility and contribute to the development of renewable energy systems. The purpose of this master thesis project is to investigate the technical and economic viability of different configurations of battery and hydrogen storage solutions in an isolated microgrid, i.e. local energy system (LES), with renewable power generation. The thesis strives to answer what operation and control strategies are necessary, what sizing methods are suitable and what measurements of performance that could be used to evaluate the system.

Power flow simulations with hourly data were conducted through creating a model based on an LES project in Simris in the south-east of Sweden. Simris is a village with 140 households supplied by a wind turbine, 500kW, and a solar power plant, 440kW. The project is run by E.ON within the framework of Interflex, in which several network operators within the EU participate to investigate flexibility options in local energy systems. This thesis investigates another promising flexibility solution than that implemented in Simris. A Li-ion battery system and a hydrogen storage system – electrolyser, fuel cell and hydrogen gas tanks – make up the proposed solution i.e. the HESS.

The model of the system was built and simulated using Python and Pandapower software. An operation strategy - a rule-based, short-term energy management strategy - was constructed, which determines the storage coordination. The first set of simulations was done to attain energy balance, resulting in the addition of a second wind turbine to compensate for high conversion losses. In the second set, the power of the fuel cell and the electrolyser, and the energy capacity of the battery were varied, to evaluate system performance through a sensitivity analysis. At a nominal storage configuration, chosen from the performance analysis, an extended analysis was performed. In one simulation, the efficiencies of the fuel cell and electrolyser were increased. In another, the minimum inner limit of battery state of charge ($SOC_{B_{min}}$), which constitutes a key control parameter of the operation strategy, was lowered.

The design of the operation strategy and the values of the corresponding control parameters affect the sizing of the storage system. The operation strategy can be formed according to several objectives; technical, economic and environmental. It can be rule-based or built on optimisation algorithms and handle data on different time scales. Performance can be evaluated with the following performance indicators: loss of power supply probability (LPSP), excess of energy (EE), annualised cost of system (ACS), loss ratio, battery cycles and electrolyser and fuel cell runtime and number of starts and stops. The performance analysis shows that the system is more reliable, lower LPSP, when both storage systems are larger. The same trend is found for EE. The ACS for the storage system seems mainly dependent on the hydrogen components. The loss ratio is similar for all configurations, 56-57% and this is mainly due to the high energy conversion losses in the electrolyser and fuel cell. The battery cycles, and electrolyser and fuel cell runtime and number of starts and stops relate to the expected lifetime of these components. More comprehensive measures and calculations are required, due to complex dynamic behaviours, to make explicit conclusions from these indicators. Increasing the fuel cell and electrolyser efficiencies gives an increase in EE and decrease in loss ratio. Lowering $SOC_{B_{min}}$ gives an increase in LPSP and battery cycles but a lower runtime of the fuel cell.

The hydrogen storage system has negative implications on the economic viability of the solution. However, according to the authors, the solution should be evaluated with regards to alternative costs of other available flexibility options and through applying different system perspectives. Thus, the applicability of a HESS with battery and hydrogen storage should be evaluated for each specific case, taking prevailing conditions and requirements into account. More instances of implementation are needed to improve the learning curve and the technical and economic viability of this solution.

Key words: *Hybrid Energy Storage System, Operation strategy, Performance indicator, Power flow simulation*

Abbreviations and units

Abbreviation	Description	Unit
ACS	Annualised Cost of System	$SEK/year$
C_{cap}	Capital cost	SEK
C_{rep}	Replacement cost	SEK
$C_{O\&M}$	Operation and Maintenance costs	SEK
CAP_B	Energy capacity of battery storage	kWh
CAP_H	Energy capacity of hydrogen storage	kWh
$CRF(i, Y_u)$	Capital Recovery Factor	$-$
DOD	Depth of discharge	$\%$
E_B	Energy level in battery storage	kWh
E_H	Energy level in hydrogen storage	kWh
EE	Excess of Energy	$\%$
i	Interest rate	$-$
$LPSP$	Loss of Power Supply Probability	$\%$
NWP	Nominal Working Pressure	$Pascal$
P_{BC}	Charge power of battery	kW
P_{BD}	Discharge power of battery	kW
P_{EL}	Power of electrolyser	kW
P_{FC}	Power of fuel cell	kW
P_{Load}	Power of loads in the grid	kW
P_{PV}	Power output of solar PV-panels	kW
P_W	Power output of wind turbines	kW
$SFF(i, Y_u)$	Sinking Fund Factor	$-$
SOC_B	State of charge in battery storage	$\%$
SOC_H	State of charge in hydrogen storage	$\%$
Y_u	Lifetime of system component	$years$
η_{BC}	Battery charge efficiency	$-$
η_{BD}	Battery discharge efficiency	$-$
η_{EL}	Electrolyser efficiency	$-$
η_{FC}	Fuel cell efficiency	$-$

Contents

1   INTRODUCTION

To restrict global warming to well below 2 °C, a target adopted at the Paris climate conference (COP21) 2015, urgent actions are required on an international scale. Reductions of global greenhouse gas emissions are a prerequisite to achieving this goal and actions are already taken within the European Union to achieve goals of cutting their emissions by 40% by 2030 (European Commission 2018). The energy sector accounts for two-thirds of the total global greenhouse gas emissions, suggesting that measures within this sector are crucial to achieving the aforementioned goals successfully. As a result, the development and implementation of more efficient, low-carbon energy production technologies have increased significantly during the past years (International Energy Agency 2015). Also, projections of future energy scenarios, conducted by the International Energy Agency (IEA), state that fossil fuels are continuously decreasing in favor of renewable energy sources (RES). Due to rapid deployment and cost reductions in renewable energy technologies, these are predicted to account for as much as 40% of the total primary demand by 2040. On an international scale, solar power production will be the dominating technology, due to rapid deployment in China and India, followed by wind power. Direct investments in solar PV-technologies, e.g., from businesses or private-owned households, further explains their increasing share of the energy market. However, within EU, the energy production from renewable resources will almost exclusively rely on wind power (International Energy Agency 2018). Even though hydropower and bioenergy will still remain the dominating renewable energy sources of the energy mix in Sweden 2040, the largest increase is expected in wind power and solar power production sources (IVL Sweden Environmental Institute 2011).

Another possible feature of the future energy sector is the dominating share of electricity for end-use demands. An increase in global population from 7.4 to approximately 9 billion by 2040 entails an increase in global energy demand. Thus, electricity will play a significant role to meet this need. During 2016 the global investments in electricity generation sources exceeded that of oil and gas for the first time. This further verifies that a substantial transformation of the energy sector is about to occur (International Energy Agency 2018). Electricity generation from renewables, in particular that from non-hydropower renewables, is expected to increase significantly during the following years. By 2040, electricity generation from RES is expected to exceed that of coal on a global scale. This is due to environmental policies and regulations to reduce emissions, which could result in an expected annual rate of increase at 2.8% for renewable electricity generation in comparison to that of 0.4% for coal-based electricity generation (U.S. Energy Information Administration 2017).

The incorporation of intermittent RES entails challenges due to their variable power output characteristics, which stresses the need for proper grid balancing functions (Rudnick and Barroso 2017). However, conventional centralized electricity grids are unable to sufficiently provide such flexibility due to control characteristics (Kwasinski, Weaver, and Balog 2016a). This can be combated through integrating smaller distributed networks to the bulk power system. These networks are referred to as microgrids, which can operate connected to or isolated from the bulk grid (Ton and Reilly 2017). Microgrids facilitates the incorporation of RES as the electricity production transitions from a centralised to a more decentralised power system, which is in favor of the implementation of RES (Farrokhabadi et al. 2017). Microgrids enhance the resiliency, reliability, and flexibility of the entire large-scale grid as it can disconnect from the grid in case of outages and operate in isolated mode (Ton and Reilly 2017). An isolated mode of operation also allows for low-cost clean energy from RES to be offered in remote areas.

However, the fluctuating nature of power output from RES still entails challenges that need to be addressed to achieve a stable and reliable microgrid operation (Farrokhabadi et al. 2017). There is a critical need to develop appropriate flexibility options that can provide sufficient grid balancing services. Energy storage systems have proven to be particularly suitable for this type of application (Rudnick and Barroso 2017). Hybrid energy storage systems (HESS), in which multiple storage technologies with complementary characteristics are incorporated in the system, is an advantageous solution. For isolated systems, with a high penetration of RES, the combination of a long-term hydrogen storage system and a short-term battery storage system is considered a promising solution (Bocklisch 2015). The international energy supply company E.ON is currently implementing a local microgrid as a part of a project called Interflex (E.ON Energidistribution 2018a). This is developed within the research and innovation programme, Horizon 2020, within EU. Projects implemented within the Interflex-context explore the operation of smart-grids and flexibility options, such as demand-side response, energy storage, smart-charging of vehicles, etc (European Commission 2017).

The local energy system is implemented in Simris, a small village located in the south of Sweden (E.ON Energidistribution 2018a). The system is comprised of a wind turbine, solar PV-panels, a battery storage system (BESS) and a backup biodiesel generator (E.ON Energidistribution 2018c). Thus, the system can be transformed into a HESS through adding a hydrogen storage system, as a means of increasing system flexibility, reliability, and stability.

It is interesting to evaluate how the system performance of an isolated microgrid with RES, such as that in Simris, is affected by the implementation of this promising HESS-solution. This will be the focus of this thesis, utilising information and data related to the microgrid project developed in Simris by E.ON.

1.1   Purpose

The purpose of this master thesis is to investigate the system performance of different configurations of battery and hydrogen storage systems in an isolated microgrid to evaluate the technical and economic viability.

1.2   Problem statement

- Which control and operation strategies are required in a microgrid to achieve an overall effective grid operation and a functioning coordination between energy storage systems?

- Which sizing methods are suitable to apply to design a microgrid including renewable generation and multiple energy storage systems?

- How can the system performance of a microgrid with multiple storage systems be evaluated with regards to technical and economic feasibility and viability? Which performance indicators are suitable?

1.3   Limitations

The main limitations comprise data availability, time resolution of data and simulation time. Historic data of power levels in the microgrid in Simris is characterised by occasional measurement errors or lack of data. Hence, the time period for each simulation was limited to the length of the coherent time period without apparent errors. The data is limited to a resolution of 1 hour. If data representing long time periods is used as input for a simulation, the computional time increases. Hence, both data availability and simulation time constitute constraints on the time period of the simulations.

1.4   Delimitations

The main delimitations established for this thesis are presented below.

- The microgrid simulated in this thesis is assumed only to operate in an isolated mode, i.e. disconnected from the external grid. This is due to the fact that the incorporation of energy storage systems are of particular importance in remote, off-grid areas. This further delimits the work of this thesis and make the simulations more comprehensible.

- The backup biodiesel generator incorporated in the microgrid in Simris is excluded in the grid architecture proposed in this thesis. This enables the authors to evaluate how the hybrid battery- and hydrogen storage solution affects the system performance alone. Also, a less complex operation strategy is sufficient as the number of components of the system is diminished.

- The design objectives considered for sizing and operation of a microgrid with multiple storage systems in this thesis are technical and economic. Hence, environmental or other objectives are not included in this report.

- Only the costs of the storage systems are considered in the economic analysis. This enables a comparative analysis between configuration cases but should not be seen as a quantitative measure of the total system cost.

- The storage systems are modeled through applying energy flow models, suggesting that the dynamic and physical aspects of component behavior are not considered.

- The system boundaries applied for the sizing and design of devices encompass the equipment included in the electrical system of the microgrid. Hence, additional ancillary services required for the operation of the storage systems e.g. water and oxygen supply systems are not included.

1.5   Method

This thesis is comprised of two main parts: a literature study and a series of simulations. The literature study is conducted in order to find the information needed to build a model for running simulations of a local energy system with multiple energy storage systems. The model is built using Python and a power flow calculation package called Pandapower. The main parts of the model are the grid components and the operation strategy. Area-specific data from the LES in Simris implemented by E.ON is used for running the simulations.

The simulation part consist of four steps, which have different aims. The first step is to attain an energy balance in the system, and to find a starting point for a sensitivity analysis, hereafter referred to as the performance analysis. The performance analysis is the second step, with the ambition to investigate how different configurations of battery capacity and hydrogen storage power affect the performance of the system. The third step is to compare the results and to determine a nominal storage configuration. The fourth step includes an extended analysis of this storage configuration. In this step model parameters that are thought to have large impact on the results are varied in one simulation each. The results are analysed and discussed in connection to the findings of the literature study.

1.6   Outline of the report

Chapter 1 is the introduction of the report, where the background, purpose, limitations, delimitations and method are presented. Chapter 2 describes the theory of microgrids and gives information about the system in Simris and the input data for the simulations. Theory of battery and hydrogen energy storage systems is given in chapter 3. In chapter 4 the theory of microgrid control is explained. Information on what to consider when sizing and designing an LES with energy storage is given in chapter 5. Chapter 6 explains how the model is constructed, what performance indicators are used for the analysis, how these are calculated and how the three simulation steps are conducted. The results are found in chapter 7, and they are analysed in chapter 8. Chapter 9 contains the discussion and concludes the report.

2   LOCAL ENERGY SYSTEMS (LES)

This chapter clarifies the concept of local energy systems (LES), also referred to as microgrids. In the first section system components and the technical requirements and challenges related to microgrid operation and control are described. The subsequent section focuses on the technical data and current challenges of a microgrid project implemented in Simris. Lastly, the microgrid architecture in Simris, including a proposed flexibility option, is displayed. The terms LES and microgrid are used interchangeably in this report.

2.1   Microgrid

The design of conventional power grids is characterised by a centralised architecture, which relies on the power supply from a few large power generation units. The power needs to be transmitted to loads often located far away from the generation source. Such a large centralised grid structure generally does not allow for sufficient control at lower levels in the grid, e.g., at distribution- or specific consumer load level. Thus, conventional centralised grid architectures are often characterised by reliability and flexibility issues. Hence, incorporation of intermittent RES, e.g., solar- and wind power plants, or load devices such as plug-in-hybrid vehicles become challenging.

These problems might be combated through incorporating smaller generation sources, distributed in the grid, rather than depending on a few large centralised generation units (Kwasinski, Weaver, and Balog 2016a). Through placing the generation units closer to the electricity consumers transmission and distribution losses can be reduced. Small electrical networks, i.e., microgrids, comprised by these distributed generation units, can operate independently or connected to the large centralised grid. In the latter case, the microgrid can participate to attain a more reliable operation of the large-scale network (Schwaegerl and Tao 2014). Also, depending on the application, microgrids are more cost-effective. This is particularly true for implementations in remote and power inaccessible areas (Kwasinski, Weaver, and Balog 2016a).

2.1.1   Concept

Microgrid definition:

> *"A group of interconnected loads and distributed energy resources within clearly defined electrical boundaries that act as a single controllable entity with respect to the grid."* (Kwasinski, Weaver, and Balog 2016a)

Above, a formal definition of a microgrid is presented. This definition can be further specified and clarified through the following three key attributes and requirements that characterise a microgrid.

1) A microgrid is a distribution network for integration of generation units, storage units and dispatchable loads.

Generation units are implemented close to electricity consumers, taking advantage of local resources. Local generation sources often comprise renewable resources such as solar-PV panels or wind turbines, depending on weather and other area specific conditions (Schwaegerl and Tao 2014). The microgrid is often implemented as a distribution grid with low voltage (LV) or medium voltage (MV) levels (Xue-song, Li-qiang, and You-jie 2011).

2) Two modes of operation are required: grid-connected and isolated.

A microgrid must be able to operate independently although grid-connected operation is expected to be the most common mode of operation in future energy systems (Schwaegerl and Tao 2014). In this mode, the large-scale external grid provides secondary power supply whenever the generation units of the microgrid are not sufficient to cover the load demand (Kwasinski, Weaver, and Balog 2016a). However, in remote or power isolated areas, e.g., islands, a long-term isolated operation is required, which entails several challenges. The need for sufficient energy storage sizes, high enough capacity of generation units or other flexibility options increases to preserve high reliability and stability of the grid (Schwaegerl and Tao 2014).

3) A microgrid includes essential control strategies to operate and coordinate system resources, i.e., generators, storages and loads, in line with technical, economic and environmental objectives.

The primary differentiation between a microgrid and a grid comprised of smaller generation sources is the level of control of the resources. This functionality is enhanced and implemented in microgrids through different management strategies. These strategies are developed with regards to one or several objetives to attain optimal operation.

2.1.2   System components

The key components comprising a microgrid include:

- Distributed Energy Resources (DER)

- Energy storage systems

- Loads

(Schwaegerl and Tao 2014).

DER units are power generation units that are suitable for distributed generation, which include both generators and storage systems. Examples of applicable DER's are: solar- and wind power production units, fuel cells, and internal combustion engines. Some of the most adopted energy storage technologies are batteries, ultracapacitors, and flywheels. However, hydrogen storage is also an option, which can be obtained through implementing an electrolyser in combination with a hydrogen storage unit and a fuel cell (DER). Hence, bidirectional power flow is attained enabling energy to be stored as hydrogen (Kwasinski, Weaver, and Balog 2016a). Loads can preferably be controlled in order to achieve a flexible microgrid system with high performance (Schwaegerl and Tao 2014).

In addition to the components mentioned above, other technologies of importance for microgrid operation are power electronics. These are involved in the necessary conversion processes of electric power (Kwasinski, Weaver, and Balog 2016a). These are utilised as an interface between the DER-units, storage systems, controllable loads and the distribution grid. Their primary function is to adjust current and voltage levels properly (Planas et al. 2015).

Three types of power electronic circuits are commonly adopted. Rectifiers convert alternating current (AC) electricity to direct current (DC). In this thesis, rectifiers are implemented for the electrolyser unit and the charging direction of the battery. Inverters are usually required for the reverse conversion process of DC to AC power, which is necessary for the output from the fuel cell, the solar-PV panel and the discharge output from the battery in this thesis. Lastly, a DC to DC power converter might be required for the power production from solar-PV for it to operate at an optimal point (Kwasinski, Weaver, and Balog 2016a).

2.1.3   Technical requirements and challenges

Basic grid requirements
According to the definition of a microgrid, the ability to operate in an isolated mode, i.e., disconnected from the external grid, is required. Hence, the microgrid must be capable of performing and providing the same grid-functions and services as a large-scale grid (Ton and Reilly 2017). A fundamental requirement attributed to the operation of an electrical grid is to maintain a constant power balance between supply and demand of electricity in the grid. If an imbalance occurs, consequences such as detrimental outages or losses of power quality, in frequency and voltage level, can occur (Milligan et al. 2012). Hence, system balancing grid services are crucial to attaining high power reliability of a system (Ecofys 2014).

Preserving reliability refers to ensuring that generation sources in the grid are sufficient to cover end-consumer requirements, but also to the ability to resist disturbances to the grid. Hence, the concept of reliability can be further specified as adequacy and system security. Adequacy refers to the capability of the generation resources to match the accumulated load-demand, taking into consideration uncertainties in generation availability. System security, on the other hand, refers to the ability of the grid to tolerate and respond to unexpected disturbances to the grid (Milligan et al. 2012).

It is also vital to maintain grid stability, which refers to the ability of the system to accurately match load and supply at every time step to attain an equalized power balance (Milligan et al. 2012). If an imbalance occurs between supply and load, this will result in frequency fluctuations, which in turn will have adverse effects on power quality and the stability of the system (International Electrotechnical Commission 2011). The nominal frequency of the grid in Europe is 50 Hz, and any deviations from this value must be adjusted to attain power balance. Hence, grid frequency serves as an indicator and control variable for the stability of the system (Schäfer et al. 2015). When frequency fluctuations occur in the grid, a control strategy is required to restore the frequency to its nominal value. Such a control strategy comprises primary, secondary and tertiary frequency control (Sioshansi 2011).

Hence, to attain a reliable and stable operation, flexible generation reserves that can participate in this control strategy need to be incorporated into the system. The concept of flexibility refers to the ability to adjust to changes in supply and demand in the system to maintain continuous operation (Papaefthymiou, Grave, and Dragoon 2014). Several flexibility technologies can offer such system-balancing services (Sauer 2015). Generation reserves can provide either short- or long-term flexibility for the system.

- *Short-term flexibility:*
  Generation reserves that can offer fast responses to changes in the grid are utilised to provide flexibility at shorter time-scales. Hence, central attributes that enable a resource to provide short-term flexibility services are high ramp rates and minimum start-up/shut-down time. These units are participating in the aforementioned primary, secondary and tertiary frequency control to attain stability of the system. (Papaefthymiou, Grave, and Dragoon 2014). Primary control assures automatic reaction to frequency deviations in the grid to restore balance, which can be achieved through the inertia of spinning masses in the system (Sioshansi 2011). The primary control must occur during the first seconds, then the generation reserves of slower response time join in within five minutes to provide secondary control (Papaefthymiou, Grave, and Dragoon 2014). The secondary control is required to deal with the frequency steady-state errors resulting from the primary frequency control (Minchala-Avila et al. 2015). Lastly, within fifteen minutes the tertiary control units respond and participate in the system balancing process (Papaefthymiou, Grave, and Dragoon 2014). Tertiary control relates to the energy management of the system (Minchala-Avila et al. 2015).

- *Long-term flexibility:*
  In power systems with seasonal variation in the power supply, generation resources that can offer long-term flexibility are required. For such long-term applications response-time is of less importance, but rather units with large storage capacity (energy density) are advantageous to incorporate in the grid structure (Papaefthymiou, Grave, and Dragoon 2014).

Technical challenges of isolated microgrids with renewable resources
The integration of RES in electricity grids adds additional challenges related to system balancing. This enhances the importance of incorporating technical resources to provide flexibility of the system, more so if the system relies exclusively on generation from RES. More specifically, systems characterised by high penetration of renewable energy sources induces the need for higher system flexibility due to the following reasons:

- Intermittent and unpredictable power output

- Seasonal variation in power output

- Reduced share of conventional resources that traditionally provide inertia for primary control

(Papaefthymiou, Grave, and Dragoon 2014)

The uncertain and stochastic nature of RES, such as wind- and solar-power, make scheduling of power supply difficult due to errors in forecasting. As of today, the inaccuracies of such power supply forecasts are also strongly related to the impact of weather conditions. Not only are predictions of weather conditions uncertain, but also the effect of weather on the operation and power output of the device is hard to predict, resulting in forecast errors. For example, forecast errors of solar radiation to the PV-panel in solar power plants might be significant during dusk and dawn due to unpredictable shadowing effects (Schäfer et al. 2015). Hence, such forecast errors increase the need to incorporate flexibility options in the system to avoid supply and demand mismatch and to assure that stability and adequacy is maintained. Also, to attain adequacy in renewable energy systems with high seasonal variations, the requirement for suitable long-term flexibility options is significant (Papaefthymiou, Grave, and Dragoon 2014).

As mentioned above, many traditional generation sources are characterised by rotating masses, and hence they can participate in primary control since they can provide inertia to adjust frequency fluctuations (Schäfer et al. 2015). However, inverter connected renewable energy sources, such as wind turbines and solar-PV panels, cannot offer this inertia response (Ulbig, Borsche, and Andersson 2014). Instead, primary control can be addressed through the use of power electronics to attain virtual inertia (Minchala-Avila et al. 2015). However, microgrids are comprised of many small scale generation sources; such as wind- and solar power plants, thus requiring many power electronic interfaces. Since power electronics are also sensitive to power fluctuations, microgrids tend to be less tolerant to frequency deviations, especially in isolated mode. In grid connected mode, these variations are addressed through the inertia offered by conventional generation sources in the external grid. If grid connection is not an option, primary control in isolated microgrids with renewable sources is of particular importance to maintain stable and reliable operation of the system (J. Li et al. 2016).

Microgrids often comprise a high share of several different DER that should participate in the balancing of power supply and loads in the system. To implement an autonomous, isolated microgrid the challenge of coordinating the operation of these DER's need to be addressed to avoid technical problems during grid operation. Hence, to incorporate suitable control and protection of grid components also poses a central and crucial challenge considering microgrid implementation (Salam, Mohamed, and Hannan 2008).

Conclusively, isolated microgrids with a high penetration of renewable energy sources require flexibility options that can make up for forecast errors, seasonal variations and the loss of inertia to preserve grid stability and reliability (Papaefthymiou, Grave, and Dragoon 2014). Also, adequate control and coordination of DER operation is crucial for the implementation of microgrids (Salam, Mohamed, and Hannan 2008).

2.2   Simris

2.2.1   Area description

Simris is a small village in the size of 140 households and there are also a few minor companies connected to the grid. It is located in the south eastern part of Skåne, southern Sweden, with coordinates: latitude 55.5362°N and longitude 14.3237°E. Close to the village there is a wind turbine which was set up in 1996. Since 2013 there is a solar power plant in the same location. Both generation units have private owners (E.ON Energidistribution 2018b). The grid is operated at medium and low voltage level and the production plants are connected at 10kV. The total cable length at low voltage level is 10707 meters and the cable length at medium voltage level is 5179 meters.

2.2.2   Technical data

The wind turbine installed at Simris is an Enercon E-40/5.40 turbine with a rated power of 500 kW. It produces around 1.4 GWh per year. The solar power plant has an installed capacity of 440 kW and produces around 0.45 GWh per year (E.ON Energidistribution 2018b). Table 2 shows an overview of the power production and consumption in Simris. The yearly production and consumption can vary between years.

Table 2: Simris: power production and consumption (E.ON Energidistribution 2018b)

Plant	Rated power	Yearly production/consumption
Wind power plant	500 kW	1.4 GWh
Solar power plant	440 kW	0.45 GWh
Grid consumption		2.1 GWh

The power production from the wind turbine and the solar power plant over the period February 23rd 2015 to February 22nd 2016, hereafter referred to as the simulation period, can be seen in corresponding figures 1 and 2. The solar power plant produces more in the summer months, while the wind production is slightly higher during the winter months. Figure 3 shows the total production: wind power and solar power added together.
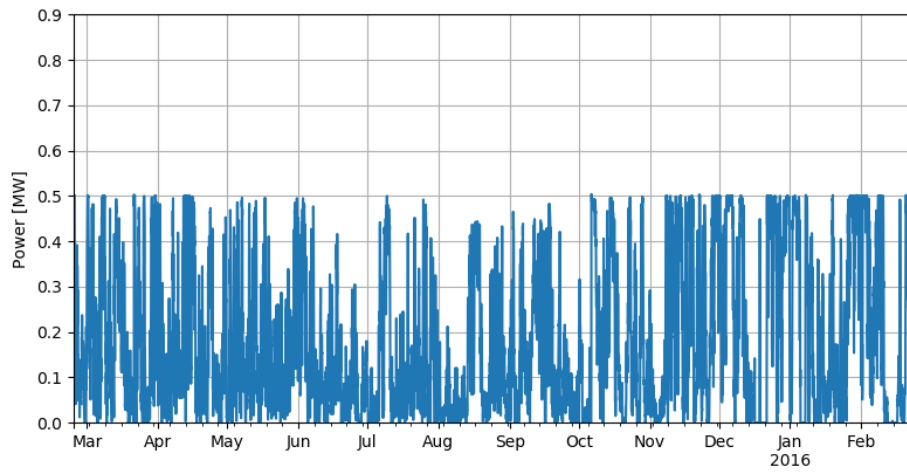
Figure 1: Wind power production.
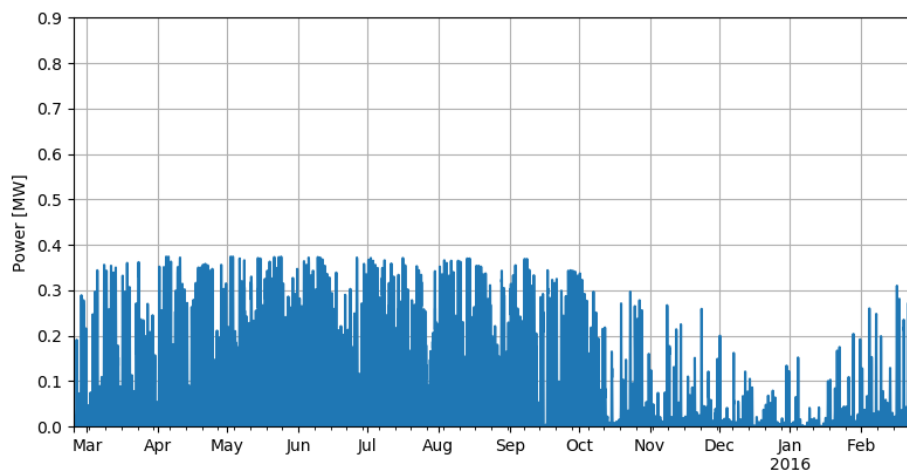
Figure 2: Solar power production.
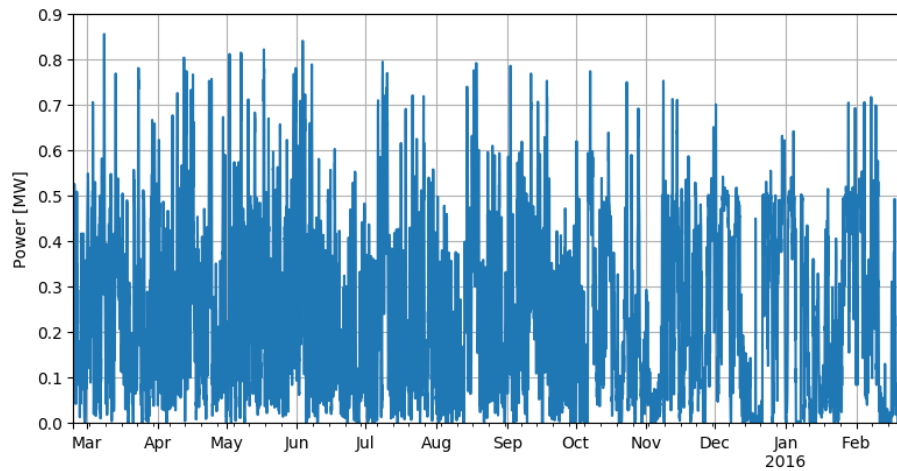
Figure 3: Total power production.

The power consumption from the households and small companies over the simulation period can be seen in figure 4. The load varies on an hourly basis with a roughly daily pattern. The consumption is higher during the winter months compared to the rest of the year. The total energy consumption over a year is approximately 2.1 GWh (E.ON Energidistribution 2018b).
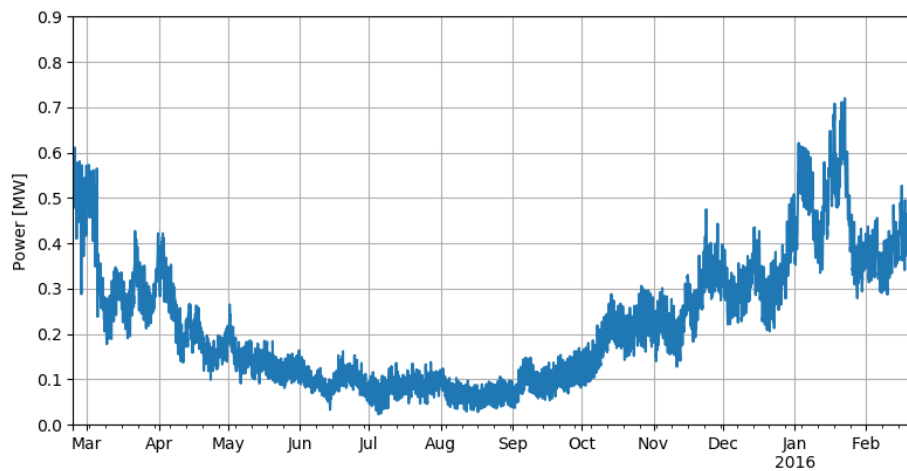
Figure 4: Load demand.

The data of the production is collected from the measurement systems of the wind power plant and the solar power plant. The data of the consumption is calcluated from the values of production and the power discrepancies. The power discrepancy is the difference between power supply and

load demand. In reality, this discrepancy represents the power transferred between the microgrid in Simris and the external grid, and vice versa. It is measured by the management system, often referred to as SCADA, at the substation where the grids are connected.

2.2.3   Challenges

Figure 5 shows the difference between the production from wind and solar power and the load demand over the simulation period. The red line in the figure indicate power balance on the grid i.e. that the power supply match the load. Positive and negative deviations from this line relates to events of power surplus and deficit respectively, displayed by the blue curve. Since the graph shows values both above and below zero it can be seen that there are power deficit and power surplus at different times all over the year. In the summer months there are more power surplus due to low load demand and high power supply from solar-PV. In contrast, the winter months are characterised by more power deficit as a result of higher load demands and lower power supply from solar-PV.
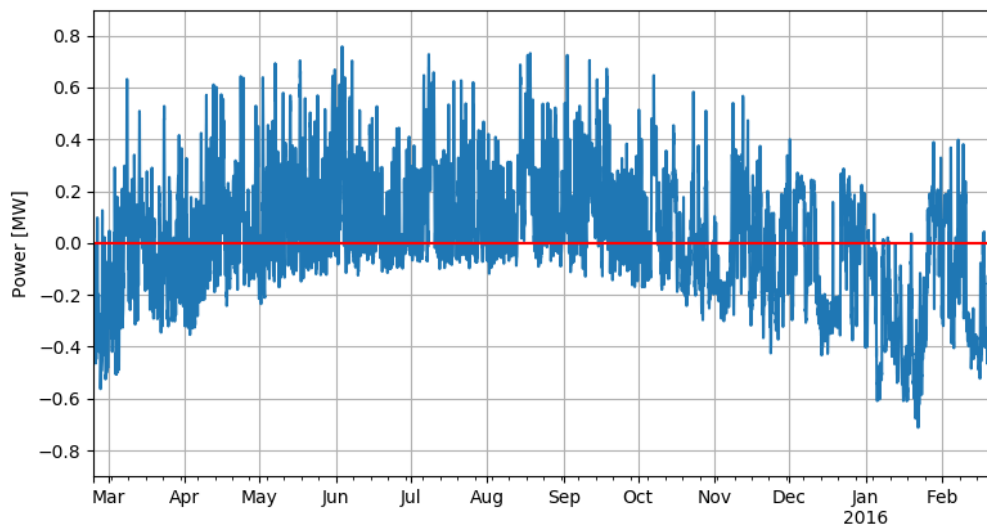
Figure 5: Power discrepancies exchanged between the microgrid and external grid in Simris.

Figure 6 shows a cumulative sum of the power differences shown in figure 5. The difference between the highest value and the lowest value in this graph could be used for an approximation of the amount of energy that could be stored on a seasonal basis. The difference between the value at the starting point and the end point indicates that more power is produced in the system than what is consumed. This is valid for the specific simulation period chosen for this study, another period could have different values of production and consumption.
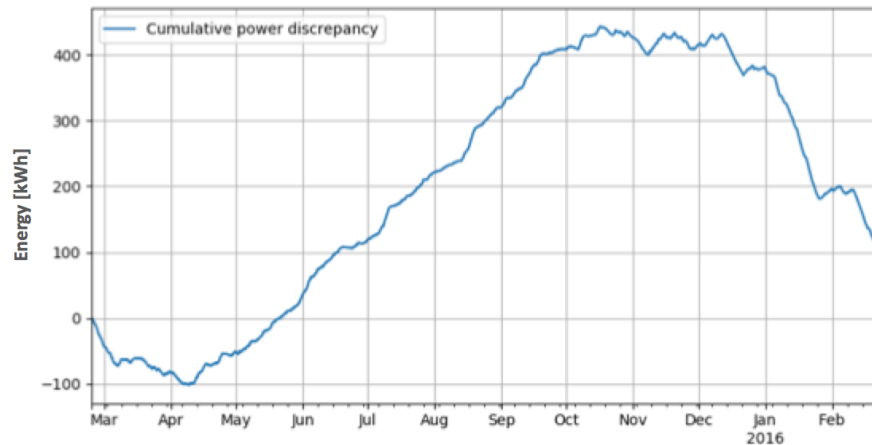
Figure 6: Cumulative power discrepancies.

In order to implement a satisfying isolated microgrid in Simris the discrepancies shown in figures 5 and 6 must be mitigated by the microgrid itself, according to the reasoning in chapter 2.1. Installing energy storage systems could be a solution.

2.2.4 Proposed microgrid architecture

The challenge of reducing the above mentioned power discrepancies might be addressed through installing energy storage systems in the grid microgrid architecture (Rudnick and Barroso 2017). In this thesis a hybrid energy storage system (HESS) solution, comprising a battery- and a hydrogen energy storage, is suggested as a promising flexibility option to enhance microgrid operation in Simris. The hydrogen storage system comprise a Proton Exchange Membrane electrolyser (PEMEL), a Proton Exchange Membrane fuel cell (PEMFC) in addition to gas tanks. The proposed microgrid architecture is displayed in figure 7.
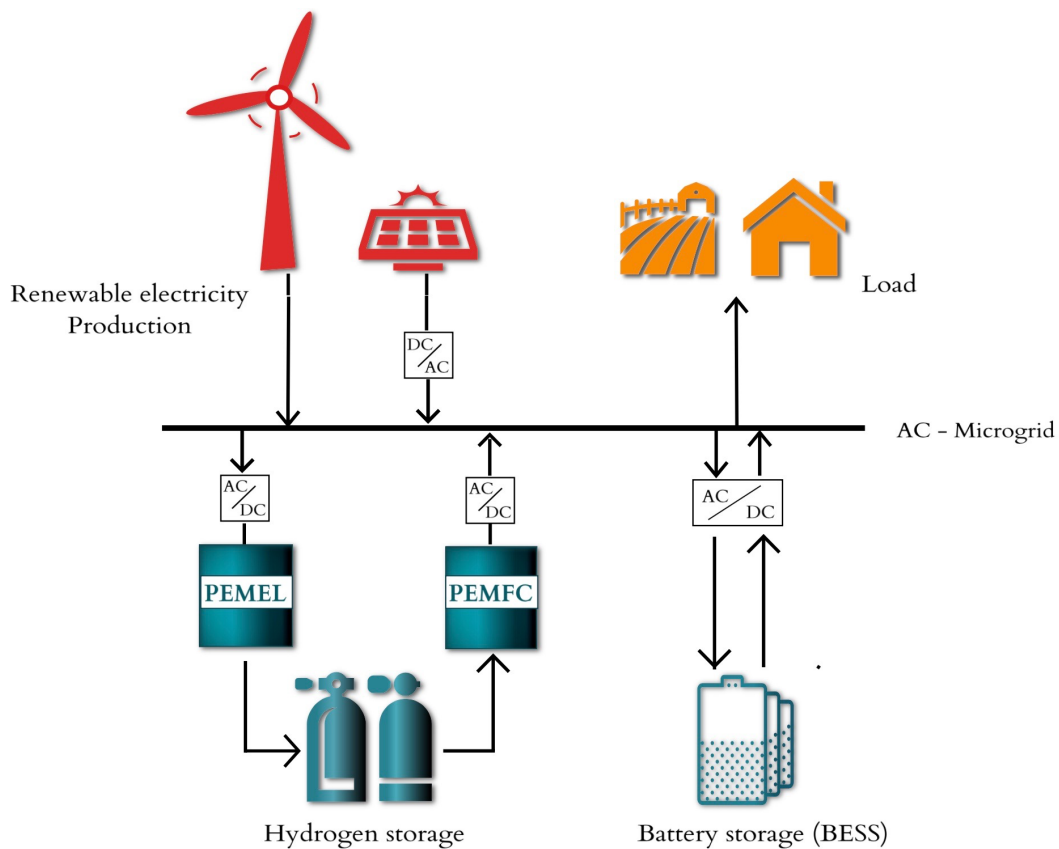
Figure 7: Proposed microgrid architecture in Simris including energy storage systems.

3   ENERGY STORAGE SYSTEMS

This chapter comprises information on energy storage systems. In the first section the general concept of energy storage systems is described, including key attributes, classification methods and potential applications. Thereafter, the concept of hybrid storage systems and their applicability to microgrids is introduced. In the third section, a more in-depth review of the energy storage technologies, incorporated in the proposed microgrid architecture, is presented.

As mentioned above, the prevailing challenges related to the operation and control of microgrids with a high share of renewable resources can be combated through incorporating suitable flexibility options (Rudnick and Barroso 2017). A range of flexibility solutions exists to address power discrepancies in the grid. Examples of such measures include demand response, curtailment of power generation, power-to-heat technology, energy storage systems etc (Sauer 2015). In this context, energy storage systems (ESS) are a promising and advocated option since they provide the sought flexibility in addition to other services to preserve a high stability and reliability of the grid (Rudnick and Barroso 2017). However, as of today, it might not always be the most economically viable solution and hence other flexibility options should not be discouraged (Sauer 2015). Nevertheless, in this thesis only energy storage systems are evaluated as a means of attaining a more reliable, safe and efficient operation of a microgrid.

3.1   Energy storage system (ESS)

As stated earlier, grid power balance is essential for the operation of an electrical grid. Hence, the main purpose of implementing an energy storage system (ESS) is to offer a means of storing energy at times of positive power discrepancies and releasing energy at times of negative power discrepancies (Sauer 2015).

3.1.1   Key attributes

Energy storage technologies are characterised and differentiated by certain key attributes, which are important to consider in the process of selecting the appropriate technology for a specific application:

- Rated Power [kW]

- Energy Capacity [kWh]

- Efficiency [%]

- Ramp rate [kW/min or percentage of rated power/min]

The rated power represents the maximum power that the device is able to attain during charge and discharge. The rated power can be different for discharging and charging. Energy capacity refers to the maximum amount of energy that can be stored in the device. When considering the efficiency of the storage system it is important to differentiate between the conversion efficiencies and the storage efficiency. Conversion efficiencies relate to losses occurring during the charge and discharge processes whereas the storage efficiency describes the losses occurring during the time energy is stored and not utilised. The ramp rate indicates the capability of a storage system to increase or decrease its power flow during discharging and charging and is commonly expressed in kW/minute. Hence, it describes the rate at which the power output and input can be altered (Byrne et al. 2017).

Further attributes of value are the energy density or physical storage size, capital costs, operation time, cycling constraints and emissions. Also, cost per unit energy stored [SEK/kWh] is a key attribute to consider when implementing an ESS. In general, storage technologies characterised by high costs of energy are optimised to provide services on shorter-time scales i.e. frequency control. Hence, these are more economically viable when providing power balancing services. An example of such an ESS is a battery storage system, BESS. On the other side of the spectrum, technologies with low energy costs are suitable for energy balancing services. For example, hydrogen storage systems are characterised by a low cost for the storage device, e.g. tank, but high costs for the power conversion devises, i.e. fuel cell and electrolyser (Ecofys 2014). Thus a hydrogen storage is more suitable for energy balancing.

3.1.2   Classification methods

Due to the diversity of storage technologies available on the market a classification system is required. It should be noted that several different classification methods exist and the methods described below are selected since they are frequently adopted in literature and add value to this thesis. Only energy storage technologies suitable for electricity-to-electricity applications are considered.

Storage method
On a basic level, the energy storage technologies can be differentiated by the approach used to store energy (Sauer 2015). They can be classified as mechanical-, electrical-, thermal-, chemical- and electrochemical storage (Ecofys 2014). In this thesis, a lithium-ion battery storage system and a hydrogen storage system are incorporated as flexibility options for the microgrid in Simris. Hence, they are the technologies of focus in this report.

Batteries are classified as electrochemical storage with internal energy storage suggesting that electricity is converted to a chemical potential to store energy (Ecofys 2014). This implies that the power conversion process and the storage level are directly dependent and occur within one unit, the battery, which makes individual sizing of power and energy capacities impossible (Sauer 2015). A hydrogen storage system is classified as a chemical storage technology due to the conversion of energy from the form of electricity to a fuel, the hydrogen gas. An advantage of chemical storage is their high energy density [kWh/l] (Ecofys 2014). In contrast to batteries, this power conversion process is external, performed by fuel cell and electrolyser units, and separated from the energy storage, the hydrogen tank. This allows for the hydrogen system to be designed to meet the needs of a specific application with regards to both energy and power through individual sizing of these components.

Duration of charge and discharge

The power to energy (P2E) ratio indicates the duration of discharge or charging at maximum power that a certain energy storage technology can accomplish. In this respect, technologies characterised by high P2E-ratios only allow for discharging and charging during short time-scales, often at high power levels. In contrast, low P2E-ratios apply to technologies with the ability to charge and discharge for a long period of time (Sauer 2015). More specifically, energy storage technologies can be classified according to their mode of operation. If they operate frequently in short intervals they are said to have a power-delivery profile, i.e. high P2E. If a storage technology is characterised by working less frequently but during longer time periods they can offer continuous supply of energy and thus have an energy-delivery profile, i.e. low P2E (Kwasinski, Weaver, and Balog 2016).

Battery storage systems (BESS) are categorised as a short-term storage system with a high P2E and a discharge time of about several minutes, depending on the device, resulting in a high number of cycles during its operation. Due to the high-power profile, BESS often act to provide primary frequency control to provide stability and instantaneous power balance to the grid. Hydrogen storage systems are categorised as long-term storage systems with a very low P2E and a discharge time of days, weeks or more at maximum power, depending on application and design. This implies a low number of cycles during its operation.

It should be noted that short-term energy storages, such as batteries, are available on the market. Long-term energy storages, such as hydrogen storage systems, have not been implemented in energy systems to the same extent since these still entail some challenges related to their economic viability due to the low amount of cycles per year (Sauer 2015).

3.1.3   Applications from a utility perspective

Since energy storage system technologies differ with regards to the abovementioned attributes, it is important to select the appropriate technology with attributes that are required for a specific application (Sauer 2015). An ESS can offer a variety of services, which makes them suitable for a range of applications. The main roles and functions that ESS can provide to a microgrid are presented below (Farrokhabadi et al. 2017).

Frequency and voltage regulation

As stated earlier, frequency and voltage regulation are important grid services to maintain a stable grid operation. Frequency regulation relates to active power balancing of the grid and is executed through properly adjusting active power output from DER-units (International Electrotechnical Commission 2011). Particularly, in isolated microgrids characterised by fluctuating power outputs from RES the need for frequency control is enhanced. Storage technologies characterised by high ramp rates, such as BESS, can be incorporated to participate in such frequency control. Such technologies can also participate in voltage control through their quick response to fluctuations in reactive power by adjusting the system voltage (Farrokhabadi et al. 2017). Hence, high-power short-term storage systems with high cycling capability can be utilised as a means to preserve stability and acceptable power quality of the grid (International Electrotechnical Commission 2011).

Time (energy) shifting
Time shifting refers to the concept of storing energy during times of power surplus and utilising it later during times of power deficit. Electricity can be stored during off-peak hours when the electricity price and the demand is low. At times of high demand and high electricity prices this stored energy can be utilised, which is an example of a time shifting strategy applied by utilities. This is especially beneficial and vital in microgrids with a high share of RES (Farrokhabadi et al. 2017). ESS technologies that are most suitable for this application are long-term storage systems characterised by few cycles (International Electrotechnical Commission 2011). The storage needs to have sufficient energy capacity to cover the load for a couple of hours. Hydrogen storage is suitable but BESS can also provide this service depending on design (Farrokhabadi et al. 2017).

Long-term storage
Seasonal power variations from intermittent RES and in load-profiles can be addressed by utilising an ESS. Through incorporating a storage technology that is capable of storing energy for longer periods of time, i.e. months, the costs of otherwise over-dimensioned generators can be excluded. The need for additional generation units during time periods of higher demand is diminished since stored energy can be utilised. A suitable technology for this application is a long-term hydrogen storage system (Farrokhabadi et al. 2017).

Grid forming (isolated microgrids)
Through offering important grid services, as the ones mentioned above, an ESS can enable stable operation of isolated microgrids (International Electrotechnical Commission 2011). Any storage technology that is implemented to assure that a microgrid can operate in an isolated mode, without support from an external grid, is referred to as a grid forming ESS (Farrokhabadi et al. 2017).

3.2   Hybrid Energy Storage Systems (HESS)

Due to the need for grid services at different time-scales it is beneficial to implement multiple storage systems with different attributes (Bocklisch 2015). Through selecting storage technologies with complementary characteristics the reliability and power quality can be enhanced (Gou, Na, and Diong 2016). Hence, in such hybrid energy storage systems (HESS) it is advisable to combine a long-term, energy balancing storage system with a storage that can provide short-term, power balancing services. The supplementary storage characteristics infer several technical and economical advantages. For example, the total investment cost is generally reduced due to that the energy and power services are decoupled. The high cost of utilising a long-term storage for power balancing services is diminished since the short-term storage can cover a higher share of these power discrepancies at a lower cost. This further suggests that optimal operation points can be established for each storage device, resulting in higher system efficiencies and prolonged lifetime of components (Bocklisch 2015).

Renewable energy system applications
For an isolated microgrid including solar and wind power generation units the combination of a battery- and hydrogen storage system is considered a suitable HESS-solution, which is proposed by Caisheng Wang, M. H. Nehrir, and Shaw (2005). Hence, this system configuration is implemented in this thesis due to its applicability in Simris, where solar and wind power are the power sources. The battery offer short-term power balancing services and complements the long-term energy balancing services provided by the hydrogen storage (Eriksson and Gray 2017).

The fuel cell, i.e. the device responsible for electricity generation in the hydrogen storage system, provides back-up energy and offers several advantages over more conventional back-up biodiesel-generators. Through implementing fuel cells, the high operation and maintenance costs, green house gas emissions and scalability issues associated with biodiesel generators can be avoided (Bizon, Oproescu, and Raceanu 2015). In addition, fuel cells are capable of operating at higher efficiencies even at part-load situations, which is not the case for biodiesel generators (Gou, Na, and Diong 2016).

The electrolyser, i.e. the device responsible for hydrogen production in the hydrogen storage system, is a dispatchable load and provides flexibility to the system as it converts surplus electrical renewable energy into energy stored as hydrogen gas. Hence, curtailment of the solar and wind power production is avoided (Eichman, Harrison, and Peters 2014).

Batteries are critical elements in many HESS-systems (Bocklisch 2015). BESSs are employed to smooth the transients and discrepancies between the load demand and the power supply from solar panels, wind turbines and fuel cells (J. Li et al. 2016). In particular, Lithium-ion batteries are commonly utilised in HESS-applications as they can provide both efficient power and energy management services if needed (Bocklisch 2015).

3.3   Hydrogen storage system technology

Hydrogen storage systems are means of incorporating intermittent renewable energy sources, such as wind and solar, through enhancing the flexibility of the system. Hydrogen is an energy carrier, which can be generated through endothermic conversion processes utilizing primary or secondary energy sources. The generation is often conducted through utilizing an electrolyser in which water molecules are split into hydrogen and oxygen molecules. The process is referred to as electrolysis, and the energy source required for the chemical reactions to occur is electricity. Subsequently, the produced hydrogen can be stored until it is further converted to meet end-use energy demands (International Energy Agency 2015). If the end-use demand is electricity, the conversion can be executed by applying a fuel cell in which hydrogen molecules combine with oxygen to form water and electricity. In contrast to electrolysis, this process is exothermic, suggesting that energy is released in the form of heat (U.S. Department of Energy 2006).

Hence, the conversion of Power–to–Power through hydrogen storage system technology comprises three parts:

- *Hydrogen production:* conversion of electrical to chemical energy in electrolyser.

- *Storage of hydrogen:* chemical energy storage of hydrogen.

- *Electricity production:* conversion of chemical to electrical energy in fuel cell.

The functions are allocated to three devices, i.e. electrolyser, fuel cell and storage, suggesting that the hydrogen storage system can be viewed as a system comprised of three individual sub-systems. This allows for the hydrogen storage system to be designed to meet specific power and energy demands to attain optimal operation of the system in different applications (Steilen and Jörissen 2015). In this chapter the technology of these sub-systems are reviewed in more detail.

3.3.1   Electrolyser

As described previously an electrolyser is an electrochemical device in which an electrical current (DC) is utilised to split water into hydrogen and oxygen molecules through a process called electrolysis (Mittelsteadt et al. 2015).

General principle
The general principle of an electrolyser cell involves connecting an electrical current (DC) to two electrodes, a positive anode and a negative cathode. These half-cells are separated by an electrolyte (Smolinka, Ojong, and Garche 2015). This is a thin proton-conducting but electrical insulating solid electrolyte membrane (Proton Exchange Membrane, PEM) (Rost, Roth, and Brodmann 2015). The electrolyte is a medium characterised by high ion conductivity required to close the electrical circuit. To enable ion transport either an acid or alkaline electrolyte is utilised (Smolinka, Ojong, and Garche 2015). Apart from having a high proton conductivity, the main characteristics of the membrane is to have high water absorption abilities and to provide a barrier between the fuel and reactant gases (Sammes 2006). In each half-cell, bi-polar plates (BPP) are situated. These provide the supply and removal routes for water, oxygen and hydrogen. Hence, the BPP keep the gas and fluid flows separated in channels and enables a uniform distribution over the catalytic area to enhance the reaction. Electrolysers are often mounted in stacks comprised of several cells and the BPP also aid to conduct electrical current between adjacent cells to close the electrical circuit.

As stated earlier the reactions to be attained in the electrolyser are endothermic, thus requiring an input of energy, often as heat, from the surroundings to proceed (Smolinka, Ojong, and Garche 2015). Also, input of energy in form of electricity is required for the electrolysis reactions to occur. Through applying a power source (DC) to the electrolyser cell, a voltage difference between the anode and cathode is established. The constituent atoms of water molecules are held together by electromagnetic forces. Hence, when liquid water experiences this voltage difference the molecule is separated into positively and negatively charged ions. These ions are attracted and transported to the electrode of opposite charge (Roebuck 2003).

Hence, when liquid water is supplied and temperature and the voltage applied between the electrodes are sufficiently high, redox reactions take place at the anode and cathode respectively, and the products from the reactions are oxygen- and hydrogen gas (Smolinka, Ojong, and Garche 2015).

Different electrolyser technologies
There are many kinds of electrolysers, which can be differentiated by the type of electrolyte, operating temperature and charge carrier utilised. The most common types are:

- Alkaline electrolyser (AEL)

- Proton Exchange Membrane electrolyser (PEMEL)

- Solid Oxide electrolyser (SOEL)

Of these, AEL represents the most mature electrolyser technology present in the market with the lowest investment costs and higher efficiencies than PEMEL and SOEL. However, with regards to future cost reduction potentials, both PEM- and SO- electrolysers have evident advantages (International Energy Agency 2015). Although the AEL historically has been the dominant

electrolyser technology utilised in hydrogen storage demonstration programs there has been an increased focus on and development of PEMEL. This technology provides several advantageous features, which makes it more suitable for renewable energy storage applications than AEL why it is the recommended option to apply for such systems. In particular, PEMEL can provide load-following services due to almost immediate start up and shut down (Mittelsteadt et al. 2015). Besides, it has the highest current density and operational range (International Energy Agency 2015). Furthermore it can produce high pressure hydrogen gas of up to 350 bar, which in turn allows for the implementation of smaller volumetric designs of the hydrogen storage tank (Mittelsteadt et al. 2015). Also, a thin and solid electrolyte is utilised in PEMEL in contrast to the liquid electrolyte in alkaline electrolyser. Thereby, faster ion transport and enhanced reliability and safety are attained (Bessarabov et al. 2016). Due to the apparent advantages of the PEM-electrolysers in renewable energy system applications a more in depth review of this technology is provided in this chapter.

Redox reactions in PEMEL
In PEM-electrolysers liquid water is supplied to the anode half-cell at which the water is oxidised to produce oxygen gas, protons and electrons with the aid of catalysts on the electrode surface, see equation 1.

$$Anode: \quad H_2O(liq.) \rightarrow \frac{1}{2}O_2(g) + 2H^+ + 2e^- \tag{1}$$
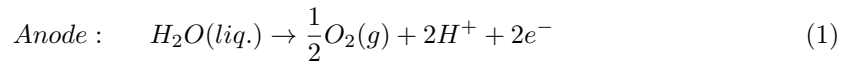
The charge carriers in this technology are the protons, i.e. the postively charged hydrogen ions (H^+), which are transported across the electrolyte to the cathode half-cell (Mittelsteadt et al. 2015). The electrons are conducted through the electrodes, current collectors and BPP and further transported through an external circuit to the cathode half-cell. At the cathode side, the migrated protons are reduced by the electrons and thus the electrical circuit is closed and hydrogen gas is produced, see equation 2 (Bessarabov et al. 2016).

$$Cathode: \quad 2H^+ + 2e^- \rightarrow H_2(g) \tag{2}$$
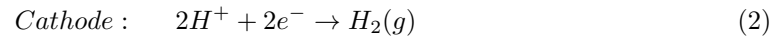
Hence the overall reaction of the conversion process is:

$$Overall: \quad H_2O(liq.) \rightarrow H_2(g) + \frac{1}{2}O_2(g) \tag{3}$$
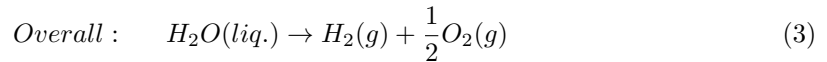
A scheme of operation and cell reactions of an electrolyser is visualised in figure 8.

Electricity source
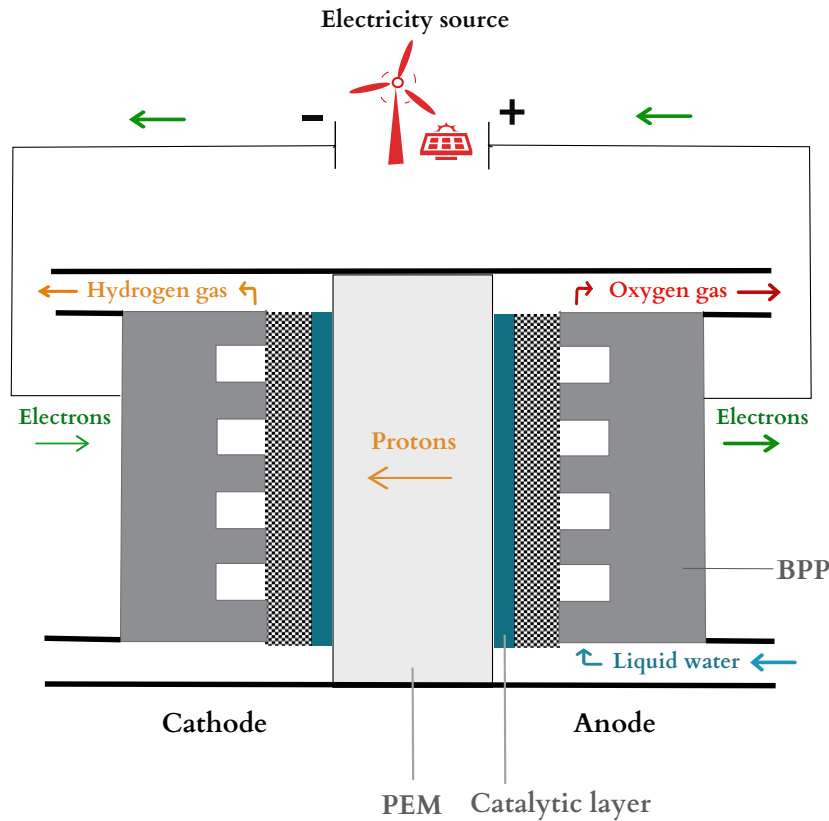
Figure 8: Schematic of electrolyser operation and reactions.

Efficiency and performance

Conversion devices that are part of Power-to-Power application systems, e.g., electrolysers and fuel cells, in which the produced hydrogen is converted back to electricity the lower heating value (LHV) should be utilised to calculate the efficiency for the energy conversion (Smolinka, Ojong, and Garche 2015). The efficiency of the electrolyser can be derived using Faraday's law:

$$\eta_{EL} = \frac{LHV \cdot \dot{n}_{H_2}}{P_{EL}} \tag{4}$$

Where LHV is the lower heating value of hydrogen, $\dot{n}_{H_2}$ is the molar flow of produced hydrogen, P_{EL} is the electrical power applied to the electrolyser and η_{EL} is the efficiency of the conversion process in the electrolyser (Cau et al. 2014). The efficiency of an electrolyser is typically in the interval of 64 - 82 percent depending on the technology used (Smolinka, Ojong, and Garche 2015).

As a part of the research programme Horizon 2020, established within the EU, the Fuel Cell and Hydrogen 2 Joint Undertaking programme has been initiated. Within this context, 2020 targets for fuel cell and electrolyser efficiencies have been determined. The fuel cell efficiency target is an increase by 10 %-units, whereas a target for electrolyser efficiencies is 80% (Niakolas et al. 2016).

The efficiency of the electrolyser decreases considerably with higher power flows, i.e., higher cell voltage, see equation 4. However, the hydrogen production rate increases as the cell voltage increases, which poses an operational dilemma in which a compromise between attaining optimal efficiency and high hydrogen production is required (International Energy Agency 2015). In addition, at low power levels ancillary losses are prominent, which results in a decrease in efficiency. Hence, to assure efficient operation of the electrolyser maximum and minimum power flow limits are established (Cau et al. 2014).

The loss mechanisms in electrolysers and fuel cells are of complex nature related to thermodynamics and kinetics (Mittelsteadt et al. 2015). This is not however reviewed in detail in this thesis .

Lifetime
An estimated lifetime for a device is based on the predicted time a device is able to operate until the performance decrease considerably. A decrease in performance occurs due to degradation processes resulting in lower operation efficiencies (Kwasinski, Weaver, and Balog 2016b). The lifetimes of electrolysers and fuel cells are closely related to how the system is operated. In particular, a high frequency of start/shut down of the devices results in a decreased life expectancy due to higher degradation (Ipsakis, Voutetakis, Seferlis, Stergiopoulos, Papadopoulou, et al. 2008). As previously mentioned, operation at too high or too low power levels reduces the efficiency due to loss mechanisms, which results in chemical and mechanical degradation of the system. Hence, frequent starts/stops degrades the electrolyser components and should be avoided (Valverde, Pino, et al. 2016). The expected lifetime of PEMEL remains one of the limiting factors for its applications (International Energy Agency 2015).

PEMEL system level
In addition to the electrolyser stack, several ancillary components and services are required for the system to operate. A supply of DC power and pure water is needed in addition to thermal management (Mittelsteadt et al. 2015). Hence, power conditioning, a feed water pump and heat exchangers are required. Furthermore, both the oxygen and hydrogen production side of the system constitutes a circulation loop including several stages such as water purification, gas/water separation, heat removal, etc (Smolinka, Ojong, and Garche 2015).

3.3.2   Fuel cell

As described previously, a fuel cell is an electrochemical device in which the chemical energy stored in hydrogen (fuel) and oxygen (oxidant) is converted into electrical power (DC). In contrast to batteries the chemical energy is not stored in the device, and hence a continuous supply of fuel and oxidant is required for the conversion process to proceed (Gou, Na, and Diong 2016).

General principle
Fuel cell operation is very similar to electrolysers, except the process is reversed. As for electrolysers, redox reactions take place at the anode and cathode respectively, but in contrast to electrolysers the electricity is generated through the conversion process. The reactants are hydrogen- and oxygen gas and liquid water is the product. Through conducting the electrons through an external circuit with a load, the power can be used for electricity consumption (Rayment and Sherwin 2003). In addition, the process is exothermic rather than endothermic suggesting that energy is released in the form of heat to the surroundings (Gou, Na, and Diong 2016).

Different fuel cell technologies
As with electrolysers, the various technologies available on the market can be distinguished by the type of electrolyte, operating temperature and charge carrier utilised. The most common types are:

- Alkaline fuel cell (AFC)

- Proton Exchange Membrane fuel cell (PEMFC)

- Solid Oxide fuel cell (SOFC)

(International Energy Agency 2015).

AFCs and PEMFCs are characterised by low working temperatures of about 80 C° in contrast to SOFCs which operates at temperatures of up to 600 C°. Thus, SOFC is the most suitable technology applied in combined heat and power (CHP) systems (International Energy Agency 2015). However, for energy system applications requiring the incorporation of renewable energy sources, SOFC is unsuitable due to long start-up times (Mittelsteadt et al. 2015). Instead, through applying fuel cell technologies of low operating temperatures fast start-ups are attained as desired. Specifically, for hybrid renewable energy systems, PEMFC is the fuel cell technology recommended (Uzunoglu, Onar, and Alam 2009). Hence, PEMFC is the technology of interest in this thesis, and a more in-depth review is provided in this chapter.

Redox-reactions of PEMFC
In PEM-fuel cells, hydrogen gas is supplied to the anode half-cell where the catalysts enable oxidation of hydrogen molecules to its constituents; protons and electrons, see equation 5.

$$Anode: \quad H_2(g) \rightarrow 2H^+ + 2e^- \tag{5}$$
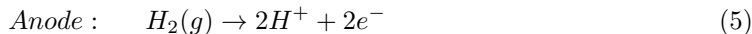
Similar to electrolysers, the PEM prohibit the transportation of electrons. These are instead conducted through an external circuit to the other half-cell. At the cathode side, the reduction reaction occurs in which the supplied oxygen reacts with the electrons and protons to form liquid water, see equation 6.

$$Cathode: \quad \frac{1}{2}O_2(g) + 2H^+ + 2e^- \rightarrow H_2O(liq.) \tag{6}$$
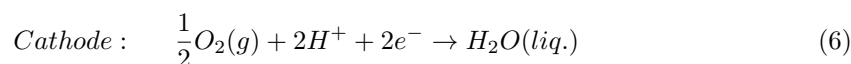
Hence, the overall fuel cell redox reaction is reversed that of an electrolyser, see equation 7.

$$Overall: \quad H_2(g) + \frac{1}{2}O_2(g) \rightarrow H_2O(liq.) \tag{7}$$
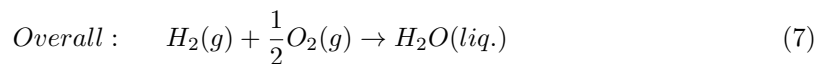
A scheme of operation and cell reactions is visualised in figure 9 (Sammes 2006).

Load
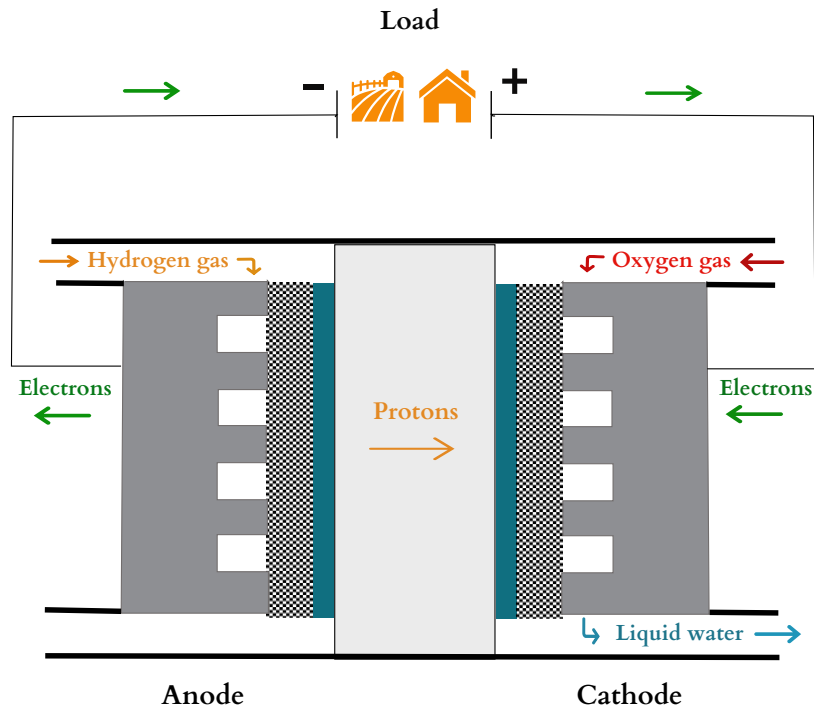
Figure 9: Schematic of fuel cell operation and reactions.

Efficiency and performance
As for electrolysers, the efficiency of fuel cells is determined using Faradays' law, see equation 8.

$$\eta_{FC} = \frac{P_{FC}}{LHV \cdot \dot{n}_{H_2}} \tag{8}$$

Where LHV is the lower heating value of hydrogen, $\dot{n}_{H_2}$ is the molar flow of consumed hydrogen, P_{FC} is the electrical power generated, and η is the efficiency of the conversion process in the fuel cell. (Cau et al. 2014) In general, the efficiency of a low-temperature fuel cell, such as PEMFC, is about 50 percent depending on the application (Steilen and Jörissen 2015).

Similar to the trade-off between efficiency and hydrogen production during electrolyser operation, a compromise between efficiency and electricity production is required for fuel cell operation (International Energy Agency 2015). Thus, maximum and minimum power flow limits are established to assure efficient operation of the fuel cell (Cau et al. 2014). Since the conversion process is exothermic, the overall system efficiency can be increased through recovering the heat released. However, if low temperature fuel cells are utilised, the temperature of the recovered heat is in the range of 60-70 °C. Hence, suitable applications are limited to heating of domestic water or floors rather than heating for industrial purposes (Steilen and Jörissen 2015).

Lifetime
Fuel cell lifetime and degradation rate correlates with the frequency of starts/stops during its operation, similar to that of electrolysers, see explanation in electrolyser section (Ipsakis, Voutetakis, Seferlis, Stergiopoulos, Papadopoulou, et al. 2008).

For fuel cells, as for electrolysers, no unanimous value of the lifetime is found. The lifetime ranges from 5000 to 50 0000 run hours and it is strongly related to the type of fuel cell technology used. The number of run hours of PEMFC ranges from 8000 to 15000 hours (Niakolas et al. 2016).

PEMFC system level
A high level of purity of the oxygen and hydrogen gases is essential. Eventual impurities in the hydrogen gas may accumulate at the anode and have a negative impact on the operation. The ancillary components and services required include heat exchangers and power conditioners. Besides the fuel cell stack, the fuel cell system also comprises separated oxidant and fuel supply systems and a water management system (Sammes 2006). The water management system may include a closed loop through which water is recycled back to the electrolyser, where it can be reused as a reactant (Ipsakis, Voutetakis, Seferlis, Stergiopoulos, and Elmasides 2009).

3.3.3   Hydrogen storage tank

There are several ways to store hydrogen:

- Gas at high pressure

- Liquid at low temperature

- Adsorbed or bound into hydrides

(Riis et al. 2006).

Storage of hydrogen gas at high pressure is a commercially available technology, common both for stationary applications and for vehicles. Cryogenic storage as liquid is costly, but used where space is scarce (Riis et al. 2006). Storage in hydrides is done in several different ways, which could all prove to have higher energy density than liquid storage and to have less security risks (Steilen and Jörissen 2015).

For this study hydrogen gas tanks of 200 bar is used. They represent a well known technology, which is common for stationary use and it is also applied in an isolated microgrid project implemented at Utsira in Norway (Ulleberg, Nakken, and Ete 2010).

For this technology the state of charge is in reality a measure of the density of the gas in the tank (ρ_{H_2}) compared to the nominal density $(\rho_{H_{2\,nom}})$. The density depends on the pressure of the gas in combination with the temperature, according to equation 9 used by Miguel et al. (2015). In the equation P is gas pressure [Pascal], T gas temperature [C°] and NWP is the nominal working pressure.

$$SOC_H(\%) = \frac{\rho_{H_2}(P,T)}{\rho_{H_{2\,nom}}(NWP,T_{nom})} \cdot 100 \tag{9}$$

However, since this thesis treats power and energy flows equation 10, used by Brka, Al-Abdeli, and Kothapalli (2015), is used in the simulations. This equation is a simplification of the reality, as it only considers the energy content of the storage. It is convenient to use as conversion of energy into complex pressure and temperature relations is avoided.

$$SOC_H(\%)(t) = \frac{E_H(t)}{E_{H,max}} \cdot 100 \tag{10}$$

3.4   Battery storage system technology

A battery is an electrochemical device which uses chemical reactions to store and provide electrical energy. Generally a battery consists of two half-cells where a positive electrode and a negative electrode are separated by an electrolyte (Dell and Rand 2001) and sometimes a membrane separator (Berg 2015). Redox reactions occur at the electrodes and the ions formed in the reactions are transported through the electrolyte, from one electrode to the other. The redox reactions can be written on a general form as in equations 11 and 12 (Dell and Rand 2001).

$$Negative\ electrode: \quad M \to M^{n+} + ne^- \tag{11}$$

$$Positive\ electrode: \quad nX + ne^- \to nX^- \tag{12}$$
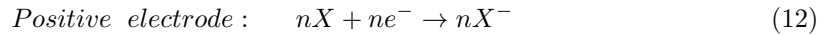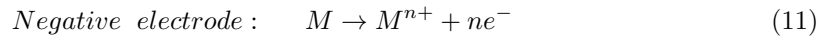
Where e^- represents electrons, M is a metal and X is an oxidising agent.

The capacity and voltage level of the battery depend on how the electrochemical cells are connected. Series connection adds up the voltage of each cell giving high voltage level, while cells connected in parallel have the same voltage level as one cell but larger capacity. The depth of discharge, DOD [%], describes how much capacity is consumed compared to the total energy available at that discharge rate. The state of charge, SOC [%], describes how much energy capacity is left (Dell and Rand 2001). How the battery is cycled can have large impact on the State of Health, SOH, and the lifetime of the battery. To preserve the battery life it is rarely cycled to its full extent, it is common to use a more narrow interval of SOC (Xu et al. 2016).

There are different types of batteries. The first division is between primary and secondary batteries, where the secondary batteries are rechargeable whereas the primary batteries are not. The electrodes and electrolytes can be made of several different combinations of materials; these often give name to the battery type. For example there are Lead-Acid batteries, commonly used in conventional vehicles with combustion engines, and Li-ion batteries (Dell and Rand 2001). The latter is used in the simulations conducted for this thesis.

Li-ion batteries are quick to start, ramp up and down, and stop running. Therefore they are suitable for performing frequency control. Li-ion batteries have a ramp rate of 15 MW/min or 250 kW/s (Byrne et al. 2017). The efficiency of Li-ion batteries is in the range of 90-95% (Cau et al. 2014) (Byrne et al. 2017). One drawback with batteries is that they self discharge and therefore are not suitable for long term energy storage (Cau et al. 2014).

4   CONTROL AND OPERATION

This chapter focuses on the control and operation of microgrids. The first section provides information on the features of control management and a review of the key controllers responsible for the microgrid operation. The second section addresses the operation strategy required to deal with the energy management of the system. A review of different operation objectives and energy management strategies is given.

4.1   Grid control

As mentioned previously, management and control strategies are required to enable incorporation of DER in the microgrid (Schwaegerl and Tao 2014). Also, the microgrid must be capable of performing and providing the same grid functions and services as a large-scale grid. These functions include:

- Equalized balancing of power supply and demand to preserve stability

- Scheduling and coordination of DER units and loads

- Maintaining grid reliability considering both adequacy and security

(Ton and Reilly 2017)

The higher penetration level of DER units in microgrids in comparison to the penetration level of DER in regular distribution networks makes control and coordination of these units even more urgent for implementation of stand-alone microgrids (Olivares, Cañizares, and Kazerani 2014). Microgrids can utilise either a centralised or distributed controller. In the former case, a centralised controller is in charge of controlling the power and energy flows in the system and hence controls the operation of the entire grid (Kwasinski, Weaver, and Balog 2016a). In isolated microgrids, centralised control is preferable due to the importance of proper coordination of the DER units (Olivares, Cañizares, and Kazerani 2014). The centralised control comprises three controllers:

1. Power Conversion System (PCS)

2. Microgrid Central Controller (MGCC)

3. Device Management System (DMS)

These three controllers are together responsible for the efficient execution of the aforementioned hierarchal control: primary, secondary and tertiary control (Minchala-Avila et al. 2015). To achieve a coordinated control scheme, these three controllers are communicating to provide each

other with information about the state of the system etc., see figure 10 (Byrne et al. 2017).
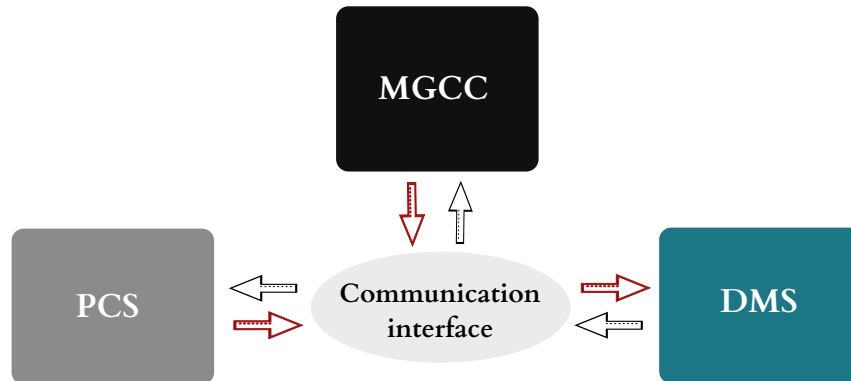
Figure 10: Communication and dataflow scheme between control levels.

Power Conversion System (PCS)
The PCS controllers are applied at device-level to ensure that DER's are operating correctly. This concerns their participation in primary and secondary control to maintain accurate voltage, frequency and power flow levels of the grid (Minchala-Avila et al. 2015). As stated earlier, power electronics enable renewable resources and storages to participate in the primary control and most commonly, through applying traditional Proportional-Integral (PI) control. The PCS enables DER to participate in secondary control through controlling the bi-directional power flows between the grid and the device. Hence, the PCS can execute three different commands to the DER's to attain secondary control: charging, discharging and stand-by mode (Byrne et al. 2017).

Device Management System (DMS)
The DMS is responsible for ensuring that the DER units operate safely and that MGCC and PSC control levels are provided with this information. To assure that the DER's are operated safely with regards to their technical constraints and power limits, the DMS must be able to monitor and evaluate the state of the device. The state of charge of a battery, for example, is indirectly determined through measuring temperature, voltage levels, current and its lifetime. The state of health (SOH) relates to the condition of the component relative to its ideal state. In batteries, it is indirectly measured through evaluating the impedance of the device. Information about the state of the device is also essential information for the control decisions made in the PCS and MGCC (Byrne et al. 2017).

Microgrid Central Controller (MGCC)
The MGCC is responsible for providing tertiary control, i.e., energy management of the system based on data obtained from the other control levels; PCS and DMS. Hence, based on information such as load demand, power levels of generation sources and storage state, the MGCC determines suitable reference values for the power levels of the different DER units. Then the PCS ensures that this set-point value is attained for the device through initiating either the charging, discharging or stand-by mode (Minchala-Avila et al. 2015). Conclusively, the MGCC is the controller responsible for the vital coordination between the DER units and thus optimised operation of the microgrid (Byrne et al. 2017).
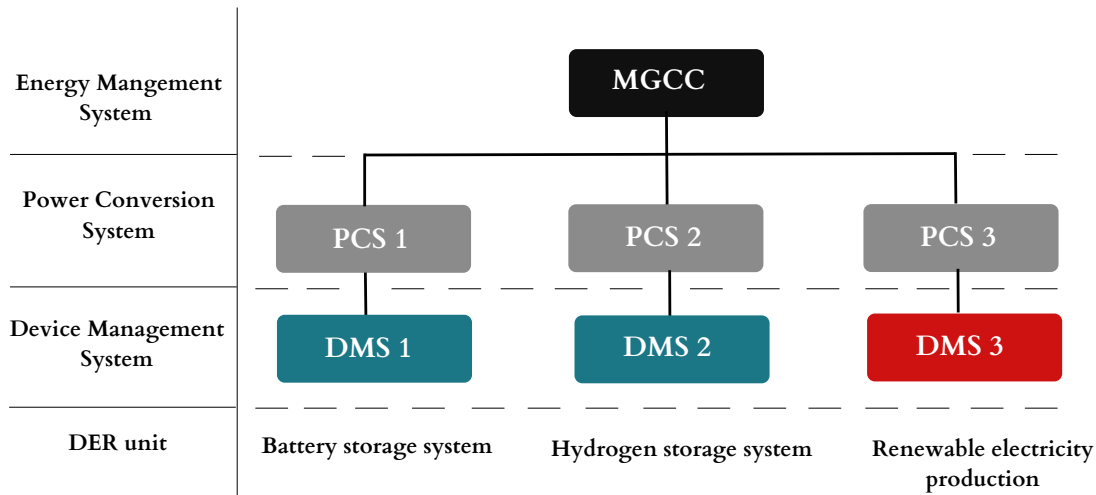
Figure 11: Hierarchal control architecture including DER units: energy storage (blue) and renewable generation (red).

In figure 11 an example of a hierarchal control architecture is displayed (Byrne et al. 2017). The figure includes the DER's incorporated in the microgrid studied in this thesis. However, it should be noted that for this thesis, pre-determined historical data from Simris is used for the simulations. Thus, the MGCC does not calculate and determine power output set-point levels for next time step.

Conclusively, in this thesis, the power output set-point levels for the wind and solar power plants is not evaluated through a control strategy. Hence, the control strategy implemented in this thesis only determines reference values for charge and discharge power levels of the battery- and hydrogen storage systems taking the pre-determined production and load power levels into consideration. Thus, henceforth only the control and coordination of the battery and hydrogen storage systems is addressed in this report.

4.2   Operation strategy

The MGCC is an entity responsible for ensuring optimal operation of the microgrid through controlling the energy flow management of the system. This is done by designating set-point power levels, of charge or discharge, to the storage systems (Minchala-Avila et al. 2015). As mentioned earlier, the incorporation of renewable resources puts a stress on the need for energy storages that can offer vital grid services. This results in a higher demand for energy flow and optimization techniques of the grid to preserve reliability and stability (Eriksson and Gray 2017). An Energy Management System (EMS) is implemented in the MGCC. (Meng et al. 2016). The EMS comprise algorithms responsible for determining the energy management of the system (Etxeberria et al. 2010). The development of such energy management strategies is essential to take full advantage of the flexibility potential that the energy storage systems provide. Energy storage systems are a new flexibility option, and many system operators lack sufficient experience and knowledge

regarding their implementation and operation. Hence, suitable energy management strategies still need to be developed in order to facilitate the integration and coordination of multiple storage systems (Byrne et al. 2017). This is of high importance since the energy management strategy strongly affects the performance of the system. Since the EMS controls the operation and coordination of the DER's, e.g., energy storages, the operation strategy implemented in the EMS will strongly affect the lifetime of these components. In turn, the lifetime of the equipment strongly influences the economic viability of the system. This further emphasises the importance of addressing the challenge of developing innovative energy management control strategies to attain a technically and economically viable microgrid operation (Valverde, Rosa, et al. 2016).

4.2.1   Objectives

The energy management strategy, and thus the final microgrid architecture configuration, are developed with regards to microgrid operational objectives. Hence, the operation strategy varies depending on the interest of the stakeholders involved, e.g. system operators, DER owners, and customers. In general, three objectives exist: technical, economic and environmental, which can be combined or applied independently.

Technical
For system operators, a technical objective is essential since it relates to optimising the operation of the grid to ensure security, reliability, and stability. Often constraints such as voltage limits etc. are utilised to achieve the technical objective. Production costs and revenues are not taken into consideration.

Economical
If an economic objective is applied, the aim is to minimize the cost of the microgrid operation. Effects on the technical performance of the grid are not included however. For customers or owners of the generation resources, this objective might be of interest.

Environmental
Environmental and climate targets are attained by operating the microgrid with regards to environmental objectives. Greenhouse gas emission from the integrated generation source is the primary indicator to evaluate. Hence, generation units with low emission levels are prioritised in this operation strategy, disregarding technical and economic aspects (Schwaegerl and Tao 2014).

4.2.2   Energy management strategy

As stated earlier, the energy management strategy should ensure that the storage units are coordinated correctly and operated with regards to load demand and renewable power production to preserve an equalized power balance of the grid. The primary objective is to assure that the electricity demand of customers in the microgrid is met but, as stated previously, the strategy can be further customised with regards to the established operation objectives (Valverde, Rosa, et al. 2016). Due to the high penetration of RES and sharper load variations in microgrids, the energy management strategy differs considerably from that constructed for conventional grids. Since energy storage systems provide important flexibility services to microgrids, the operation of the microgrid is strongly affected by the strategy implemented in the EMS to control these storage systems (Petrollese et al. 2016).

The algorithms implemented in the EMS can be differentiated into simple rule-based algorithms or complex optimisation algorithms. Optimisation algorithms can consider several variables and might encompass forecasting of weather, electricity prices, and electricity demands, etc. A more in-depth review of different energy management concepts is outlined below, see 4.2.3.

The EMS is characterised by the ability to schedule the energy and power management at different time-scales: short-term and long-term management (Valverde, Rosa, et al. 2016).

Long-term management
To attain an economically viable operation and coordination of the storage systems long-term planning is required (Petrollese et al. 2016). Long-term scheduling can be divided into daily and hourly management. For example, daily management may involve weather forecasting to predict renewable electricity production or prediction of electricity load demands. Hourly management can include energy storage availability (Valverde, Rosa, et al. 2016). The long-term management system is responsible for scheduling and determining suitable reference values for SOC in the storage systems for the following couple of hours. The scheduling is conducted on the basis of the forecast predictions of the generation and load that is made for the coming days (Petrollese et al. 2016).

Short-term management
As for long-term scheduling, short-term management can be divided into control at different time scales, milliseconds to hours, to offer regulatory services and power management availability (Valverde, Rosa, et al. 2016). Regulatory services refer to the instantaneous management of energy flows in the grid in the time interval of milliseconds to seconds (Suzdalenko and Galkin 2013). It includes frequency control and balance of active and reactive power. Power management comprises assuring that the power levels of the storage devices are within proper limits to ensure that the device is optimally operated with regards to, e.g., lifetime and O&M costs (Valverde, Rosa, et al. 2016). The long-term and short-term management systems work simultaneously and cooperate to achieve optimal operation. In figure 12 a schematic of their cooperation is displayed.
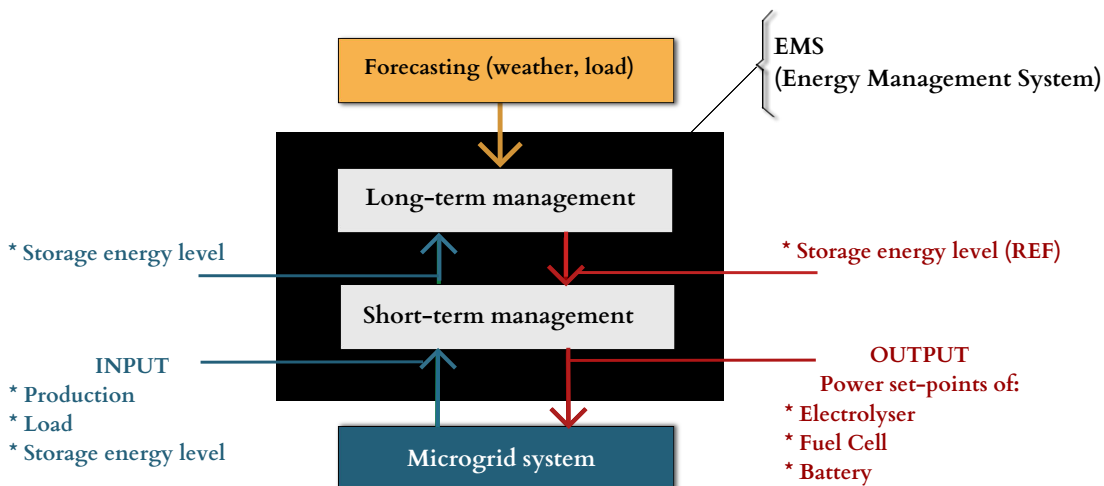

Figure 12: Overview of the long- and short-term management included in an EMS.

Hence, the long-term management schedules reference values for the energy level of the storage systems, i.e., SOC based on predictions and forecasts of load and power generation. The short-term management provides real-time power management through comparing the production and load predictions from the long-term management with the actual, real-time, load and generation profiles. If any deviations between predicted and actual power levels occur, this is accounted for by the short-term management system to achieve an equalised power balance. Thus, the short-term management system is responsible for the real-time control and power balancing, i.e., determining the power levels of the storage devices, fuel cell, electrolyser, and battery, to assure that grid stability and long-term objectives are attained (Petrollese et al. 2016).

However, for this thesis only a short-term energy management strategy is implemented for the EMS. This is in line with the research method applied by Valverde, Rosa, et al. (2016) who conducted research regarding an evaluation of different energy management strategies for microgrids with hydrogen storage. Instead of forecasting generation and load profiles, the control strategy was developed through utilising real historical yearly data for production and load. Hence, a short-term control strategy that can calculate and determine the power set-points for the storage units, electrolyser, fuel cell, and battery, based on information about production, load, and SOC levels is developed. This short-term strategy is described in detail in chapter 5.3.

4.2.3   Different energy management strategies

Several types of energy management strategies can be implemented for HESS, and the choice and design of this strongly influences the operation of the microgrid (Petrollese et al. 2016). As stated in section 4.2.2, the EMS concept can be divided into two categories of control strategies, rule-based and optimisation based strategies (Bocklisch 2015). What mainly distinguishes the two categories is the ability to achieve an optimised operation with regards to several aspects, which is possible through applying optimisation control algorithms. This is accomplished through forecasting of weather, electricity prices, degradation, etc. For example, economic objectives can be addressed through cost functions, which enable a techno-economic optimisation of the system (Valverde, Rosa, et al. 2016). Such an optimised operation and management of resources in the microgrid cannot be achieved through applying rule-based strategies. However, an optimization strategy is more complex and entail a higher computational burden than a rule-based strategy. Furthermore, rule-based approaches are simple, reliable and widely reviewed and adopted in research and literature (Petrollese et al. 2016). Lastly, they are also suitable for real-time applications (Bocklisch 2015). Hence, since short-term energy management is responsible for the real-time power management, the strategy deployed for this thesis is rule-based.

Rule-based control strategies

As stated earlier, rule-based strategies can be constructed through programming using if-statements in which rules are formed to manage the energy discrepancy in the grid (Valverde, Rosa, et al. 2016). The main control variable utilised in this control strategy is the SOC of the battery storage system or sometimes the SOC of the hydrogen storage system. Hence, the SOC level strongly affects the coordination of the storage systems as it indirectly determines and allocates the power flows between the storage devices (Petrollese et al. 2016). In a HESS including a high power, short-term storage, e.g., battery storage, and an high energy, long-term storage, e.g., hydrogen storage, it is custom to let the SOC of the short-term storage to be the governing control variable (Bocklisch 2015).

5   SIZING AND DESIGN

In this chapter, the sizing and design methodology applicable for microgrids with multiple storage systems (HESS) is reviewed. The first section presents different design objectives and their corresponding performance indicators. In section 2, the concept of grid power balance and the design constraints required to model the energy storage systems are presented. Lastly, in section 3, a detailed description of the energy management strategy constructed for the proposed microgrid solution in Simris is given.

Sizing and configuration of system components are essential to attain an accurately functioning microgrid, which operates in line with design objectives (Eriksson and Gray 2017). Sizing and design considerations are strongly related to energy management considerations, and hence these operation strategies are utilised to determine the storage sizes required to attain power balance of the grid (Bocklisch 2015). Unit sizing of storage systems in an isolated microgrid with renewable resources is complex. To obtain an optimal storage configuration based on prevailing conditions for a specific microgrid, an optimisation approach is required (Bizon, Oproescu, and Raceanu 2015). In practice it means that a mathematical function is constructed with regards to objectives of the stakeholders. The function is to be minimised with regards to system constraints to find an optimised solution, which can be done by utilising complex mathematical optimisation programming techniques (Eriksson and Gray 2017).

However, it should be noted that due to time and scope limitations, the primary purpose of this thesis is not to determine and present an optimised storage configuration solution. Instead, a sensitivity analysis is conducted to compare and evaluate system performance for different storage configurations.

5.1   Objectives

Since sizing of a system is closely related to the construction of an EMS the design and sizing of system components are conducted with regards to the same objectives mentioned in section 4.2.1; technical, economic and environmental (Behzadi and Niasati 2015). Several suitable configuration solutions can be attained for a given design problem, which stresses the importance of carefully selecting the appropriate design objective(s) (Eriksson and Gray 2017). Often, the selected objectives are in conflict with each other resulting in that the final design and configuration of the system components represents a trade-off between these goals. For each objective one or several performance indicators are determined, which serve as design criteria (Bizon, Oproescu, and Raceanu 2015). Below, a more in-depth description of the objective functions is given. It should be noted that only the objectives of relevance for this report are presented.

5.1.1   Technical objective

There are several technical objectives to consider and select from when designing an energy system. Technical goals that might be regarded are system feasibility, performance, risk management, efficiency, energy availability, and reliability, to name a few. When designing a system characterised by high penetration of intermittent renewable resources, it is essential to include system reliability in order to ensure that the system is adequately designed to meet the load demand. This is particularly true for systems comprising a long-term hydrogen storage solution, which should be designed to account for seasonal variations. The most utilised and renowned performance indicator to evaluate system reliability is Loss of Power Supply Probability (LPSP) (Eriksson and Gray 2017). Hence, this is the primary performance indicator employed for the system design in this thesis.

Furthermore, sometimes the power produced by the renewable sources exceeds the load demand and storage capability. Hence, this excess energy is wasted, either through curtailment of the generation sources or through dumping the energy. It has been found that, depending on system configuration, up to 50 % of generated power from renewable sources eventually becomes excess power, which needs to be wasted. Excess power may also represent an indication for over dimensioned generation units, PV-panels, wind turbines and fuel cells, and may serve as an indirect indicator of the techno-economic viability of energy systems. Excess of Energy (EE) as a design parameter has only been adopted by Brka (2015) who implemented an optimisation strategy for stand-alone energy system focusing on minimising EE while assuring that targets for LPSP was met. However, the results showed that, due to high costs of energy storage units, lower EE was always associated with higher system costs. Hence, due to higher system costs in addition to low level of occurrence in literature EE is not a prioritised performance indicator in this thesis to size the system. However, despite aforementioned disadvantages, the dilemma of avoiding excess power is considered an important and interesting aspect to consider for renewable energy systems. EE is calculated and used for analysing and evaluating system configuration performance in this thesis. Hence, EE is included but little emphasis will be put on sizing the system with regards to minimizing this indicator.

Loss of Power Supply Probability (LPSP)
The Loss of Power Supply Probability (LPSP) function is defined as a ratio of the accumulated time of power deficits and total time, see equation 13.

$$LPSP = \frac{\sum_{t=0}^{T} Power\ deficit\ incident}{T} \quad = \quad \frac{\sum_{t=0}^{T} Time(P_{available} < P_{load})}{T} \tag{13}$$

The parameter T represents the total number of hours of the analysed period, which in this study is a year, i.e. 8760 h. The time of deficit implies the time when the available power from generation sources, PV and Wind, and storage systems, battery and hydrogen storage, is unable to meet the load demand resulting in a negative power discrepancy. A system with high reliability can ensure that sufficient power is available to meet the load for a specific time-period, i.e. the LPSP is low. The value for LPSP is in the range of 0 to 1. Hence, an LPSP of 0 suggests a system that can assure that load is satisfied during the entire period and a value of 1 implies that the demand is never met (Yang et al. 2008).

Excess of Energy (EE)
Brka (2015) evaluated EE with regards to energy, however, in this thesis EE is evaluated with regards to time to make it more compatible with the results from LPSP, see equation 14.

$$EE = \frac{\sum_{t=0}^{T} Power\ excess\ incident}{T} = \frac{\sum_{t=0}^{T} Time(P_{available} > P_{load})}{T} \tag{14}$$

As for the performance indicator of LPSP, the parameter T represents the total number of hours of the analysed period. The time of excess power implies the time when the available power from generation sources exceeds the combined load including electricity demand of consumers in the grid and storage system resulting in a positive power discrepancy. Similar to LPSP, a value of 0 implies a system with no excess power and a value of 1 suggests that there is excess power every hour (Brka 2015). A positive power discrepancy would mean that the power production has to be curtailed to maintain grid balance.

5.1.2   Economic objective

Depending on the interest of the stakeholders, a suitable economic objective can be selected. Examples of potential economic aspects to evaluate include return on investment, availability of funds, generation cost of energy and system cost. In literature, the most adopted performance indicator is Annualised Cost of System (ACS), which is utilised to design a system based on the economic objective of minimising system cost (Eriksson and Gray 2017). This method was also deployed by Hongxing Yang et al. to size a stand-alone hybrid solar-wind system. Hence, the method is assumed applicable for this thesis. The ACS is a sum of the annualised values for the capital-, replacement- and operation and maintenance cost of the parts and components considered, see equation 15.

$$ACS = C_{acap} + C_{arep} + C_{aO\&M} \tag{15}$$

A more in-depth description of these annualised costs is presented below.

Annualised capital cost
The total annualised capital cost [SEK/year] of the components of the system is calculated by adding the individual annualised capital costs. To calculate the annualised capital cost of one unit (u) the initial capital cost of the equipment has to be multiplied by a capital recovery factor (CRF), see equation 16. Hence, the value of CRF is utilised to convert the present value into an annualised value.

$$C_{acap} = \sum_{u=0}^{U} CRF_u \cdot C_{cap_u} \tag{16}$$

In equation 16, U is the total number of units included in the economic evaluation. The recovery factor takes the lifetime of the unit (Y_u, [years]) and interest rate (i) into account, see equation 17 (Yang et al. 2008).

$$CRF_u(i, Y_u) = \frac{i \cdot (1 + i)^{Y_u}}{(1 + i)^{Y_u} - 1} \tag{17}$$

Annualised replacement cost
Many devices degrade during operation and have a limited lifetime, which may require replacement of these during the project life. The total annualised replacement cost of the units of the system is calculated as the sum of the annualised replacement costs of the individual units (u). The latter is calculated as a product of the Sink Fund Factor (SFF) and the replacement cost (C_{rep_u}) (Yang et al. 2008). According to Y. Zhang et al. (2017) the unit replacement cost can be assumed the same as the unit capital cost [SEK], which will be utilised in this paper, see equation 18.

$$C_{arep} = \sum_{u=0}^{U} SFF_u \cdot C_{rep_u} \quad = \quad \sum_{u=0}^{U} SFF_u \cdot C_{cap_u} \tag{18}$$

The SFF is a ratio utilised to determine the future value, in this case the replacement cost (C_{rep}), from a series of annualised values. Hence, SFF can also be used to calculate the annualised costs if the replacement cost is given, which is applied in this thesis. The SFF takes the lifetime of components (Y_{rep}, [years]) and the interest rate (i, [%]) into account, see equation 19 (Yang et al. 2008).

$$SFF_u(i, Y_{rep}) = \frac{i}{(1 + i)^{Y_{rep}} - 1} \tag{19}$$

Annualised operation and maintenance cost
The annualised operation and maintenance cost ($O\&M$) for a unit (u) is calculated as a product between the $O\&M$-ratio ($r_{O\&M}$, [%/year]), the capacity (CAP, [kWh]) and the capital cost [SEK]. The total annualised operation and maintenance cost is determined by summing up the individual annual operation and maintenance costs of the units, see equation 20 (Y. Zhang et al. 2017).

$$C_{aO\&M} = \sum_{u=0}^{U} r_{O\&M_u} \cdot CAP_u \cdot C_{cap_u} \tag{20}$$

5.2   Models and constraints

5.2.1   Grid power balance

Power balance is a requirement for a proper functioning microgrid i.e. the input and output power flows must match at each time-step (Petrollese 2015). Ideally, the production profile matches the load profile and eventual losses in the system, see equation 21:

$$0 = P_{prod} - P_{load} - P_{Loss} = (P_{PV} + P_{Wind}) - P_{load} - P_{Loss} \tag{21}$$

However, unwanted positive or negative discrepancies between electricity supply and load demand can occur, particularly in microgrids with a high share of intermittent renewable sources, see equation 22.

$$P_{diff_1} = (P_{PV} + P_{Wind}) - P_{Load} - P_{Loss} \tag{22}$$

Hence, the microgrid should be constructed and controlled with the aim of minimising this power difference (P_{diff_2}), which can be achieved through adding flexibility options such as battery and hydrogen storage and implementing a suitable energy management strategy, see equation 23. A positive value for P_B or P_H implies discharging of the storage devices, whereas negative values represents charging processes.

$$P_{diff_2} = (P_{PV} + P_{Wind} + P_B + P_H) - P_{Load} - P_{Loss} \tag{23}$$

A negative value of P_{diff_1} suggests that the power supply from PV-panels and wind turbine is unable to match the load demand (Yusof and Ahmad 2016). Such a negative power discrepancy indicates a power deficit, which is critical to address in order to assure reliability and a low LPSP (Yang et al. 2008). Hence, a smaller, i.e. less negative, value of P_{diff_2} can be achieved through discharging the storage devices.

In contrast, a positive value of P_{diff_1} implies that the power supply from PV-panels and wind turbine exceeds the load demand (Yusof and Ahmad 2016). A positive power discrepancy indicates a power excess, which relates to minimising the performance indicator EE (Brka 2015). This can be combated through charging the battery or hydrogen storage systems (Yusof and Ahmad 2016). However, as stated earlier, ensuring reliability, i.e., minimising the negative power discrepancy of, $P_{diff_1} < 0$, to attain a low LPSP, is crucial and considered the prioritised objective over EE for the microgrid design in this thesis.

5.2.2   Energy storage models and constraints

Energy storage systems, e.g. battery and hydrogen storage, can be modelled in several ways depending on the purpose of its implementation. The prevailing methods used to model energy storages are categorised as either dynamic-, energy flow-, physic-based- or black-box models. Modelling of energy storages is complex and challenging due to the variety of different technologies and complicated operation dynamics. Thus, the presented methods mainly differ with regards to the level of complexity that is included in the model and their applicability considering time-scales. The choice modeling method should be evaluated with regards to the purpose of the study, level of complexity required and the time-scale under which the simulations are performed.

The purpose of this thesis is to design an energy management strategy utilising input data of power and load profiles in the time-scale of hours, which motivates the choice of applying energy flow models. The simulations are not capturing the complex dynamics or underlying physical behaviors affecting the energy conversion processes in the storages. To achieve that, dynamic- or physics based models are required, which often are implemented at lower levels in the hierarchal control architecture, e.g. in the DMS. However, energy flow models are typically implemented in the EMS and it provides a high-level understanding of the power flows in the charging and

discharging processes. Hence, it is beneficial to deploy energy flow models at an early stage, e.g. feasibility studies, to enable an initial analysis of the system performance or to select appropriate energy storage technologies. This further motivates the choice of applying energy flow models in this study (Byrne et al. 2017).

Power flow: charge and discharge
By convention, the power parameters for the load and power supply, P_{load} and P_{prod}, in equation 23 are always positive. In contrast, energy storages provide bi-directional power flows. Thus, the power parameters representing the energy storages in equation 23, P_B and P_H, are negative for charging and positive for discharging processes (Gulin, Vašak, and Baotić 2015). The charging and discharging scenarios are presented below.

Charge of storage systems
As stated earlier, a positive value for P_{diff_1} can be combated through charging the battery or hydrogen storage systems (Yusof and Ahmad 2016). If the battery is charging, the charge power is positive (P_{BC}). In the hydrogen storage, the electrolyser is performing the conversion process of electricity to hydrogen to charge the hydrogen storage (Gulin, Vašak, and Baotić 2015). This is represented by a positive value for the electrolyser power level (P_{EL}). The power balance condition and sign conventions for the power parameters representing the storages are presented below.

Power balance condition: $P_{diff_1} > 0$

Battery storage system:

$$P_B < 0 \implies \begin{cases} P_{BC} > 0 \\ P_{BD} = 0 \end{cases}$$

Hydrogen storage system:

$$P_H < 0 \implies \begin{cases} P_{EL} > 0 \\ P_{FC} = 0 \end{cases}$$

Disharge of storage systems
A negative value for P_{diff_1} can be combated through discharging the battery or hydrogen storage systems (Yusof and Ahmad 2016). If the battery is discharging, the discharge power is positive (P_{BD}). In the hydrogen storage, the discharging process is performed by the fuel cell through converting hydrogen to electricity to discharge the hydrogen storage (Gulin, Vašak, and Baotić 2015). This is represented by a positive value for the fuel cell power (P_{FC}). The power balance condition and sign conventions for the power parameters representing the storages are presented below.

Power balance condition: $P_{diff_1} < 0$

Battery storage system:

$$P_B > 0 \implies \begin{cases} P_{BC} = 0 \\ P_{BD} > 0 \end{cases}$$

Hydrogen storage system:

$$P_H > 0 \implies \begin{cases} P_{EL} = 0 \\ P_{FC} > 0 \end{cases}$$

However, it should be noted that these scenarios are general. Depending on the design of the operation strategy it is possible to run the battery and hydrogen storages simultaneously e.g. discharging the fuel cell at a high enough power level to meet the load demand and charge the battery (Ipsakis, Voutetakis, Seferlis, Stergiopoulos, Papadopoulou, et al. 2008). This scenario suggests that the strategy is constructed to allow the battery to be charged ($P_{BC} > 0$) even at times when $P_{diff_1} < 0$.

Energy level: State of Charge (SOC)
Energy flow models are applied to represent the storage units and thus the state of charge of the storages can be described using first-order equations, see equations 24 and 25.

$$SOC(t+1)_B = SOC(t)_B + \frac{\triangle t}{CAP_B}\left(\eta_{BC} \cdot P_{BC}(t) - \frac{1}{\eta_{BD}} \cdot P_{BD}(t) \right) \tag{24}$$

$$SOC(t+1)_H = SOC(t)_H + \frac{\triangle t}{CAP_H}\left(\eta_{EL} \cdot P_{EL}(t) - \frac{1}{\eta_{FC}} \cdot P_{FC}(t) \right) \tag{25}$$

The time-step ($\triangle t$) utilised in the simulations conducted for this thesis is one hour. In the above equations, $SOC(t+1)$ represents the state of charge calculated for the following time-step, which is determined based on information of:

- State of charge of the previous time-step ($SOC(t)$)

- Charge efficiencies (η_{BC} and η_{EL})

- Discharge efficiencies (η_{BD} and η_{FC})

- Capacity of storages (C_B and C_H)

- Charge power levels of the previous time step ($P_{BC}(t)$ and $P_{EL}(t)$)

- Discharge power levels of the previous time step ($P_{BD}(t)$ and $P_{FC}(t)$)

The control strategy should ensure that a storage unit is unable to perform discharging and charging processes simultaneously as this would entail unacceptable and unnecessary power losses and higher operational costs. For example, during charging of the hydrogen storage the value of P_{FC} must be zero as the value for P_{EL} is positive. Thus, charging processes results in an increase in SOC and discharging processes will lead to a decrease in SOC (Gulin, Vašak, and Baotić 2015).

Design constraints of storage systems
Design of the energy management strategy and the storage systems require design variables. Typical variables applied for the design of battery- and hydrogen storage systems are SOC, charge- and discharge powers. The variables utilised in the design process should only be allowed to adopt values within defined boundaries. Such boundaries strongly affect the outcome of the design process and are referred to as design constraints. Hence, the values for these constraint parameters should be carefully selected. The constraints are chosen based on functional limitations and other requirements that need to be fulfilled for the system to operate in accordance with design goals (Eriksson and Gray 2017).

Power flow constraints
Due to technical and functional limitations, constraints regarding discharging- and charging- power levels are required. More specifically, the operation efficiency of batteries, fuel cells and electrolysers decrease significantly at too high power levels. Hence constraints for maximum power levels need to be established. Also, to attain proper and efficient operation of the fuel cells and electrolysers, a minimum power level is required as a design constraint. If the fuel cell and electrolyser are operated at too low power flows, their efficiency will decrease due to ancillary losses, which should be avoided through applying the design constraint mentioned above. The design variables of power flow for the battery, fuel cell, and electrolyser are displayed below in equations 26, 27, and 28.

$$P_{BC}, P_{BD} \leq P_{B_{max}} \tag{26}$$

$$P_{ELmin} \leq P_{EL} \leq P_{EL_{max}} \tag{27}$$

$$P_{FCmin} \leq P_{FC} \leq P_{FC_{max}} \tag{28}$$

Energy level constraints
Constraints of the energy level are required for the battery and hydrogen storage system operation, and are commonly represented as boundary values for the state of charge (SOC), see equations 29 and 30 (Petrollese 2015). Both maximum and minimum SOC-constraints are imposed on batteries due to the substantial damage and decrease in battery life that over-charging and over-discharging events cause (Valverde, Pino, et al. 2016). For example, the minimum SOC is determined based on the lowest depth of discharge (DOD) allowed by the manufacturer. If the batteries are discharged to low DOD levels, the number of cycles that the battery can complete before replacement is drastically reduced. The SOC constraint can be expressed according to equation 29.

$$SOC_{B_{min}} \leq SOC_B \leq SOC_{B_{max}} \tag{29}$$

For hydrogen storage systems, minimum and maximum hydrogen energy levels commonly refer to the pressure limits in the tank. In order for the fuel cell to operate properly, requirements on the hydrogen supply pressure level are needed. This constitutes the minimum pressure allowed in the tank. The maximum permitted tank pressure determines maximum hydrogen energy level in

the tank (Petrollese 2015). In accordance with equation 9 in section 3.3.3 the SOC of hydrogen tanks is indirectly an indicator of the hydrogen pressure in the tank. Hence, minimum pressure level allowed is represented by constraints of SOC, see equation 30:

$$SOC_{H_{min}} \leq SOC_H \leq SOC_{H_{max}} \tag{30}$$

5.3   Energy management strategy for simulations

Figure 13 shows how the MGCC works along with the components of the proposed HESS system in Simris. The MGCC contains the EMS and thus the energy management strategy constructed for this thesis. Information about the power discrepancy, battery state of charge and power and energy limits of both energy storage systems are taken into account by the EMS. Based on this information, the energy management strategy evaluates appropriate power set-point levels for the battery and hydrogen storage systems to achieve power balance on the grid.
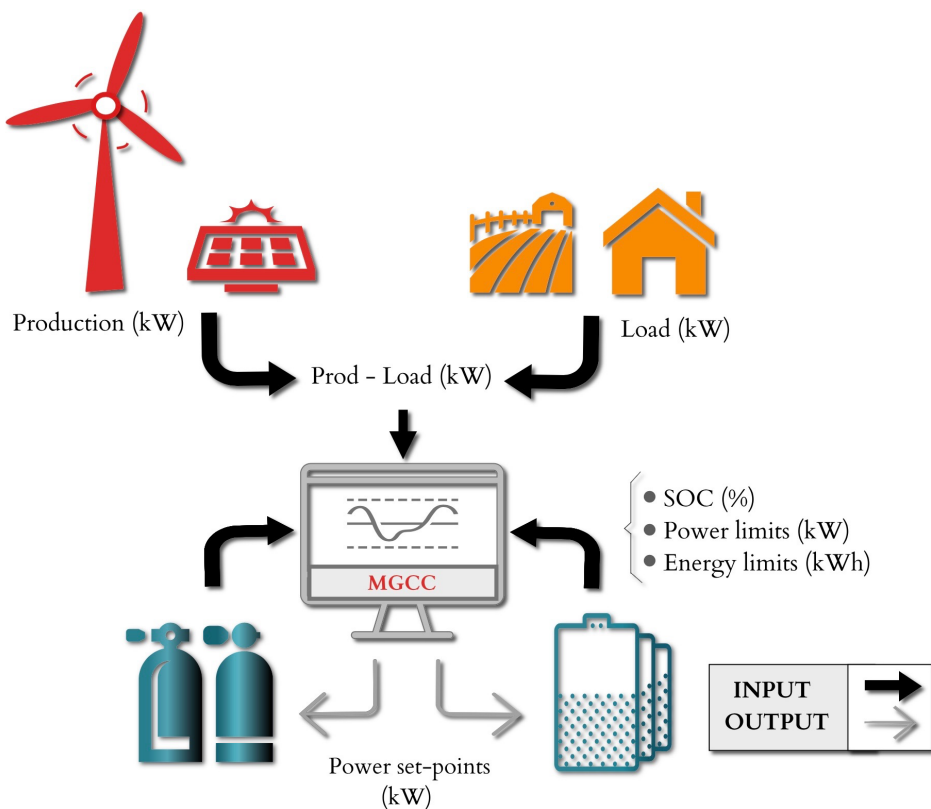

Figure 13: Overview of how the MGCC is connected to the LES in Simris

The operation strategy constructed for this thesis is a combination and an extension of the strategies used by Ipsakis, Voutetakis, Seferlis, Stergiopoulos, and Elmasides (2009) and Brka, Al-Abdeli, and Kothapalli (2015). When studied it was noticed that one strategy covered situations that the other did not, and vice versa. There were also situations that neither strategy covered. Ipsakis, Voutetakis, Seferlis, Stergiopoulos, and Elmasides (2009) do not consider the state of charge of the hydrogen storage in their control strategy. Neither do they make sure that the battery cannot be over-charged. One function that is included in their strategy is that the fuel cell will run at full power and charge the battery when the battery SOC is low. This is not included in the strategy of Brka, Al-Abdeli, and Kothapalli (2015). However, the latter strategy includes considering the energy level in the hydrogen storage as well as preventing both the battery or hydrogen storage from being over-charged or over-discharged.

Neither of the strategies use the double state of charge limits for the battery that are used in the energy management strategy for this thesis. The concept is displayed in figure 14. The inner limits allow the system to prioritise charging and discharging the battery within a small interval of SOC, 65-75%, which prolongs the battery lifetime. Thereafter the electrolyser or fuel cell will take over balancing the power in the grid. If the power of the fuel cell or electrolyser is not enough to cover the load or surplus power, the battery can discharge or charge further, until the outer limits are reached, 25% and 85%. Avoiding power discrepancy is prioritised higher than preserving the battery lifetime. How the SOC_B limits are set is explained in section 6.2.2.
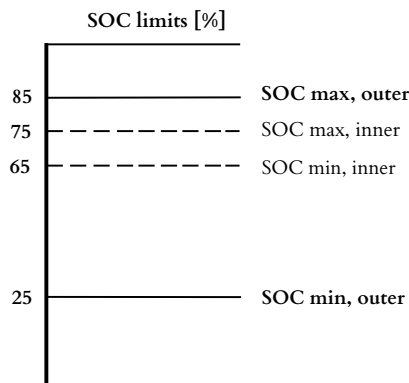
Figure 14: Battery SOC constraints utilised in the operation strategy.

The strategy with double state of charge limits is similar to a different control strategy called hysteresis band control. This strategy is deemed as simple and reliable and is implemented in several real systems (Valverde, Rosa, et al. 2016). A hysteresis band control strategy was written for this thesis, implemented in the system and tested. However, the hysteresis band strategy does not, for example, prevent the electrolyser from running at the same time as the battery is discharging. Thus, this operation strategy was discarded in favor for the above mentioned energy management strategy.

Figure 15 shows an overview of all possible management situations that can occur and that will be dealt with by the operation strategy constructed for this thesis. Below follows a description of the figure from left to right. A detailed block diagram of this rule-based energy management strategy can be found in Appendix A.
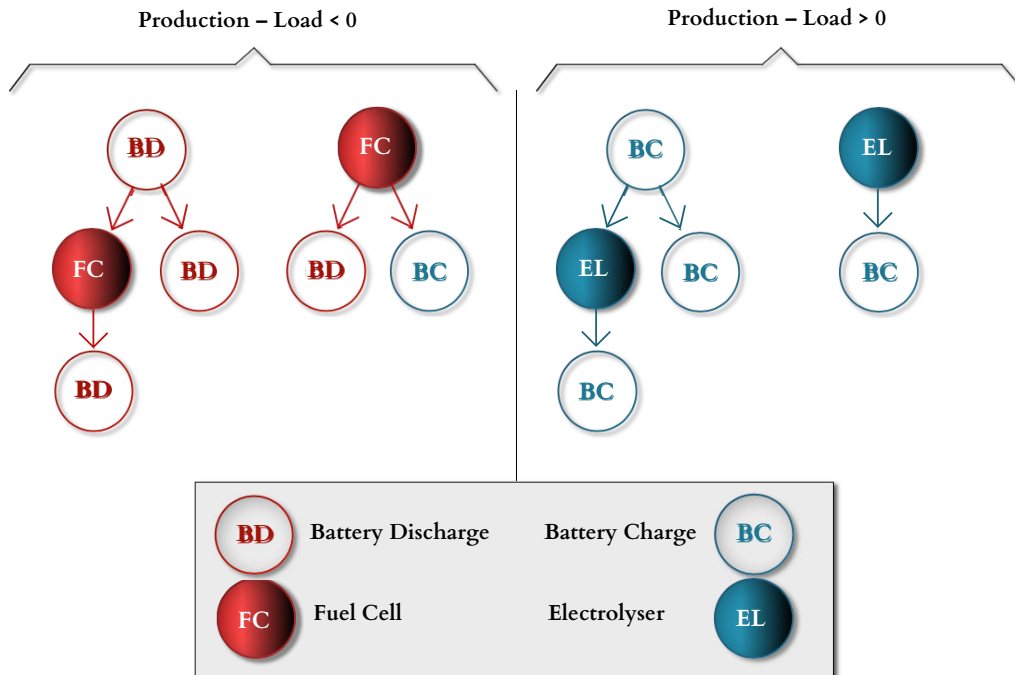
Figure 15: Overview of Energy Management Strategy designed for the simulations.

The left side of figure 15 shows the situations when the load power demand is larger than the power production. These management strategies are implemented to deal with negative power discrepancies. Depending on the SOC in the battery either the battery will discharge or the fuel cell will start running. The right side shows the situations when the power production is larger than the load power demand. These management strategies are implemented to deal with positive power discrepancies. In these situations, the SOC in the battery will determine if the battery will charge or if the electrolyser will run.

Left side, first column, starting with BD, Battery Discharge
If SOC_B is above the minimum inner limit the battery will discharge. If this is enough to meet the power demand, no further action will be taken (BD). If discharging the battery is not enough to meet the demand the fuel cell will run. If this action is enough to meet the demand the process will stop here (BD:FC). If the demand is still not met the battery can discharge further, if the minimum outer limit of SOC_B allows (BD:FC:BD). In some cases the fuel cell cannot run, for example the power demanded could be below the minimum power of the fuel cell or the SOC_H could be too low. Then the battery can discharge further, if the minimum outer limit of SOC_B allows (BD:BD). In the two latter cases, the discharge power from both battery discharge steps will be added.

Left side, second column, starting with FC, Fuel cell
If SOC_B is below the minimum inner limit, the fuel cell will run. If the limit of SOC_H allows, the fuel cell will run at its rated power and use the residual power, after meeting the load demand, to charge the battery (FC:BC). If running the fuel cell is not enough to meet the load power demand the battery can discharge further, if the minimum outer limit of SOC_B allows (FC:BD).

Right side, first column, starting with BC, Battery Charge

If SOC_B is below the maximum inner limit the battery will charge. If this is enough to meet the power surplus no further action will be taken (BC). Else the electrolyser will start. If this is enough to meet the power surplus the process will stop here (BC:EL). If it is not enough, the battery can be charged further, if the maximum outer limit of SOC_B allows (BC:EL:BC). In some cases the electrolyser cannot run, for example the required power could be lower than the minimum power or the SOC_H could be too high. Then the battery can charge further, if the maximum outer limit of SOC_B allows (BC:BC). In the two last cases the battery charging power from both steps will be added.

Right side, second column, starting with EL, Electrolyser

If SOC_B is higher than the maximum inner limit the electrolyser will run. If this is enough to cover the power surplus no further action will be taken (EL). Otherwise, the battery can charge, if the maximum outer limit of SOC_B allows (EL:BC).

6   MODELLING AND SIMULATION METHOD

This chapter describes how the model for the simulations is constructed. First the software tools are presented. The subsequent section explains how each component is modelled, which parameters are used and how their values are chosen. In section three, general assumptions are presented and motivated. Thereafter the performance indicators, selected for the performance analysis, are described. Finally the simulation strategy is explained

6.1   Simulation tools

The model is coded in Python, using the scientific python development environment Spyder. Microsoft Excel is used for input data and for saving result data. A python extension for grid models, Pandapower, is used to conduct power flow calculations of the grid (Thurner et al. 2017).

The Pandapower library contains several predefined datastructures and elements, some of which are used in the model. Buses and Lines are used to build up the grid. The element External grid is mandatory for the program to work and is used to model the battery. For modeling loads, power generation sources and the hydrogen storage components the elements Load and Static Generator are utilised. These components contain a parameter called scaling, which is used to control how much of the rated power, for load or generation, is used. Scaling is calculated according to equation 31.

$$scaling = \frac{P_{actual}}{P_{rated}} \tag{31}$$

6.2   Parameters and models

6.2.1   Hydrogen storage system

The hydrogen storage solution is made up of three parts: the electrolyser, the storage tank and the fuel cell.

Electrolyser
The electrolyser is modelled with the grid component Load. The rated power is set when implementing the model and the variability is acquired by using the load model parameter scaling, equation 31. The parameters are shown in table 3. The electrolyser unit has a maximum power of 40 kW (Areva 2014) and a minimum power of 10 kW. The minimum power is calculated as 25% of the maximum power according to Cau et al. (2014). To run simulations with higher electrolyser power the rated power of several electrolyser units are added, as if they are connected in parallel.

47

The minimum power remains 10 kW regardless of the number of units in the simulation. The efficiency of 70% is an average value based on PI and Newton (2015) who claim 72% and H. Zhang et al. (2012) who claim 68%. When the calculations are performed an efficiency of 95% for the inverter is used (Brka 2015). The hydrogen gas compressor efficiency is estimated using methods proposed by Pellow et al. (2015). These efficiencies are multiplied with the electrolyser efficiency.

Table 3: Electrolyser

Parameter	Symbol	Value	Unit	Reference
Maximum power	$P_{EL_{max}}$	40	$kW/unit$	(Areva 2014)
Minimum power	$P_{EL_{min}}$	10	$kW/unit$	(Cau et al. 2014)
Efficiency	η_{EL}	70	%	(H. Zhang et al. 2012), (PI and Newton 2015)

Fuel cell
The fuel cell is modelled with the grid component Static Generator. The rated power is set when implementing the model and the variability is acquired by using the generator model parameter scaling, equation 31. The parameters of the fuel cell are shown in table 4. The maximum power of a fuel cell unit is set to 20 kW based on devices produced by PowerCellSwedenAB (2017). The minimum power of 10 kW per unit is based on larger fuel cell units of 100 kW, as these can run at the lowest power 10% of maximum. This is approximated from an efficiency-power curve made for the 100kW-units, supplied by Per Ekdunge from PowerCell Sweden AB, see appendix B. Below 10% of the rated power the efficiency is too low. This is similar to the results of Cau et al. (2014). To run simulations with higher fuel cell power the rated power of several fuel cell units are added, as if they are connected in parallel. The minimum power remains 10 kW regardless of the number of units in the simulation. The efficiency of 50% is approximated from the above mentioned efficiency-power curve. It is also supported by Eriksson and Gray (2017) and Pellow et al. (2015). When the calculations are performed, an inverter efficiency of 95% is multiplied with the fuel cell efficiency.

Table 4: Fuel cell

Parameter	Symbol	Value	Unit	Reference
Maximum power	$P_{FC_{max}}$	20	$kW/unit$	(PowerCellSwedenAB 2017)
Minimum power	$P_{FC_{min}}$	10	$kW/unit$	(Cau et al. 2014)
Efficiency	η_{FC}	50	%	(Eriksson and Gray 2017), (Pellow et al. 2015)

Hydrogen storage tank
The hydrogen storage is made up of tanks with a pressure of 200 bar and its parameters are shown in Table 5. The storage size is kept constant through all simulations for the performance analysis, 1 GWh, 1887 m^3. It is over-dimensioned in order to avoid becoming full or empty, thus letting the fuel cell and electrolyser maximum power be the limiting factors. The model calculates how much of the storage space that is unused. The state of charge is calculated in the same way as for the battery storage. The control strategy checks the state of charge to decide if maximum power of the fuel cell or electrolyser can be used. The maximum state of charge is 100% and the minimum state of charge is 10% (Brka 2014). The initial SOC of the hydrogen tank for the performance analysis is set to 30%, which is lower than half the tank. This is done since the starting point of the time series used for the simulation is in the end of February. This

date is in the middle of the winter, why it is likely that the hydrogen storage would be closer to empty than full.

Table 5: Hydrogen tank

Parameter	Symbol	Value	Unit	Reference
Capacity	C_H	1	GWh	
Volume	V_H	1887	m^3	
Maximum State of charge	$SOC_{H_{max}}$	100	%	(Brka, Al-Abdeli, and Kothapalli 2015)
Minimum State of charge	$SOC_{H_{min}}$	10	%	(Brka, Al-Abdeli, and Kothapalli 2015)
Initial State of charge	$SOC_{H_{init}}$	30	%	

6.2.2   Battery storage

In the grid model the battery is represented by the compulsory component for the External grid. A grid model cannot work without this component. The external grid component acts as a slack bus, meaning it balances the grid through taking care of the residual load. The power allocated at the external grid component comprise the battery power, the grid loss power and possible deficit or excess powers. The charge and discharge powers of the battery, in addition to the deficit and excess powers, are determined through the energy management strategy described previously. This allows the grid loss power to be calculated from the external grid component.

In table 6 the parameters of the battery model unit are shown. It has rated values of charge and discharge power, 833 kW and 1332.8 kW, and maximum capacity per unit, 333.2 kWh. These values are based on the real system installed at Simris, which is made up of 7 Samsung 192S 1P racks (E.ON 2016). To run simulations with higher battery capacities the capacities of several units are added, as if they are connected in parallel. The maximum charge power and discharge power remain the same regardless of the number of units, as if they are connected to the same inverter. The battery capacity and state of charge is not included directly in the grid model but are calculated separately.

The state of charge determines the energy available to charge or discharge the battery. If the level is close to the maximum or minimum states of charge respectively, charging or discharging at rated power might not be possible. This is calculated by the control strategy. The inner levels of minimum and maximum SOC, 65% and 75%, are set to preserve the battery lifetime. Lithium batteries cycled within these limits are found to last longer (Xu et al. 2016). However, these limits can be passed if deficit or excess power is thus avoided. The outer levels of SOC, 25% and 85%, are based on an average of what is used by Xu et al. (2016) and Kurzweil (2015). How the SOC limits are set can have a significant impact on the performance of similar systems (Ulleberg 2004). The initial SOC is set between the inner limits, 70%.

The battery efficiencies for charging and discharging are based on the round trip efficiency of 95% (E.ON 2016). It is assumed that the charging and discharging efficiencies are equal and thus calculated as the square root of the round trip efficiency. The converter and inverter efficiencies are assumed to be 95% and are multiplied with the other efficiencies for the simulations.

Table 6: Battery

Parameter	Symbol	Value	Unit	Reference
Rated charge power	$P_{BC_{rated}}$	833	kW	(E.ON 2016)
Rated discharge power	$P_{BD_{rated}}$	1332.8	kW	(E.ON 2016)
Charge efficiency	η_{BC}	97.47	%	(E.ON 2016)
Discharge efficiency	η_{BD}	97.47	%	(E.ON 2016)
Capacity	CAP_B	333.2	$kWh/unit$	(E.ON 2016)
State of charge max outer	$SOC_{B_{max_2}}$	85	%	(Xu et al. 2016), (Kurzweil 2015)
State of charge min outer	$SOC_{B_{min_2}}$	25	%	(Xu et al. 2016) , (Kurzweil 2015)
State of charge max inner	$SOC_{B_{max}}$	75	%	(Xu et al. 2016)
State of charge min inner	$SOC_{B_{min}}$	65	%	(Xu et al. 2016)
State of charge initial	$SOC_{B_{init}}$	70	%	

6.2.3   Photovoltaics and wind power plant

Hourly values of the power production from the wind turbine and the solar power plant are the first part of the indata for the simulations. The two plants are modelled separately. Each is represented by a Static Generator connected to the same bus, just like they are connected in the real grid. The rated powers are the same as in reality, 500 kW and 440 kW respectively, and the parameter scaling provides the variability, equation 31. How the power from wind turbine and solar power plant varies can be seen in figures 1 and 2, chapter 2.

6.2.4   Electricity consumption

Hourly values of the power consumption in the LES are the second part of the indata for the simulations. On each bus in the grid the maximum load, active power, has been registered. These values are used as the rated load power of the Load components used to model all the loads connected to each bus. An approximated value for reactive power of 33% of the rated active power is added to each load, corresponding to a power factor of $\cos\phi = 0.95$. The variability of the active and reactive loads in each time step is controlled by the parameter scaling, see equation 31, where P_{rated} is the sum of all the loads. How the total load, P_{actual}, varies can be seen in figure 4 in chapter 2.

6.2.5   Grid

The cables, transformators and buses in the model, as well as corresponding dimensions, are based on those existing in the real grid in Simris. The external grid connection that exists in reality is excluded for this thesis since an isolated mode of operation is simulated. The External grid

element is instead connected to the bus where the battery storage system is located. The grid has losses, which show in the external grid component. The grid losses are calculated as power in the external grid subtracted by power of the battery and eventual deficit or excess powers, equation 32.

$$P_{gridloss} = P_{externalgrid} - P_{BC} - P_{BD} - P_{excess} - P_{deficit} \tag{32}$$

6.2.6   Economic parameters

Table 7 shows the values used for the economic calculations of the project. Costs are stated in SEK and have sometimes been converted from other currencies.

Table 7: Economic Parameters

Parameter	Symbol	Value	Unit	Reference
Electrolyser				
Capital cost	$C_{Cap_{EL}}$	15100	SEK/kW	(Niakolas et al. 2016)
Lifetime	Y_{EL}	10000	*run hours*	(Valverde, Pino, et al. 2016)
O&M cost	$r_{O\&M_{EL}}$	5	% of C_{Cap}/year	(Mittelsteadt et al. 2015)
Fuel cell				
Capital cost	$C_{Cap_{FC}}$	44600	SEK/kW	(Niakolas et al. 2016)
Lifetime	Y_{FC}	8000	*runhours*	(Niakolas et al. 2016)
O&M cost	$r_{O\&M_{FC}}$	5	% of C_{Cap}/year	(Eichman, Townsend, and Melaina 2016)
Hydrogen tank				
Capital cost	$C_{Cap_{HT}}$	3800	SEK/m^3	(Ulleberg, Nakken, and Ete 2010)
Lifetime	Y_{HT}	20	*years*	(Y. Zhang et al. 2017)
O&M cost	$r_{O\&M_{HT}}$	2.5	% of C_{Cap}	(Ulleberg, Nakken, and Ete 2010)
Battery				
Capital cost	C_{Cap_B}	17900	SEK/kWh	(E.ON 2016)
Lifetime	Y_B	20	*years*	(E.ON 2016)
O&M cost	$r_{O\&M_B}$	0.5	% of C_{Cap}/year	(Y. Zhang et al. 2017)
Additional				
Interest rate	i	5	%	(Nelson, M. Nehrir, and C Wang 2006)

6.3   Assumptions

- The ramp rate up and down of all the components; battery, electrolyser and fuel cell are assumed to be instantaneous. In reality they all have ramp rates on the scale of milliseconds to seconds (Eichman, Harrison, and Peters (2014), Per Ekdunge PowerCell AB (2017), Byrne et al. (2017)), but since this investigation uses time steps of 1 hour these can be neglected.

- The primary control of power and frequency in the microgrid is conducted by the battery storage system.

- The efficiencies of the components in the system are assumed to be constant, regardless of operation mode and working condition, such as power level or temperature.

- The self discharge of the battery and hydrogen storage are neglected.

- The data selection, from February 23rd 2015 to February 22nd 2016, is assumed to be representative.

- The compressor required to compress the gas further between the electrolyser and the hydrogen storage tank is included by multiplying a factor with the efficiency of the electrolyser.

- The minimum power of the electrolyser and the minimum power of the fuel cell are based on a percentage of the smallest corresponding unit in the model.

- Environmental control, e.g. temperature and air humidity, is assumed to be maintained to keep acceptable working conditions for the storage components, but is not included in the calculations.

- The lifetime of components are assumed constant regardless of operation characteristics e.g. number of starts/stops and cycles.

6.4   Performance indicators

This subsection describes the performance indicators used in the performance analysis. Firstly, the use of these parameters is motivated and then a description of how each is calculated and included in the model follows.

As Valverde, Pino, et al. (2016) mention there is a lack of standard definitions and use of performance indicators for hydrogen and battery storage systems in different operation modes. However, one that appears in several articles is LPSP or Loss of Power Supply Probability. It describes the reliability of the system, that is how well the systems covers the demand for power. This is the primary function of the system. (Nelson, M. Nehrir, and C Wang 2006) (Yang et al. 2008) (W. Zhou et al. 2010) (Luna-Rubio et al. 2012) (Brka, Al-Abdeli, and Kothapalli 2015) (Dong, Y. Li, and Xiang 2016). This is very similar to GSD, Grid Supplied Demand, that Valverde, Pino, et al. (2016) suggest as their primary performance indicator.

In the study of Brka, Al-Abdeli, and Kothapalli (2015) a performance indicator called EE, Excess of Energy, is used. It describes how often the storage system cannot receive all renewable energy that is produced in the system. The authors conclude that EE should not be used as criteria for optimisation as of todays situation, since hydrogen devices are very expensive. But it might be important in the future and still interesting to look at. EE is very similar to the performance indicator REG, Renewable Exported to Grid, used by Valverde, Pino, et al. (2016).

When considering economic performance, several studies use NPV, Net Present Value (Brka, Al-Abdeli, and Kothapalli 2015) (W. Zhou et al. 2010) (Luna-Rubio et al. 2012), LCOE, Levelised Cost of Energy (W. Zhou et al. 2010) (Luna-Rubio et al. 2012), ACS, Annualised Cost of System (Nelson, M. Nehrir, and C Wang 2006) (Yang et al. 2008) (Luna-Rubio et al. 2012) (Dong, Y. Li, and Xiang 2016). Valverde, Pino, et al. (2016) suggest splitting the cost into several parts, overlooking for example the operation and maintenance costs for each part separately. This study uses ACS. However, the economic analysis of this study is only meant to present a relative cost estimation for comparing different configurations of energy storage in the system. Thus the figures of the economic analysis should only be considered as relative measurements, not an exact price for installing the system.

The performance indicators showing electrolyser and fuel cell starts and stops are important since these factors have an impact on the lifetime of the components. Valverde, Pino, et al. (2016) suggest looking at these factors as well as the run time for each component. This study looks at the number of starts and stops and at runtime. The run time is used to calculate the lifetime of the components. The battery cycles are considered as well since these have an impact on battery lifetime.

Loss of Power Supply Probability
The LPSP is calculated by dividing the time with deficit power with the total simulation time, see equation 13. For each time step in the simulation, one hour, the deficit power is stored in an array which has zero as default value. Calculating the number of array positions, which have a value other than zero, gives the number of hours with power deficit.

LPSP is the key performance indicator of this performance analysis. It is used to direct the proceeding of simulation setups. When LPSP equals zero the system experiences no deficit power during the simulation. However, according to Dong, Y. Li, and Xiang (2016) an acceptable level of LPSP in a stand-alone hybrid system is <0.1%. This corresponds to less than nine hours per year of power shortage in the grid. For the simulation proceedings this means that when early simulations reach above LPSP = 0.1% the configuration is changed no further in that direction.

Excess Energy
The excess energy, EE, of the system is calculated similarly to the LPSP, see equation 14. For each simulation time step the excess power is stored in an array. The number of array positions with values other than zero is calculated and thereafter divided by the total number of time steps, i.e. number of hours.

ACS
The annualised cost of system, ACS, is calculated according to equations 15-20, using the parameters in table 7, Economic parameters. Since the lifetimes of the electrolyser and the fuel cell are given in run hours the lifetime in years is calculated by dividing the lifetime with number of run hours per year. The O&M-cost of the hydrogen storage is not presented in % of capital cost per year, as are the others. However, this is accounted for in the economic calculations.

Loss ratio
The loss ratio is the sum of all losses, relating to conversion efficiencies in storage systems and grid transmission, divided by the total energy produced. The losses in the electrolyser, fuel cell and battery are calculated by summarizing the product of ingoing power in each time step multiplied with one minus the corresponding efficiency, see equation 33 below. The grid losses are calculated by subtracting the calculated battery power and the deficit and excess powers from the slack bus power in each time step.

$$P_{loss} = P_i \cdot (1 - \eta_i) \tag{33}$$

Electrolyser and Fuel cell: runtime, start and stop
The runtime fractions for the fuel cell and electrolyser are calculated by summarising all the time steps when they are running and dividing by the total number of time steps.

The number of electrolyser starts is calculated during the simulation. The number of stops is assumed to be equal to the number of starts as it can only be one unit smaller. If the power of the electrolyser was equal to zero in the previous step but is above zero in the present step the number of starts is increased by one.

The number of fuel cell starts is calculated similarly to the number of electrolyser starts. During the simulation the number of starts is increased by one if the fuel cell power is above zero in the present step and was equal to zero in the previous step.

Battery cycles
The number of battery cycles is calculated by summarizing the energy level increases and decreases respectively into complete total fillings and drainings of the battery and calculating the number of these. This way of calculating battery cycles might not be very true to the actual physics and chemistry of the aging mechanisms of lithium ion batteries. Han et al. (2014) use more complex methods to describe the aging of batteries, which are out of the scope of this thesis. However, the method described above was found on a web-page describing how to calculate the battery cycles of lithium ion batteries in computers (Page 2015). It is simple and provides a relative measurement, which is sufficient for this work.

6.5   Simulation strategy

6.5.1   Energy balance

Before conducting the performance analysis to investigate the behaviour of the system, energy balance must be achieved. This is done by altering model parameters to find an appropriate set of parameter values, which gives a simulation result showing that the final state of charge in the hydrogen storage is on the same level as the initial. A starting point for the performance analysis, where LPSP equals zero, is found by altering the parameters further.

6.5.2   Performance analysis

The performance analysis is meant to investigate how the performance of the system varies when the sizes of battery and hydrogen storage systems are varied. To visualise this the rated power of the hydrogen storage system is placed on the x-axis of a diagram and the capacity of the battery storage is placed along the y-axis, see figure 16. This type of diagram is generated for each of the key performance indicators (KPI) described above.
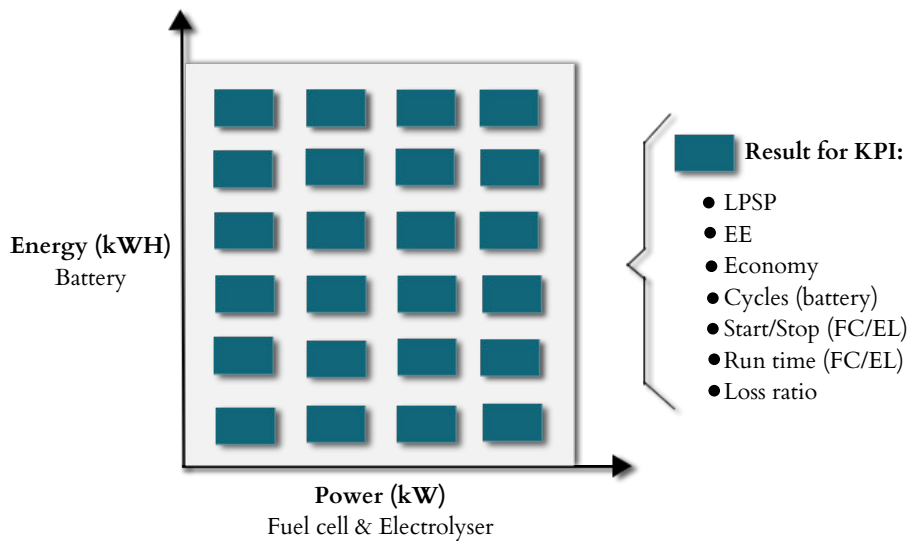

Figure 16: Performance analysis: strategy and shape of results

The performance analysis is conducted with the top right corner as starting point. The starting point is found through adjustments of several parameters of the system, as is described in chapter 7.1. While keeping the rated power of the hydrogen storage system constant, the capacity of the battery system is systematically decreased with unit steps until the battery size is reduced to one battery unit, 333.2 kWh. Then the parameters are reset to the values at the starting point, in the top right corner. While keeping the battery capacity constant, the rated power of the hydrogen storage system is systematically decreased with unit steps until LPSP>0.1% is reached. Thereafter simulations are performed for every combination of battery capacity and hydrogen system power in the mesh that the previous simulations define.

6.5.3   Nominal storage configuration

A nominal storage configuration is chosen from the results of the performance analysis. This configuration is used in the extended analysis.

6.5.4   Extended analysis

In order to evaluate the model settings, two parameters are chosen and altered. One simulation is run for each of the parameters and the results are compared to the original, nominal, simulation with the same input parameters of battery capacity and fuel cell and electrolyser power.

7   SIMULATIONS

In this chapter the results attained from the simulations are presented. Section 1 focuses on the results from the first part; attaining energy balance in the system. The results of the performance analysis simulations are displayed in section 2. In the last section, additional results are presented. The results are analysed in chapter 8.

7.1   Energy balance

This section describes how several parameters of the model are altered to find a relevant starting point for the performance analysis. The input parameters of the seven simulations described below can be found in table 8. The parameter values changed between the simulations are displayed bold text in the yellow cells.

Table 8: Energy balance simulations

Simulation	P_W [kW]	P_{EL} [kW]	P_{FC} [kW]	CAP_H [MWh]	$SOC_{H_{init}}$ [%]
1	500	400	400	500	55
2	500	400	400	500	**90**
3	**1000**	400	400	500	**30**
4	1000	**800**	400	500	30
5	1000	800	400	**750**	30
6	1000	**1200**	**600**	750	30
7	1000	1200	600	**1000**	30

The initial size of the hydrogen storage is estimated from the cumulative sum of power discrepancies seen in figure 6, the difference between the maximum and minimum values. The initial values of maximum power of the electrolyser and fuel cell are set equal since the maximum power discrepancies, seen in figure 5 , positive and negative, are almost equal. The initial battery size is set to six battery units, 1999.2 kWh, which enables the battery supply the grid at full load for two hours. The rated power of the solar power plant is kept constant, at 440 kW, throughout the simulations. In simulation 3 the rated power of the wind power production doubles as a second wind turbine is added.

The results from the seven simulations are shown in seven sets of two figures. The figures to the left in the figure sets, figures a, show how the power discrepancy, deficit power and excess power vary over the simulation period. The figures to the right, figures b, show the variation of state of charge in the battery and hydrogen storage over the same period. The simulations are referred to according to their number in table 8.

Figure 17 shows the results from simulation 1. It can be seen that the initial SOC in the hydrogen storage, set to 55%, is higher than the final SOC at the end of the simulation. The hydrogen storage reaches SOC_{Hmin} at 10% already in December, figure 17b.

(a)   (b)
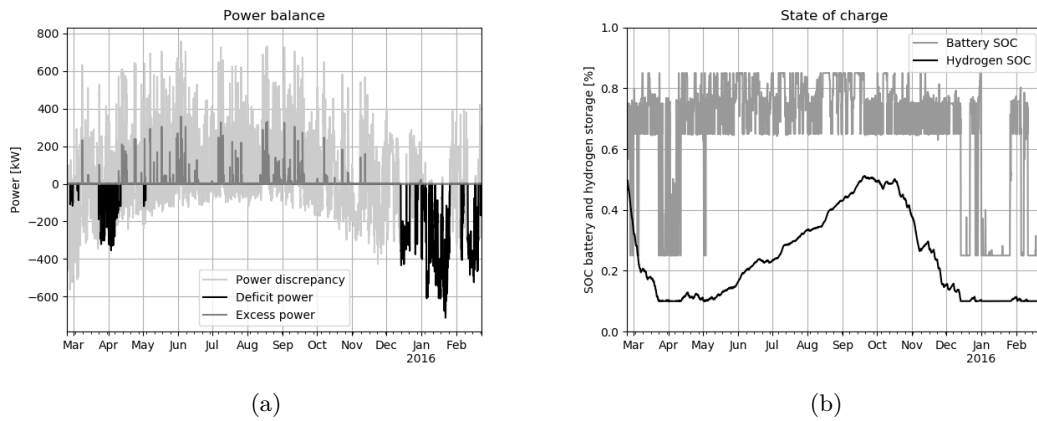
Figure 17: The results from simulation 1.

In simulation 2, seen in figure 18 , the SOC is set to 90%. This is unrealistically high, since the storage is unlikely to be almost full in the middle of the winter. But it shows that even though the storage begins at a very high level it will still be emptied a few months before the simulation period is over, figure 18b. This suggests that when including the conversion losses connected to the energy storage more production is required in the system to achieve energy balance. Energy balance, or a small surplus, over the year is a prerequisite to conduct further performance analysis of the system. Energy balance is achieved when the final value of SOC in the hydrogen storage being at the same level, or slightly above, compared to the initial level.

(a)   (b)
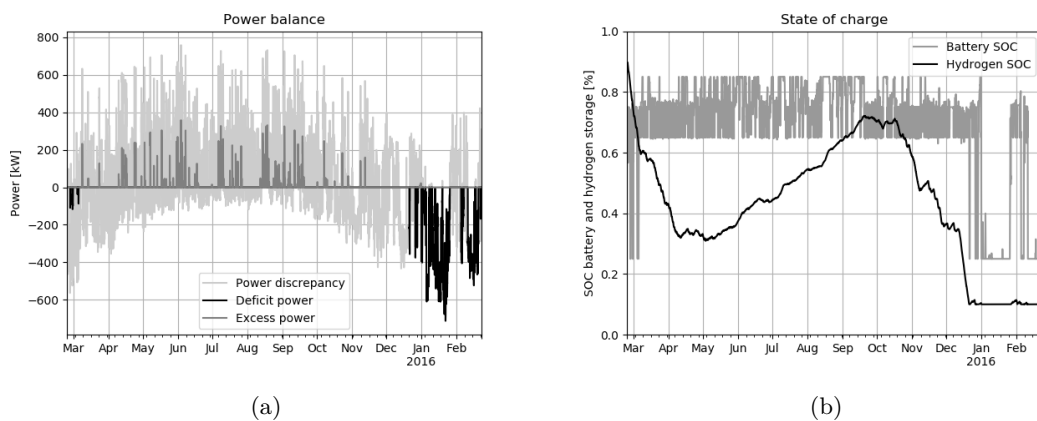
Figure 18: The results from simulation 2.

A means to achieve energy balance is to increase the rated power of any of the generation sources. In simulation 3, figure 19, the wind power production has been doubled, as an identical wind turbine is added to the original one. The SOC in the hydrogen storage has been set to 30%, as it is reasonable that the storage is closer to empty than full at the end of February. The solar plant produces very little during the critical months, November to February, as can be seen in figure 2. However, the wind power production is fairly evenly distributed over the year, figure 1. Another argument for choosing to increase the wind power production, is that it is better to be able to use the power at once than storing it, due to the conversion losses. The consequence of doubling the wind power production is that the initial and final SOC_H come closer to each other, figure 19b.

(a)   (b)
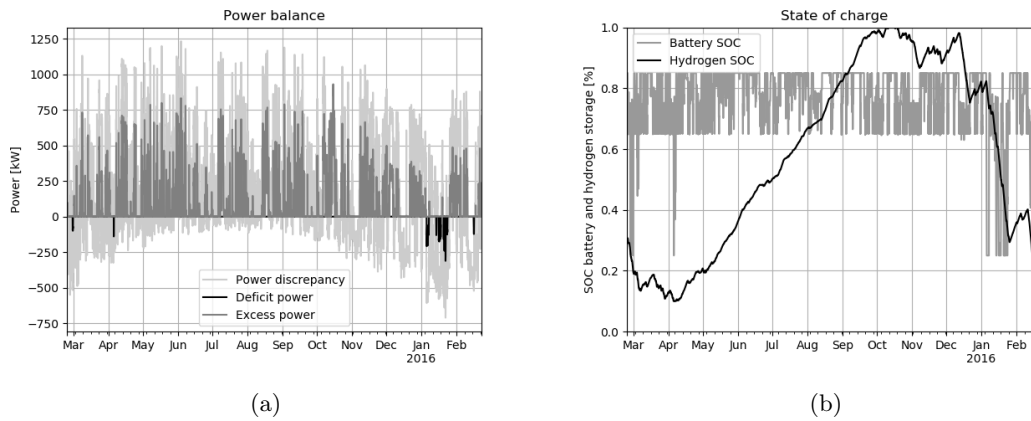
Figure 19: The results from simulation 3.

In simulation 4, seen in figure 20, the maximum power of the electrolyser has been doubled in order to match the new, higher production. This means that it is twice as high as the maximum fuel cell power. It can be seen in figure 20a that there is still excess and deficit power, but the initial and final SOC_H are closer than in the previous simulation, figure 20b. Most of the excess power is resulting from the hydrogen storage becoming full in August. This is why the hydrogen storage is increased by a factor 1.5 to simulation 5.
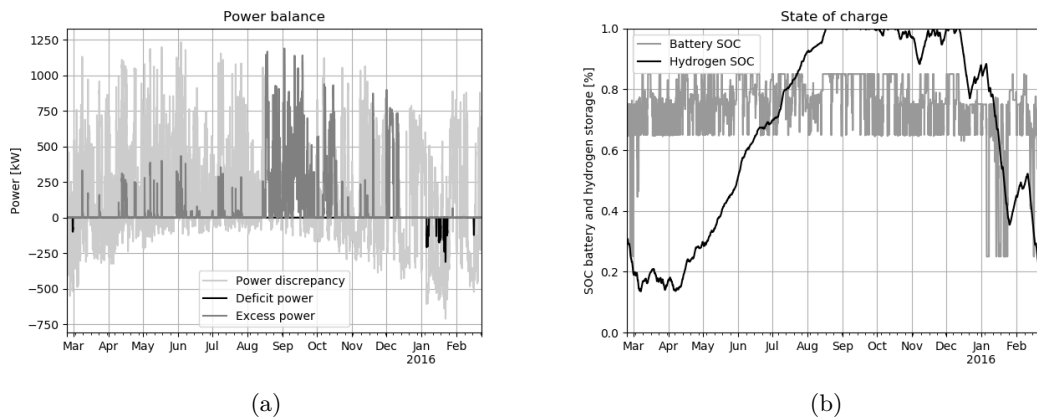
Figure 20: The results from simulation 4.

Figure 21 shows the result of increasing the hydrogen storage size, simulation 5. The final SOC_H is now above the initial, which means that energy balance is achieved with margin, figure 21b. However, there is still too much deficit power to fulfill the LPSP criteria, which can be seen on the black line below zero in figure 21a. The deficit power can be decreased by increasing the maximum power of the fuel cell. Since the ratio of the electrolyser and fuel cell maximum powers are to be maintained, the electrolyser maximum power is increased as well. It was also attempted to increase the battery capacity instead of the fuel cell power. But since the measure of increasing fuel cell power gave a better result, lower LPSP, no further attempts with increased battery capacity were made.
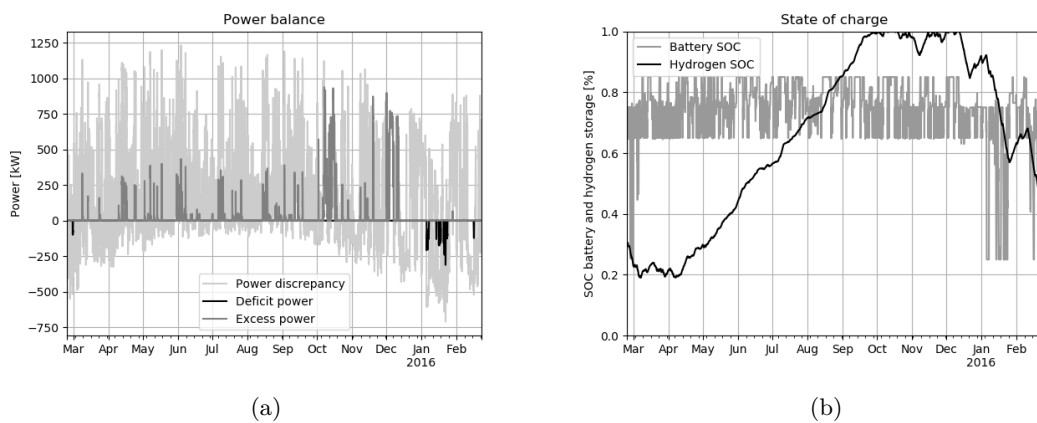
Figure 21: The results from simulation 5.

The result of increasing fuel cell and electrolyser powers by a factor of 1.5 is shown in figure 22, simulation 6. Since there is no black line in figure 22a there is no deficit power, giving an LPSP value of 0.

(a)   (b)
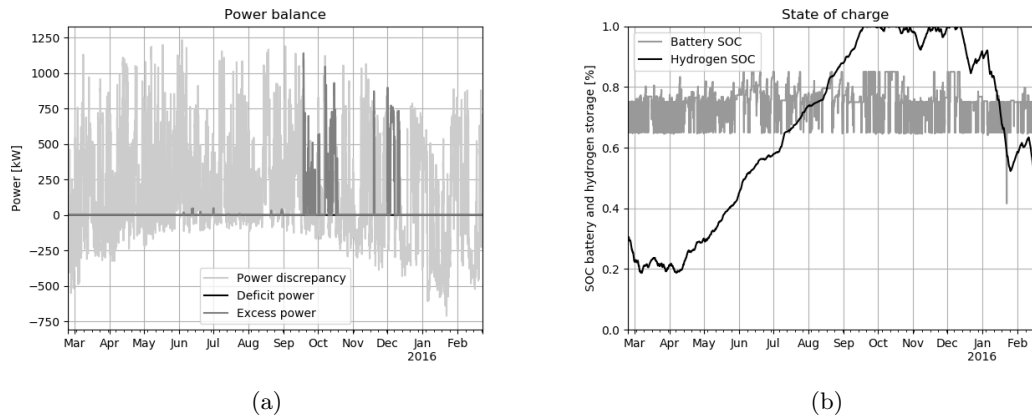
Figure 22: The results from simulation 6.

As a final step the size of the hydrogen storage is increased further, to 1 GWh, in order to accommodate more of the produced energy, simulation 7. The result of this simulation can be seen in figure 23. This simulation represents the starting point for the performance analysis.

(a)   (b)
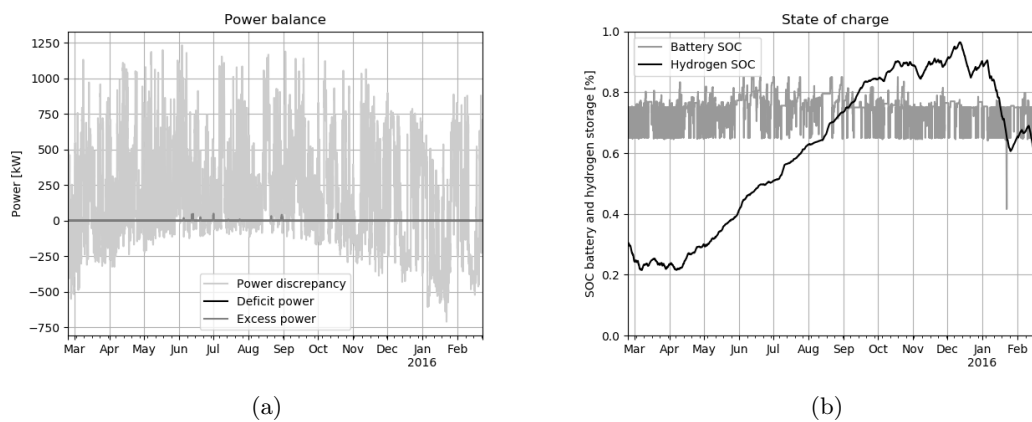
Figure 23: The results from simulation 7: the starting point of the performance analysis.

7.2   Performance analysis

In this section the results from the performance analysis are presented. Results for each performance indicator are displayed in a graph, where light colours represent low values and dark colours represent high values. The bar on the right side of the graph shows the range for the indicator values and the corresponding colour.

7.2.1   LPSP

The reliability is highest, i.e. the value of LPSP is lowest in the upper right corner of the diagram, figure 24. The reliability is lowest in the lower left corner. Hence, the reliability increases with the number of storage units used in the simulation.

The LPSP condition of 0.1% is not met when the dimensions of the battery storage range from 333.2-1999.2 kWh,1-6 battery units, with the smallest hydrogen storage size, and when dimensions of the battery storage range from 333.2-999.6 kWh, 1-3 battery units, with the next to smallest hydrogen storage size. This represents nine of the 24 simulations. Thus the majority of the configurations have an LPSP value lower than 0.1%. The highest value observed is 1.09%, which corresponds to approximately 95 hours of power deficit per year. The smallest value is zero, corresponding to complete reliability.
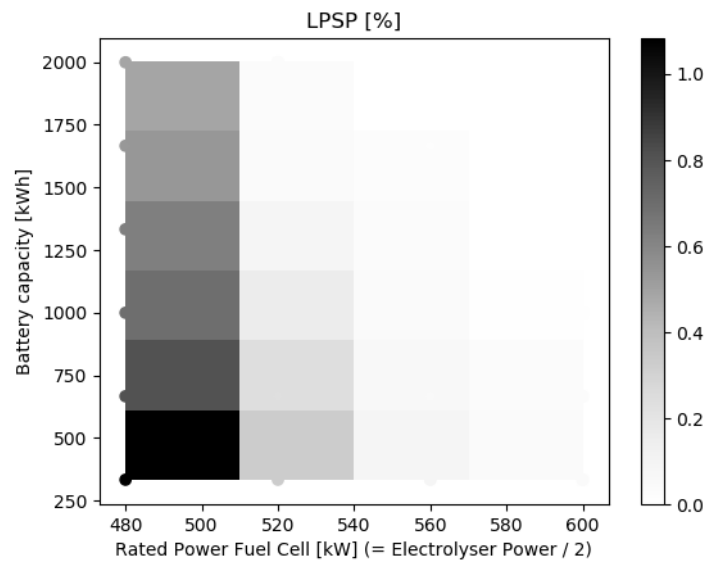
Figure 24: Loss of Power Supply Probability (LPSP) in percent for different energy storage configurations.

7.2.2   EE

The excess energy is lowest in the upper right corner and highest in the lower left corner, figure 25. The lowest value is 0.35% which corresponds to 31 hours of excess power per year and the highest value is 5,85% which corresponds to 513 hours of excess power per year.
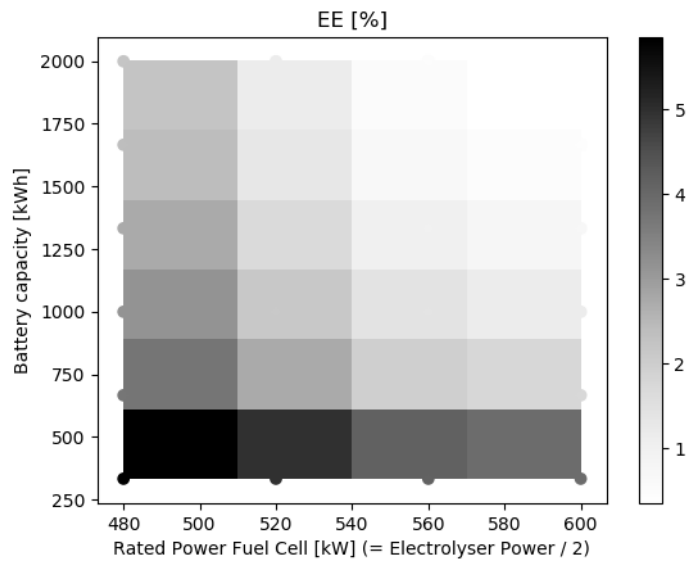
Figure 25: Excess of Energy (EE) in percent for different energy storage configurations.

7.2.3 ACS

In figure 26 it can be seen that the cost is higher when the hydrogen storage system components are larger, the right side of the diagram. The cost is highest in the bottom right corner and the trend mainly goes from left to right. For the simulations with a battery capacity of 666.4 and 999.6 kWh, 2 and 3 battery units, there is a horizontal band where the cost is reduced compared both to higher and lower battery capacities with the same number of hydrogen units. The highest ACS is 26 MSEK/year and the lowest is 19.3 MSEK/year.
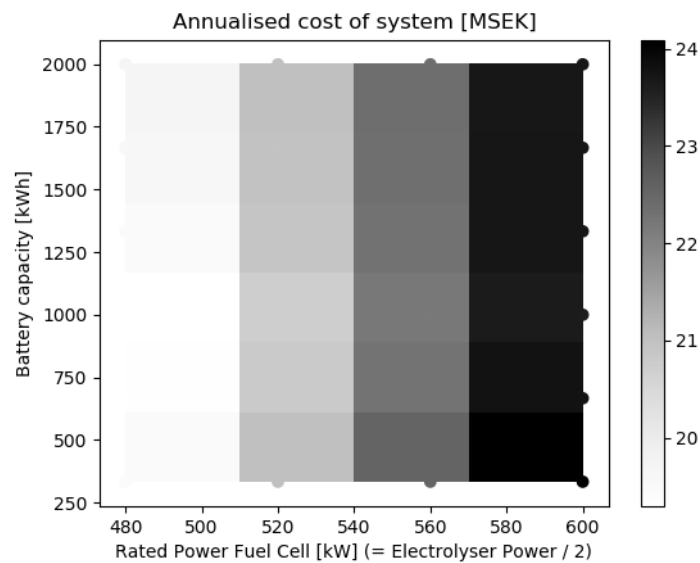
Figure 26: Annualised cost of system (ACS) in MSEK for different energy storage configurations.

7.2.4   Loss ratio

The losses are largest in the bottom right corner, i.e. when the hydrogen storage is large and the battery storage is small, figure 27. The losses are lowest in the top left corner, where the battery storage is large and the hydrogen storage is small. The highest loss ratio is 57.3% and the lowest is 56.4%. The trend is not entirely linear.
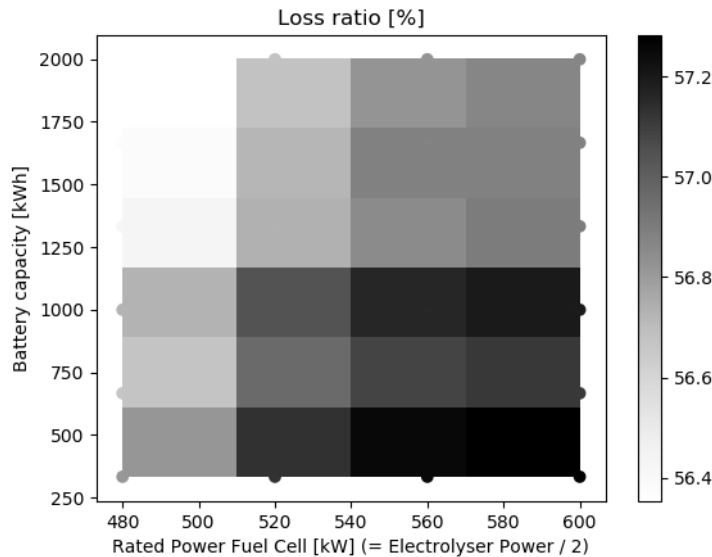
Figure 27: Power loss ratio in percent for different energy storage configurations.

### 7.2.5   Electrolyser and Fuel cell: runtime, start and stop

The coarse trend for the electrolyser start and stop is that a larger battery system gives fewer starts and stops, figure 28a. With a smaller battery system the number of starts and stops is higher. However, this trend is not linear. No trend following the size of the hydrogen storage is easily distinguished. The highest number of starts and stops is 406 times per year and the lowest is 384 times per year. This means that the configuration with the lowest number of starts and stops is 5% lower than the configuration with the highest number of starts and stops.

The coarse trend for the fuel cell is that a larger battery system gives more starts and stops, figure 28b. Smaller battery systems give fewer starts and stops. This trend is not linear. There is no clear trend following the size of the hydrogen storage. The highest number of starts and stops for the fuel cell is 383 times per year and the lowest is 295 times per year. This means that the configuration with the lowest number of starts and stops is 23% lower than the configuration with the highest number of starts and stops.

(a) Electrolyser   (b) Fuel cell
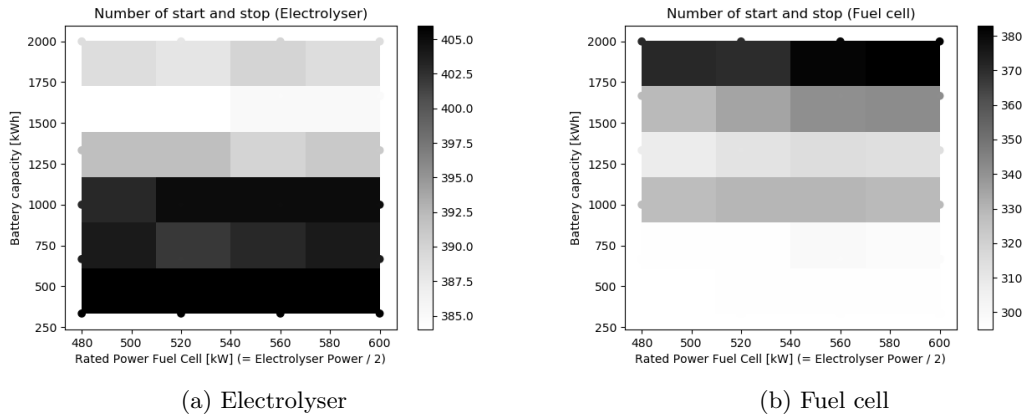
Figure 28: Number of electrolyser and fuel cell start and stop for different storage configurations.

The trend for the run times of both the fuel cell and the electrolyser is that they decrease with a larger battery capacity, figure 29. The trend for the fuel cell is linear, figure 29b. The electrolyser trend is uniform apart from having a lower run time with two battery units than with three, second and third row from the bottom, figure 29a. The run times of the electrolyser vary from 58.5 to 59.7%, which translates to a lifetime of about 1.7 years. The fuel cell run times vary between 19.2 and 28.4%, which translates to a lifetime in the range of 5.3 and 3.5 years.

(a) Electrolyser   (b) Fuel cell
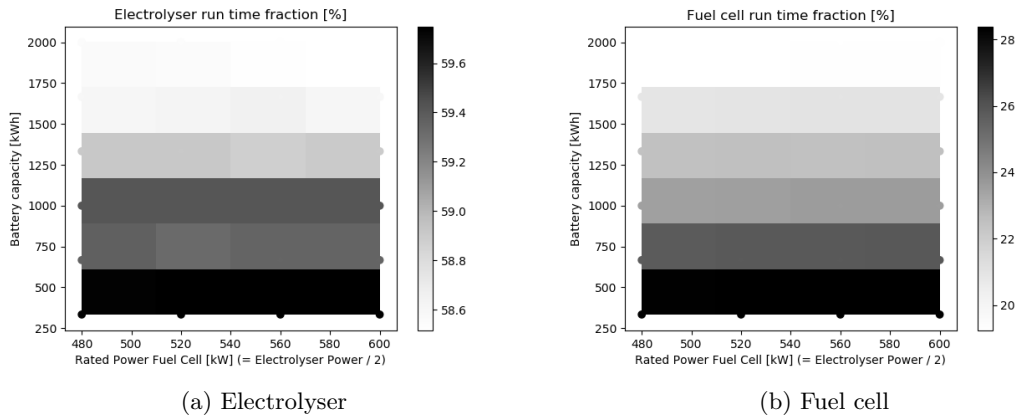
Figure 29: Electrolyser and fuel cell operation run time in percent for different storage configurations.

7.2.6   Battery cycles

There is a coarse trend for the battery cycles, following the size of the battery storage system, figure 30. When the battery storage system is larger the number of battery cycles decreases. A smaller battery system gives a higher number of battery cycles. However, this trend is not linear. There is a trend regarding the impact of the size of the hydrogen storage system, as the number

of battery cycles increases with a larger hydrogen storage. The largest number of cycles is 212 whereas the lowest number of cycles attained in a simulation was 144.
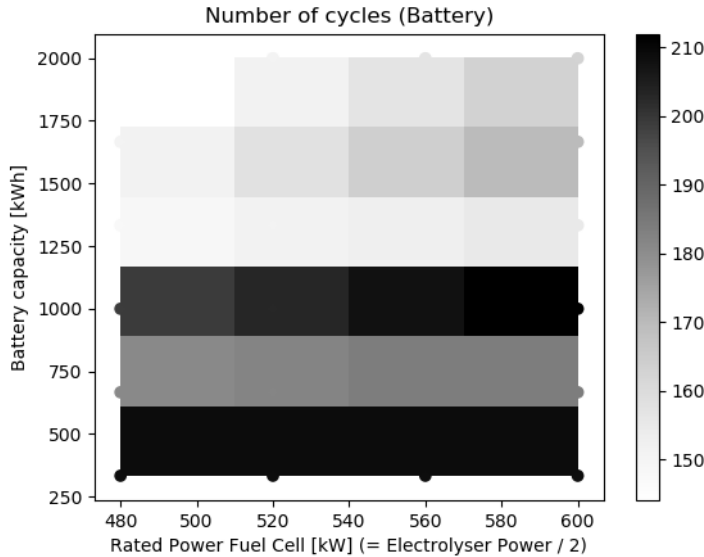
Figure 30: Number of battery cycles for different energy storage configurations.

7.3   Additional results

Other results from the simulations that are worth mentioning are: average grid loss and storage usage. The average grid loss remains the same for all 24 simulations of the performance analysis, with a value of about 4.7 kW.

The trend for the battery storage usage show that in a majority of the simulations the battery storage is used to a full extent. This implies that the outer limits for both maximum and minimum SOC are reached at least once during a simulation. But it should be noted that although the maximum SOC is reached in all simulations, the minimum SOC is not reached in all cases. In a couple of simulations, the difference between the lowest measured SOC level and the minimum SOC constraint, $SOC_{B_{min2}}$, reached as much as 16.5%. This suggests a lower utilisation of the battery storage for such storage configurations.

In contrast, the hydrogen storage is never utilised to a full extent in any of the 24 simulations. Hence, the tank is never entirely discharged to its outer minimum SOC-limit. The difference between the lowest observed SOC levels and the minimum SOC limit constitutes about 11.5% of the available storage space. This trend is consistent for all simulations. In contrast, larger variations in actual- and maximum SOC levels are deduced. The results indicate a excess in storage space ranging from 3.5 to 7 % depending on storage configuration.

8   ANALYSIS

This chapter contains the analysis of the results. In the first section of this chapter the results from the performance analysis simulations are analysed. In section 2, the performance of the different storage configurations is compared to determine a nominal storage configuration. This configuration serves as a reference case for the extended analys, which is presented in section 3.

8.1   Performance analysis

8.1.1   LPSP and EE

As can be seen in figure 24 the LPSP is lower when both the hydrogen and battery storage systems are larger. This means that isolated microgrids comprised of larger storage systems, i.e., more storage units, are more likely to be able to cover all the loads and attain a higher grid reliability. In the figure it might seem as if the size of the hydrogen system has a higher impact on reliability than the size of the battery system. However, this is very difficult to decide. Since the units of battery system and hydrogen system were shaped independent of each other they are difficult to compare. In addition, the y- and x-axis have different units since battery storage, y-axis, is represented with regards to its energy capacity whereas the hydrogen storage, x-axis, is represented through the fuel cell and electrolyser power level.

The trends showing in the figure for LPSP are similar to those showed in figure 25 displaying the results for EE. As for LPSP, the value for EE is lower with a larger storage system. The hydrogen storage is most probably over-dimensioned in this configuration in accordance with the results of storage usage, see section 7.3. These results verify a consistent redundancy in hydrogen storage space throughout the simulations. Hence, it is mainly the maximum power of the electrolyser and the capacity of the battery that limit the ability to store any surplus electricity.

8.1.2   ACS

The annualized cost of system, figure 26, is mainly dependent on the size of electrolyser and fuel cell. This is probably due to the higher investment cost, replacement cost and shorter lifetime of these components, compared to the battery. The lifetimes of the fuel cell and electrolyser are calculated through utilising the run time measurement. A shorter run time per year entails a longer lifetime in years. As can be seen in figure 29 the run time of both the electrolyser and the fuel cell are mainly dependent on the size of the battery storage system. When the battery system is larger the run times are shorter. The consequence of this is that the costs of the battery system and the hydrogen system balance each other. When the battery system is larger the cost for this naturally increases. But with the same trend the costs for the replacement of fuel cell

and electrolyser decrease, since the lifetime increases. This could be why variations of the battery storage system size seem to have little effect on the ACS, figure 26.

8.1.3   Loss ratio

The loss ratios of all the different configurations are very similar, around 56-57%, figure 27. The major part of the losses is due to conversion losses in the electrolyser and the fuel cell, since the round-trip efficiency is very low, around 33%. The coarse trend that can be observed in the figure can be explained by diminishing conversion losses when the size of the hydrogen system is reduced. Also, the larger the battery system is, the less the hydrogen system is engaged in grid operation which results in shorter run times for the electrolyser and fuel cell respectively. This allows more energy to be stored in the battery, which has significantly higher energy conversion efficiency. Thus, the lower right corner of the diagram shows configurations with the largest losses and the upper left corner shows configurations with the lowest losses. The slight decrease of loss ratio when comparing the second row from the bottom of the diagram to the ones above and below can be related to the electrolyser run time, which shows a very similar trend, figure 29a.

8.1.4   Runtime, start and stop

The runtimes for the fuel cell and electrolyser, figure 29, have similar trends: they decrease when the battery capacity increases. However, the variation of runtime for the fuel cell, 20-28%, is much larger than the variation of the electrolyser runtime, 58-60%. The starts and stops have opposite trends for the electrolyser and fuel cell, see figure 28. The fuel cell starts and stops increase with the battery capacity, while the electrolyser starts and stops decrease.

With a larger battery capacity the electrolyser is not required to participate in the power balancing process to the same extent, why its run time and number of starts and stops decrease. Hence, lowering the battery capacity entails a higher hydrogen production by the electrolyser but at the expense of more start/stop events and thus higher degradation rates and shorter lifetime.

The fuel cell run time decreases as the number of starts and stops increase. This could be due to the characteristics of the control strategy; the fuel cell has the opportunity to charge the battery, while there is no corresponding action for the electrolyser. The fuel cell can charge the battery at maximum power when the battery SOC is below the minimum, inner limit. When the battery capacity is larger it will contain more energy when it is full than a fully charged battery of lower capacity. Then the battery would be more capable of covering a load without any assistance from the fuel cell. This might result in that the fuel cell is turned off as soon as it has charged the battery, instead of continuing to run to help the smaller battery cover the load.

The increased number of starts and stops for the fuel cell when the battery capacity is larger, in addition to lower run times, suggest that it is beneficial to design a system with a low battery capacity in order to prevent degradation of the fuel cell. However, to attain effective grid operation from a system perspective other aspects need to be included. The irregularities and unclear trends in figure 28, displaying the results for number of starts and stops, are hard to analyse further as they probably arise due to the complex behaviour of the system.

8.1.5   Battery cycles

In figure 30 it can be seen that the number of battery cycles roughly decreases when the battery capacity increases. Since the power discrepancies remain the same for all simulations, a smaller portion of the battery capacity is utilised when the capacity increases. The number of battery cycles is calculated by summarising the change in energy level occurring in the battery during charge and discharge events. The outer maximum and minimum SOC limits constitute the boundaries for a complete cycle. It can also be seen in the figure that for each change in battery capacity, i.e. each row, the number of cycles decreases when the fuel cell and electrolyser maximum power levels decrease. This could be because when the fuel cell maximum power is lower the battery will reach a lower state of charge when the fuel cell charges the battery. Thus a smaller part of the battery charging cycle would be covered. There would also be less energy available for discharging, implying that a smaller part of the discharging cycle would be covered, resulting in a lower number of battery cycles.

8.2   Nominal storage configuration

Based on the results of the performance analysis presented in section 7.2, a comparative evaluation is conducted. The aim is to determine which of the simulated storage configurations is expected to provide the highest system performance. The final chosen storage configuration is referred to as the nominal case, and the results from this simulation serve as reference values for further extended analysis, see section 8.3.

Since the primary design objective is to assure a technically viable system operation with regards to reliability, all simulations with an LPSP lower than the limit of 0.1% are discarded at an initial stage. As can be seen in figure 24, the entire first column from the left is discarded, which represents all configurations with a rated fuel cell power of 480 kW. Also, three configurations of the subsequent column are rejected which are represented by battery storage capacities ranging from 333.2 to 999.6 kWh. Hence, nine of the twenty-four storage combinations are excluded in this respect.

Secondly, the remaining fifteen storage configurations are evaluated with regards to their annualised cost of system (ACS) in order select a system that operates in line with the economic objective. According to the results displayed in figure 26, storage configurations comprised of large hydrogen storage systems are associated with high costs. Thus, the storage arrangements represented by the results in the two columns on the right are not included for further analysis. This implies all storage combinations with fuel cell rated powers of 560 and 600 kW regardless of the energy capacity of the battery storage system. Thus, twelve of the remaining fifteen storage configurations are excluded concerning economic viability. In figure 31 the simulation cases discarded due to low LPSP and high ACS are visualised. Squares with a black and white texture relates to cases excluded with regards to reliability constraints, i.e. LPSP. Squares distinguished by a light grey color relates to simulations cases discarded due to high annualised cost of system, i.e. ACS.
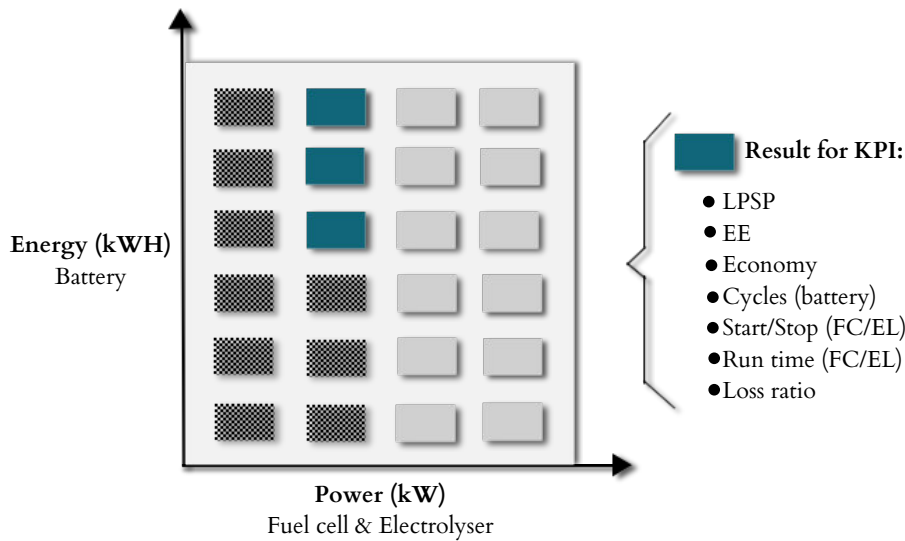
Figure 31: Visualisation of the simulation cases discarded due to low LPSP and high ACS. Squares with black/white texture relate to LPSP and light grey squares relate to ACS.

Thirdly, only three different storage combinations remain, which are more thoroughly evaluated through comparing the values attained for each performance indicator, see table 9. All configurations comprise a fuel cell with a rated power of 520 kW and electrolyser of 1040 kW. However, the battery energy capacity varies, which is utilised to differentiate the three cases in the table. The three different configurations will be referred to as case one, two and three for simplicity, starting with the lowest battery capacity. The values of the performance indicators attained for each case are compared, and the yellow cells in table 9 present the most favorable configuration for each specific indicator.

Table 9: Performance indicator results utilised in evaluation of a nominal storage configuration.

Performance indicator	C_B [kWh]= 1333	C_B [kWh] = 1666	C_B [kWh] = 1999
LPSP [%]	0.09	0.05	**0.03**
EE [%]	1.7	1.3	**1.2**
ACS [MSEK]	**20.92**	20.98	21.02
Loss ratio [%]	56.7	56.7	56.7
Electrolyser starts/stops	392	**384**	388
Fuel cell starts/stops	**312**	335	370
Electrolyser run time [%]	58.9	**58.6**	**58.6**
Fuel cell run time [%]	22.5	21.0	**19.2**
Battery cycles	**151**	158	**151**

The LPSP is the primary design parameter, and the highest reliability is obtained in case three. However, all values for LPSP are below the allowed target limit of 0.1% ranging from 0.03 to 0.09%, which translates to a probable annual time of power deficit of about 3 to 8 hours. Concerning reliability, case three should be prioritised, but as other aspects also affect the operation of the system, the remaining system performance indicators are taken into consideration.

Case three is also most beneficial with regards to the excess of energy (EE), but as this parameter is not a widely adopted performance indicator in literature, this is not prioritised in the process of selecting an appropriate system design. Also, since the loss ratio is identical for all three cases, this parameter is also disregarded in the comparison.

Case two enables more efficient operation of the electrolyser as fewer starts and stops are required. However, the difference in the number of start and stops does not differ to a great extent between the three cases. In contrast, the number of start and stops for the fuel cell varies significantly, with the lowest number attained in case one. This suggests a more efficient operation of the fuel cell and lower degradation rate resulting in a longer lifetime of the component. Also, the fuel cell run time is lower, which most probably explains the lower annualised cost of system (ACS) for case one.

Considering the above arguments, either case one or case three present the most appropriate solution. Case three might be most beneficial considering the technical objectives of reliability and reducing the excess of energy. However, this is achieved at the expense of higher annual system costs. In this thesis, an LPSP below 0.1% is considered sufficient, and thus the economic objective of the system design is prioritised secondly, which is in favor of case one. Although EE is high for case one, the cost of dumped energy might be accounted for by reducing substantial replacement costs of the fuel cell.

Conclusively, case one is selected as the nominal storage system configuration which serves as a reference case for further fine-tuning of the system performance in the extended analysis below, see section 8.3. The results describing power balance and and state of charge of the system for the nominal storage configuration is displayed in figure 32a and 32b.


(a)   (b)
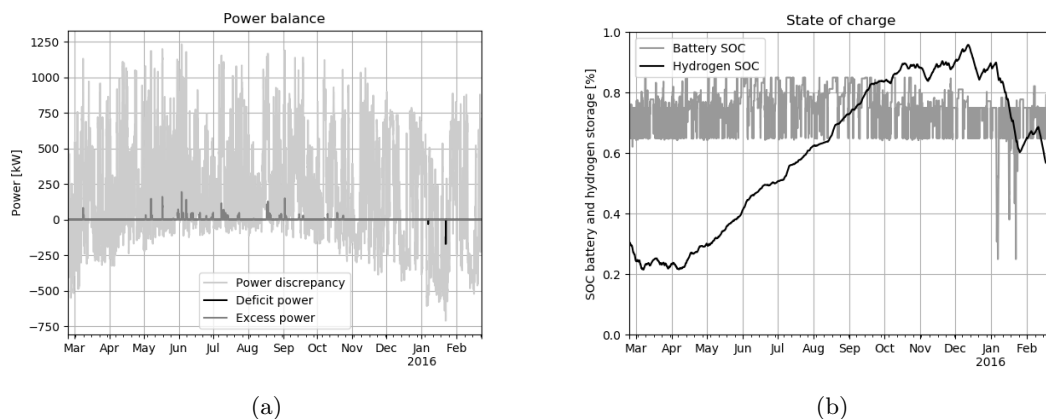
Figure 32: The results from the nominal storage configuration.

8.3   Extended analysis

An extended analysis is conducted for the nominal case deduced above. Hence, two additional simulations are conducted in order to evaluate the impact of two separate parameters of choice.

The first parameter to be altered is the efficiency of the fuel cell and electrolyser, since the low round-trip efficiency of the hydrogen system is also assumed to have a significant impact on system performance. The Fuel Cell and Hydrogen 2 Joint Undertaking within the Horizon 2020 Framework programme in EU have established 2020 targets for fuel cell and electrolyser efficiencies. Thus, the fuel cell and electrolyser efficiencies are altered in line with these objective targets. The fuel cell efficiency target is an increase by 10%-units resulting in a new simulation efficiency of 60%. The electrolyser target efficiency is about 80% (Niakolas et al. 2016).These values are used for the extended analysis.

The second parameter to be altered is the battery state of charge, SOC_B. The inner SOC_B limits are assumed to have a strong influence on the energy management strategy and the results. The new inner minimum limit was set in accordance with a study conducted by K. Zhou, Ferreira, and De Haan (2008). The proposed operation strategy in the study was characterised by a margin of 10%-units between the inner and outer limits (K. Zhou, Ferreira, and De Haan 2008). The current maximum and minimum outer SOC_B limits are retained to preserve battery life (Xu et al. 2016). The maximum inner limit is also unchanged since it is in line with values proposed by K. Zhou, Ferreira, and De Haan (2008). However, the inner minimum limit is altered from 65% to 35% to attain an SOC_B margin of 10%-units between the inner (35%) and outer (25%) minimum limits, see figure 33. The initial state of charge, $SOC_{B_{init}}$, is also assigned with a new value in between the inner boundaries, 55%.
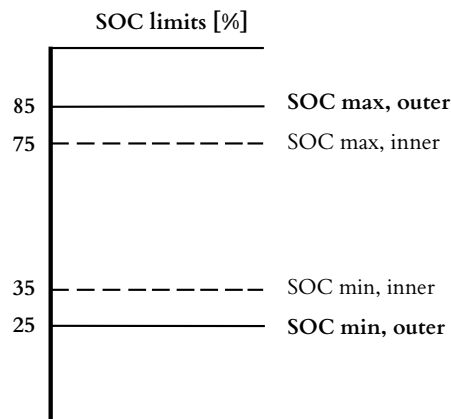
Figure 33: Battery SOC constraints utilised for an the extend analysis.

In table 10 the input values of the parameters altered in the extended simulations are displayed. The new values for the efficiencies and SOC_B limits altered for the simulations are marked in bold text in the yellow cells. The maximum battery capacity and maximum power levels of fuel cell and electrolyser remain the same for all simulations. These values represent the storage configuration attained for the nominal case; $C_B = 1332.8$ kWh, $P_{FC} = 520$ kW and $P_{EL} = 1040$ kW.

Table 10: Extended analysis simulations: Input values

Simulation	η_{EL} [%]	η_{FC} [%]	$SOC_{B_{min}}$ [%]	$SOC_{B_{init}}$ [%]
Nominal	70	50	65	70
$\eta_{EL,FC}$	**80**	**60**	65	70
SOC_B	70	50	**35**	**55**

The results from the two additional simulations in addition to the results from the nominal case are presented in tables 11 and 12. The results from the extended analysis are normalised with regards to the nominal case to enable a comparison, see figure 34.

Table 11: Extended analysis simulations: Results

Simulation	LPSP [%]	EE [%]	ASC [MSEK]	Loss ratio [%]
Nominal	0.09	1.7	20.9	57
$\eta_{EL,FC}$	0.09	8.0	20.0	41
SOC_B	0.34	1.5	18.7	55

Table 12: Extended analysis simulations: Results

| Simulation	EL start	FC start	EL run [%]	FC run [%]	BAT cycles
Nominal	392	312	59	22	151
$\eta_{EL,FC}$	376	310	53	22	152
SOC_B	364	298	57	15	268
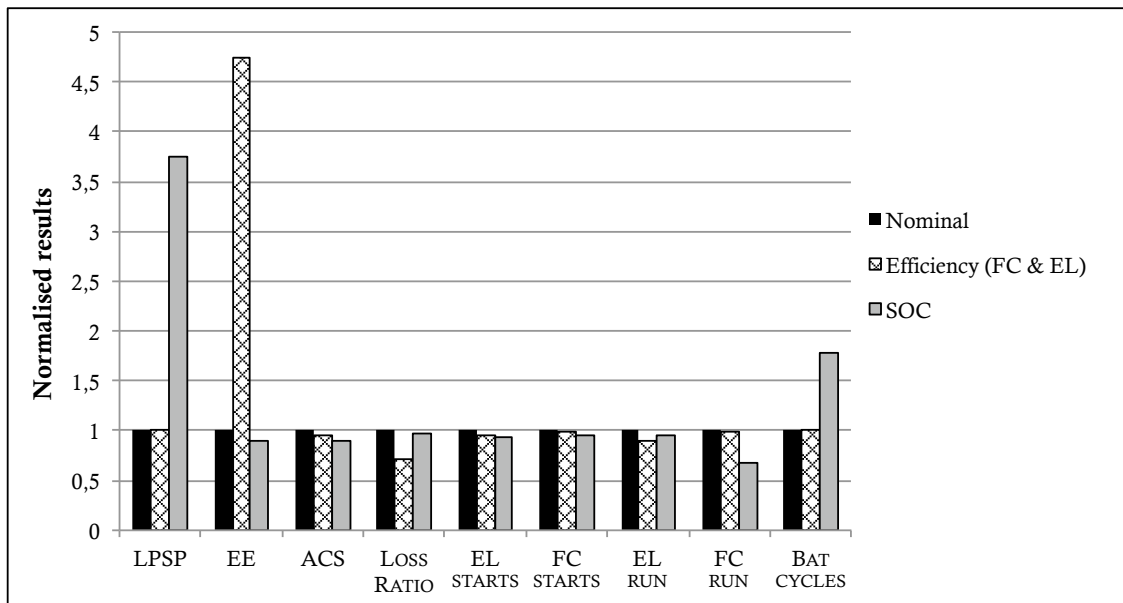
Figure 34: Impact of changing electrolyser and fuel cell efficiency, and the minimum inner limit of SOC_B in comparison the to nominal case.

Efficiency (η_{FC}, η_{EL})
From the results displayed in tables 11 and 12 and in figure 34 it can be concluded that the parameters most affected by the alterations in electrolyser and fuel cell efficiency are EE and the loss ratio. The excess of energy (EE) undergoes a significant increase, suggesting a higher amount of annual power losses. The loss ratio, however, is decreased implying improved system performance in this regard. The decreased values of the remaining parameters mainly suggest an enhanced or equal system performance in comparison to the nominal case.

Through increasing the efficiency of the fuel cell and electrolyser, the power losses allocated to the conversion pathways are lower. Thus, the rate of change of the SOC in the hydrogen tank during charge and discharge is increased. The fact that SOC_H increases with an increase in efficiency is further verified mathematically through equation 25.

(a)   (b)
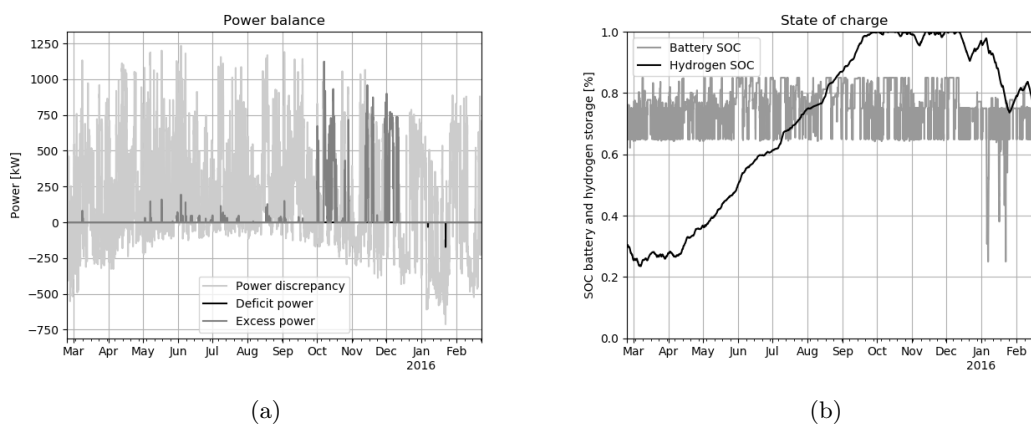
Figure 35: Results from increasing the efficiencies of the fuel cell and the electrolyser by 10%-units.

As a response to a higher rate of change in SOC_H during charging, the excess of energy increases, see table 11. As a higher amount of hydrogen per power input is produced the maximum SOC in the hydrogen tank is attained. This leads to an excess of energy that cannot be utilised by either the electrolyser or the battery and needs to be dumped. The SOC_H maximum is reached already in late September, and the majority of the excess of energy occurs during the subsequent months until the middle of December, see figures 35a and 35b.

The fuel cell runtime is more or less identical to that of the nominal case but a significant decrease in electrolyser run time is apparent. The number of fuel cell start/stop events is similar to the nominal case and for the electrolyser the number is slightly lower. The reason for a decrease in the electrolyser runtime and number of starts/stops is most likely due to the high hydrogen level in the tank during September to December. The operation of the electrolyser is prohibited by the constraint for maximum SOC_H level implemented in the operation strategy.

The number of battery cycles is very similar to that of the nominal case, only slightly higher. Identical inner SOC limits for the battery are utilised during this simulation. Thus the increase might be due to the increased charging of the battery when the hydrogen storage is full and the electrolyser cannot run, see figures 32b and 35b for the period of October to November.

With regards to economic viability, the results indicate that a lower ACS is obtained with higher fuel cell and electrolyser efficiencies. This is probably mainly related to the lower run time of the electrolyser.

State of Charge ($SOC_{B_{min}}$, $SOC_{B_{init}}$)
From the results displayed in tables 11 and 12 and in figure 34 it can be concluded that the performance indicators most affected by the lowered inner minimum SOC_B are LPSP and the number of battery cycles. The results display an increase for both of these indicators, which has negative implications for the grid operation and battery life respectively. However, values of the remaining parameters primarily indicate an enhanced system performance, in comparison to the nominal case.

Lowering the minimum inner SOC_B limit entails a higher utilisation frequency of the battery. Since the inner minimum ($SOC_{B_{min}}$) was altered, and not the maximum SOC_B limit, this affects the frequency in operation of the fuel cell. The fuel cell is not considered by the Energy management strategy until the energy level in the battery reaches the minimum inner limit of SOC_B. Since this limit is lowered, 35% in comparison to the nominal case of 65%, the battery is more frequently prioritised for discharge processes. This can be verified by a lower value of fuel cell runtime, see table 12. The run time of the electrolyser is also shorter than in the nominal case. This change is less drastic than for the fuel cell, since the maximum limits of SOC_B are retained, but the increased operation space for the battery has a visible impact. The number of starts/stops for the electrolyser and fuel cell are both lowered, which suggests lower degradation rates and hence more extended lifetimes of the components.

The loss ratio is decreased due to the higher utilisation of the battery and lower utilization of the hydrogen storage system. This is because battery round-trip efficiency is higher than that of the fuel cell and the electrolyser. Since the cost of the fuel cell and electrolyser components is affected by their degree of utilization, this affects the economic viability of the system (ACS). The annualised cost of system decreases with a decrease in fuel cell and electrolyser run times since lower run times suggest that the components need to be replaced less often due to degradation. Since the fuel cell and electrolyser have lower run times in this simulation, the ACS is lower due to decreased replacement costs, see figure 34 and table 11.

The large increase in battery cycles can be explained by how the calculation of battery cycles is implemented in the control strategy of the model. Allowing the battery to discharge further, down to 35%, increases the size of the charging and discharging events. Since the number of cycles is derived from summarising the charge and discharge events into complete cycles, the total number of cycles will increase as the events will add up to complete cycles faster. Hence, through implementing a control strategy with lower inner minimum SOC_B limit, the battery is more frequently operating at a lower depth of discharge (DOD), which results in higher degradation rate and shorter battery life.

(a)   (b)
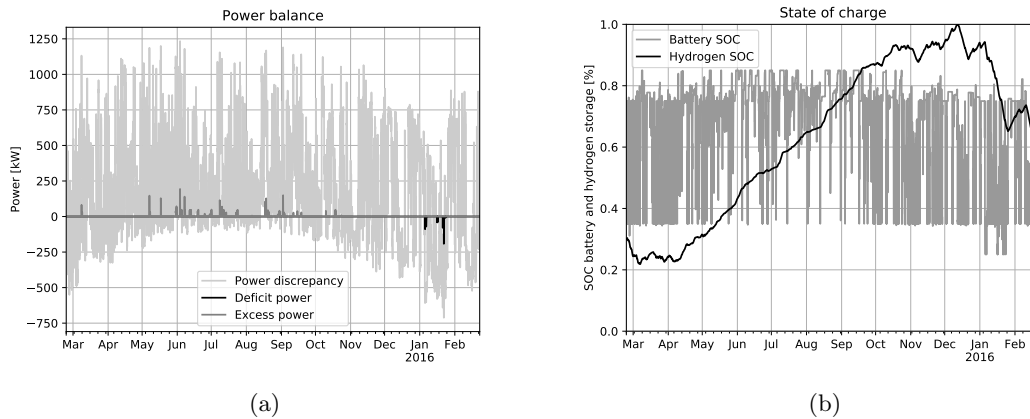
Figure 36: Results from lowering the minimum inner limit of SOC_B to 35%.

The major increase of LPSP is caused by having less energy stored in the battery while the fuel cell is running. In the nominal case the fuel cell will start running when the SOC_B reaches levels below 65% implying that there is still more than half the battery capacity left to use if the fuel cell power is not enough to cover the load. The battery has a working span between the outer SOC limits 25 and 85%, thus 25 to 65% represent two thirds of the working capacity. In the case with the lowered minimum inner SOC_B limit, set to 35%, there is only 17% of the battery capacity left to use if such demands arise. In January the discrepant power is larger than the fuel cell maximum power on several occasions, see figure 36a. where the power discrepancy reaches below 520 kW. When this happens the battery will assist the fuel cell in covering the load until it reaches the minimum outer limit of SOC_B. If the battery becomes empty while there is still a higher load demand than the fuel cell can cover alone there will be power deficit in the system. When there is less energy stored in the battery this happens more often, as is the case for this extended simulation.

9   DISCUSSION AND CONCLUSIONS

This chapter comprises the discussion and concluding remarks on the information, results and analysis presented in the preceding chapters. Section 1 contains the discussion and is divided into four parts, three of which reflect the problem statements: control and operation, sizing and design and performance evaluation. The fourth part focuses on the assumptions, delimitations and uncertainties, and elaborates on the implications these might have on the results. In section 2, the conclusions are presented. The third section presents prospect areas for future work.

9.1   Discussion

9.1.1   Control and operation

Fuel cell and battery charge strategy
The energy management strategy that is implemented in the model is constructed to allow the fuel cell to run at maximum power in order to charge the battery, when possible. The purpose of this is to maintain the main grid service function of the battery, i.e. the primary regulation of frequency. If the battery is allowed to discharge down to the minimum outer level of SOC, without having any opportunity to be charged, its regulatory abilities diminishes. However, this strategy affects the behaviour of the fuel cell. As is explained in the analysis section, the number of fuel cell starts and stops increases with the battery capacity due to this specific part of the operation strategy. This undesired effect could be avoided by making sure that the proportions of battery capacity and fuel cell power are well adapted to the system.

The battery capacity should not be large enough to cover the load alone when it has been charged by the fuel cell at maximum power. Because then the fuel cell might be turned off just to be turned on again in the next step, when the battery is almost drained. A continuous operation of the fuel cell is desired to decrease degradation. Instead of always operating the fuel cell at maximum power when charging the battery, lower set-point powers could be used to address this issue. For example a constant power for charging the battery could be added to the power required of the fuel cell to cover the load. Or perhaps, when considering the power dependency of the efficiency, which is neglected in this work, there is a power setting below the rated power at which the fuel cell efficiency is optimal. Then the fuel cell could be controlled to run at this power level for charging the battery.

Battery SOC-limits
For one of the simulations in the extended analysis the minimum inner limit of SOC in the battery is lowered from 65% to 35%. The result of this can be summarised in that the storage configuration no longer fulfills the condition of LPSP>0.1%, and the behaviour of the battery and fuel cell changes considerably. As the battery cycles and fuel cell and electrolyser runtimes are affected, the health and thereby the cost of the system is affected. Thus the storage system

and the control strategy are not compatible with each other when the SOC limit is changed. This helps establishing that how the control strategy is implemented has large impact on how the storage system is dimensioned to fulfill the technical and economic objectives.

One explanation of why the simulation no longer fulfills the LPSP condition is that there is too little capacity left in the battery when the fuel cell power is not enough to cover the loads. It could be interesting to test using different SOC_B limits depending on the time of year. For example the lower limit of 35% could be used for the spring, summer and autumn months. In the winter months, when there is power deficit, the higher limit of 65% could be used in order to save battery capacity for the critical power discrepancies.

Operation strategy
In this thesis, the operation and sizing of components are based on a rule-based energy management strategy. This is due to its suitability for real-time and short-term management and because it is considered simple, reliable and frequently adopted in literature. However, the authors of this thesis question its applicability to HESS comprising intermittent RES and long-term energy storage systems, e.g., hydrogen storage.

The rule-based strategy might be applicable if pre-determined and historical input data for the power supply and load demand exist, to attain an initial evaluation of system performance, which is conducted in this thesis. However, this strategy is unable to perform long-term management, as it cannot predict fluctuations in, e.g., weather conditions, electricity prices or load demand. This has a significant impact on the operation of long-term energy storage systems in microgrids with RES. This is because several of the advantageous grid services offered by long-term storage require long-term scheduling, which can only be obtained through implementing an optimisation-based operation strategy. It allows the system to operate with regards to multiple objectives, with the benefit of including economic and environmental as objective functions.

Thus, long-term scheduling with regards to economic, technical and environmental objectives enable optimal utilisation of hydrogen storage systems as a flexibility option. For example, through forecasting of electricity prices, weather, load demand, etc. the operation of the fuel cell and electrolyser can be scheduled to provide beneficial grid services, e.g., time-shifting and seasonal storage. The coordination of the battery and hydrogen storage would be optimised. Hence, a more economically viable operation and coordination of the storage systems can be attained.

Rule-based strategies are frequently adopted in literature, which is most probably due to their suitability for short-term storage technologies, such as batteries, which are widely implemented in energy systems. However, system operators most probably lack sufficient experience and knowledge regarding the implementation and operation of long-term energy systems since this is still a novel storage technology. Thus, innovative and suitable optimisation methods and operation strategies for HESS with long-term storage need to be further developed.

9.1.2   Sizing and design

Dimensioning of electrolyser and fuel cell
In all simulations conducted for the performance analysis in this thesis, a constant ratio of 1:2 between the fuel cell and electrolyser maximum power levels is maintained. This is done to minimise the number of free variables and the ratio is similar to several examples in literature, where it is common to let the electrolyser have a higher maximum power. This is likely due to the consequences of the high conversion losses; more energy enters the hydrogen system than the amount returned as electricity. However, when the main objective is to avoid power deficits, LPSP, the fuel cell dimensions are the most important to design well. This could be done by observing the occasions when the power discrepancies are below zero, i.e. higher load than production, and making sure that these can be covered. After this is achieved, the electrolyser could be sized in order to maintain a high enough hydrogen level in the storage to supply the fuel cell for covering the loads. Minimising EE would have a lower priority.

How the ratio between the maximum power levels would turn out depends on other factors of the system; e.g. the production levels compared to the consumption and the battery capacity. For the microgrid in Simris, with the second wind turbine included, it is likely that the ratio between the fuel cell and electrolyser would be 1:x, where $1 < x < 2$. This is because the final SOC of the hydrogen storage system is higher than the initial in all the simulations where LPSP is below the maximum limit. If minimising EE would be an objective with higher priority, the electrolyser power could be dimensioned to cover all the occasions when the power discrepancies are above zero, i.e. higher production than load. Thus, it could be interesting to evaluate the system with more configurations, disregarding the fixed ratio of fuel cell and electrolyser power.

Increased power production
In order to carry out the performance analysis it was necessary to increase the total production of the site. This could have been done in several ways. Increasing the wind power production by virtually adding a second turbine of the same size, thus doubling the wind power production at each time step, was a simple solution. The choice can be questioned, though, as there were other options available. For example the solar production could have been increased, but then there would still have been a major shortage of production in the critical months, December-February. However, since seasonal energy storages are supposed to be able to handle exactly that type of situation it could have been motivated to choose that option. Increasing the solar power production might have been reasonable considering the trend of more households installing solar panels on their roofs, thus increasing this type of power production in the future. But this would require a larger storage and would imply more energy conversion and thus more conversion losses.

9.1.3   Performance evaluation

LPSP
In this thesis the highest allowable LPSP is 0.1%, a value adopted in several other studies to design and size similar energy systems. This would permit the grid to experience power deficit for nine hours over a year. It is reasonable to question weather deficit is considered at all acceptable in design constraints, how electricity consumers are affected and what measures should be taken to alleviate the negative effects. If the microgrid is completely isolated and thus has no connection to another grid, the power deficit could mean being without electricity for those hours. It can be questioned that several studies dimension microgrids with a certain risk of experiencing a power

loss for the consumers. On the other hand, a hybrid energy system might have to be considerably oversized to avoid power deficits completely. Other ways to avoid losing power for a few hours per year could be to use demand response (DR) or to have a portable reserve generator available. DR would imply that the loads could be diminished by controlling the consumption, for example by turning off domestic heat pumps for a short period of time. The reserve generator could be plugged in during the critical hours, if these could be forecasted.

EE vs loss ratio
For one of the simulations in the extended analysis the efficiencies of the fuel cell and electrolyser are increased by 10%-units each. Summarising the results establishes that the EE increases dramatically while the loss ratio experiences a significant decrease. When less energy is lost in the conversion from electricity to hydrogen gas in the electrolyser, more energy is stored in the hydrogen storage. Thus the storage becomes full faster as the conversion losses and the loss ratio decrease. When the hydrogen storage becomes full, a power surplus will result in EE unless the battery can store the energy. As the excess energy does not enter the hydrogen storage system it will not add to the conversion losses, and thus the loss ratio is decreased further.

Considering the nominal case, and the other simulations with the nominal values of fuel cell and electrolyser efficiency, a similar reasoning can be made: If the hydrogen storage tanks has less capacity the conversion losses will probably decrease. As no energy can enter the hydrogen system if the storage tanks are full the power surplus will turn into EE. In all simulations comprising the performance analyis the final SOC of the hydrogen storage is higher than the initial SOC. This means that the hydrogen storage capacity could be decreased while still maintaining energy balance with a positive margin. This, however, would be a trade-off between losing energy in conversion losses and losing it as excess energy.

Economic viability of hydrogen storage systems
As is observed in this thesis, the ACS of a HESS with battery- and hydrogen storage is mainly affected by the size of the long-term storage. It is currently harder to attain economic viability of a long-term ESS than a short-term ESS. The economic viability of a hydrogen storage system varies depending on the application and should be evaluated with regards to project-specific conditions. For example, in remote and power isolated areas the implementation of a high-cost stand-alone microgrid might seem more legitimate if no alternative solution exists.

The economic viability of hydrogen storage systems might be enhanced through traditional technical learning curves. The high unit costs for fuel cells and electrolysers can probably be reduced through further development and research. Subsidies to R&D departments might be beneficial to address technical challenges, e.g., increasing conversion efficiencies. Another mean of promoting and improving the learning curve for hydrogen storage operation might be to implement this type of storage system in demonstration projects. Hydrogen storage systems might also be included as a part of a HESS comprising several other flexibility technologies, such as biodiesel generators and demand-side response. Thus, the size of the hydrogen storage system can be smaller and more economically viable at an initial stage. Hence, system operators would acquire knowledge about the operation and implementation of long-term storage systems. Such implementation might further support the learning curve for control strategies in microgrids, relating to the challenge of coordinating multiple DER and storage units.

Furthermore, it should be noted that the economic viability could be evaluated from a system perspective. Hydrogen storage system can provide added value and have indirect positive financial implications. For example, as mentioned in section 3.3.2, the heat released from the exothermic

conversion process in fuel cells can be recovered and utilised for domestic heating applications. Hence, the cost of this energy is allocated to the hydrogen storage system, and former heat production sources can be removed, which reduces the entire system cost.

9.1.4   Assumptions, delimitations and uncertainties

Data
The input data for production and load profiles are historical data representing the simulation period; February 23rd 2015 to February 22nd 2016. It is assumed representative for the studied area in Simris, but annual variations have been observed when selecting input data. The high availability of data measurements during the chosen period was one of the main reasons for the utilisation of this data. However, this specific time period is characterised by a slightly higher wind power production than other years. Hence, the storage configuration designed for this particular period might be over dimensioned and less applicable for other years.

Storage systems
The assumption of constant efficiency for the fuel cell, the electrolyser, and the battery might impact the results as in reality the efficiencies are highly variable, depending on, e.g., power level and temperature. The performance indicators found to be most affected by alterations in the fuel cell and electrolyser efficiencies were EE and loss ratio. Thus, to evaluate the system performance more accurately with regards to these indicators, the variations in efficiency should be included. Also, the efficiency decreases as the power output (FC) and hydrogen production (EL) of the corresponding device increase. Since the efficiency variability is not included in this thesis, this trade-off is not entirely accounted for to achieve optimal utilisation of the hydrogen storage system. However, the least optimal points of operation, characterised by low efficiencies, are discarded through the implementation of maximum and minimum power level constraints in the simulations. Furthermore, the efficiency of the compressor is assumed to be included in the electrolyser efficiency. This is also a coarse assumption since its efficiency most probably is affected in a similar manner, i.e., by the power level required to compress hydrogen gas. This would affect EE and loss ratio even further.

The assumption of pre-determined runtimes and lifetimes of components is based on values from the literature. However, considerable variation in values of the fuel cell and the electrolyser lifetimes was found, suggesting that there is no uniform measurement of this. For this thesis, lifetimes were established in line with the technology chosen, PEMFC and PEMEL. The lifetime in years was determined through values of expected runtime before replacement. Pessimistic values for this were selected in order not to under-estimate the ACS. Through utilising runtime to measure the lifetime expectancy, the lifetime in years becomes variable, which is more realistic as the runtime is evaluated with regards to the level of degradation. However, the total runtime before replacement is assumed constant, which is a simplification as it implies that the degradation rate is independent of operation characteristics. More specifically, the degradation rate of the fuel cell and the electrolyser increases as the number of starts and stops increase.

The economic performance indicator, ACS, is dependent on the lifetime of components, due to its implications on replacement costs. To evaluate the ACS more appropriately in this regard, a more accurate assessment of component lifetimes would be necessary, including effects of operation characteristics. This might be attained through applying functions and models encompassing degradation mechanisms. It might also be advantageous to evaluate the aging mechanisms in

batteries with more complex mathematical functions, which was proposed by Han et al. (2014), as there is no standardised method to calculate cycles as an indirect measure of degradation. In this way the self-discharge of batteries, which was disregarded in this thesis, could also be accounted for.

The operation of storage devices is implemented as energy flow models in this thesis as the time-scale of simulation is one hour and the energy management strategy in MGCC is the primary focus. However, to include degradation mechanisms or other behaviours of the devices, dynamic, and physics based models are more suitable as they deal with the performance at time scales of milliseconds to minutes. These deal with the control at the device level (DMS) and might complement the EMS in the MGCC to attain a more optimal operation and coordination.

The ramp rates for the fuel cell and electrolyser is in the time scale of milliseconds or seconds. As energy flow models are applied in this thesis, addressing system operation in the time scale of hours, the ramp rates can be neglected. If the time scale of the simulation is shorter than this, the constraints for ramp up or ramp down must be accounted for to avoid simultaneous operation of the fuel cell and electrolyser. The energy management strategy for this thesis is only constructed for input data in the time scales larger than milliseconds/seconds, where the assumption of instantaneous ramp up and down still holds.

Objectives
The storage configuration is designed and sized with regards to the technical objective of reliability (LPSP). The economic target (ACS) is considered secondly but not utilised as a primary objective. Environmental goals are not included in this thesis. If optimisation based design methods were implemented, accounting for multiple objective functions, it would be interesting to incorporate environmental objectives. Neither operations of the battery or the hydrogen storage system are directly associated with greenhouse gas emissions. Nevertheless, if their operation is evaluated from a life-cycle perspective, including the production of devices, etc., their corresponding environmental impacts will increase. This can be accounted for when designing the storage systems through prioritising the device associated with lowest emission levels.

The objectives utilised to assess the technical and economic viability of the system were selected since they are widely adopted in literature. Reliability, excess of energy and annualised cost of system were included in this thesis, but several other objectives can be applied. The interest of stakeholders involved in the design process determines which goals are relevant. The selected objective functions most probably have a significant impact on the outcome of the system design and should be carefully evaluated before implementation.

The ACS is not a quantitative measure of the entire system cost as it only includes the cost of the storage units. In this thesis, it is utilised to enable a comparative analysis between different storage configurations, and since the number of production units, i.e., solar-PV-panels and wind turbines, are identical these are not included. Thus, the results should not be interpreted as a price for installing the system, only a relative measurement. The cost of additional ancillary service units such as a compressor, heat exchangers, water pumps, etc. must be added to attain a more comprehensive performance analysis. These are excluded in this work due to time limitations and scope delimitations. It could also be interesting to compare the cost of installing a storage system to the cost of installing more generation sources, e.g. more wind turbines and solar cells on the household rooftops.

Results

Quantitive measures of performance are desired, to conduct a performance analysis, which is attained through utilising performance indicators. However, system performance depends on many factors and dynamics due to the complexity of real system operation. To evaluate system performance through only determining performance indicators entail a high degree of uncertainty and underlying relationships might not be accounted for or visualised in the results. Also, it is difficult to compare performance indicators as no standardised weighing methods are applied in literature. As is stated earlier, in section 6.4, the need for the development of performance evaluation methods applicable to battery and hydrogen storage systems prevails.

Due to the degree of uncertainty in the results and its specific applicability to Simris, it is difficult to make general conclusions regarding appropriate battery and hydrogen storage configurations.

9.2   Summary and conclusions

9.2.1   Results

- **LPSP** is lower when both the battery and hydrogen storage are larger.

- **EE** is lower when both the battery and hydrogen storage are larger. The over-dimensioned hydrogen storage imply that the electrolyser power and the battery capacity are the limiting factors for storing energy.

- **ACS** is mainly dependent on the size of the electrolyser and the fuel cell, due to higher investment costs and shorter replacement times. The cost of battery system and the cost of replacement of fuel cell and electrolyser seem to cancel each other out.

- **Loss ratio** is similar, 56-57%, for all simulations in the performance analysis, mainly due to the low round-trip efficiency of the hydrogen storage system, 33%. The losses are slightly lower when the battery capacity is large and the hydrogen system small.

- **Runtimes, FC and EL**, decrease when the battery capacity increase. The variation for the fuel cell, 20-28%, is larger than for the electrolyser, 58-60%.

- **Number of starts, EL**, decrease when the battery capacity increases.

- **Number of starts, FC,** increase when the battery capacity increases, the opposite trend compared to the electrolyser.

- **Battery cycles** decrease when the battery capacity increases.

9.2.2   Control and operation

Control at different levels in the system is required to achieve an overall effective grid operation and a functioning coordination between energy storage systems. Different controllers handle different parts of the coordination. A PCS can manage primary and secondary control, while the DMS monitors and controls devices' health and operation. An MGCC provides tertiary control,

i.e. energy management, and is responsible for the overall management including forecasting and optimising power set points.

The operation strategy is formed in line with the objectives established by the stakeholders of the project. These can be technical, economic and environmental. An operation strategy can be rule-based or based on optimisation algorithms. It can be valid on different time scales, which have to take different aspects, like dynamics and transients, into account.

The control strategy of this thesis connect the battery and fuel cell operation very closely. Changing the power level at which the fuel cell charges the battery to a lower level than maximum power could have profitable impacts on the fuel cell operation and lifetime. The SOC_B limits, which strongly govern the energy management of the system, are essential and how they are set affect the sizing of the system. The energy management strategy of this thesis is rule-based. For implementing a real HESS system it might be good to explore the concept of using optimisation algorithms and forecasts, thus including a long-term energy management. Hence, economic and environmental objectives can be accounted for to a higher extent and the operation of electrolyser and fuel cell could be enhanced and optimised, as unnecessary starts and stops could be avoided.

9.2.3   Sizing and design

The sizing and design of a microgrid with renewable energy sources and a hybrid energy storage system can be achieved through evaluating performance indicators reflecting the objectives established for the grid operation. In addition, physical and technical system constraints should be defined. These often include maximum and minimum charge and discharge power levels, and limits of state of charge of the storage components in the system. How the control strategy is implemented has a large impact on the operation of the components and thus their sizing.

For the simulations conducted in the thesis the ratio between fuel cell and electrolyser maximum power is kept constant, at 1:2. It could be interesting to vary this ratio since it might adapt the storage system to the rest of the Simris grid in a better way. It was necessary to increase the power production of the system to be able to analyse the behaviour of the storage system. This was done by adding a second wind turbine, identical to the prevailing turbine in Simris. An alternative measure could be to increase the solar power production, which would probably have large impacts on the results.

9.2.4   Performance evaluation

For evaluating the technical performance, LPSP, Loss of power supply probability, is a common measurement to evaluate grid reliability. EE, excess of energy, could be interesting to consider in the future, but as the market situation is today it is not considered viable to dimension the system based on this indicator. Loss ratio can be used to evaluate the energy efficiency of the system. The runtimes and number of starts and stops for the fuel cell and electrolyser can give indications of the individual component operation, rate of degradation and expected lifetimes. Battery cycles can be used to study the operation of the battery, but a more accurate method than the one used in this thesis would be required to draw any quantitative conclusions. For evaluating the economic peformance, ACS, annualised cost of system, is a common measure. In this thesis, this indicator only comprise the costs of the storage systems to make an economic

comparison between different storage configurations. To attain a quantitative measure of the entire system cost, a more comprehensive cost analysis would have to be conducted which takes all system components into account.

To design a microgrid while allowing an LPSP higher than zero can be questioned, but a system where this has to be zero would likely have to be over-dimensioned. Solutions to avoid LPSP higher than zero could be to utilise DSR, demand-side response, or to connect a portable reserve generator if the critical periods are known. The loss ratio of the system investigated in the thesis, due mainly to conversion losses, would be smaller if the hydrogen storage capacity was smaller and thus allowed less energy to enter the hydrogen system. The system could be self sufficient with a smaller storage, but more energy would be lost as EE. The economic viability of hydrogen storage systems of today depends on what surroundings and alternative power supplies the microgrid has access to. If more systems are implemented and investigated the learning curve might improve. If a system perspective is applied and for example heat could be recovered from the fuel cell, hence improving the economic viability of the solution.

9.2.5   Concluding remarks

Hybrid energy storage systems (HESS) comprising a hydrogen and a battery storage add flexibility to microgrids with a high share of renewable energy sources, such as wind and solar. The grid reliability, the main indicator for technical viability of the solution, increases with an increase in size of the energy storage systems i.e. the energy capacity of the battery and the power capacity of the electrolyser and fuel cell. The technical performance is also evaluated with regards to power losses, which is constantly very high, about 57 %, for all twenty-four simulations of different storage configurations. This is due to a large energy conversion loss in the electrolyser and the fuel cell resulting from low conversion efficiencies for these processes. This required an additional electricity production unit, a wind turbine, to achieve energy balance of the system and to conduct the simulations. Thus, the applicability of the proposed HESS in Simris can be questioned. Furthermore, the hydrogen storage system has a negative impact on the economic viability of the HESS solution due to a high capital cost of the electrolyser and fuel cell. In combination with the short lifetimes of these components, resulting in high replacement costs, these components constitute a dominant share of the total annual cost of the system.

Hence, the opinion of the authors is that the technical and economic viability of a hybrid energy storage system (HESS) with a hydrogen and a battery storage, must be evaluated specifically for each case. The system performance must be compared to other prevailing flexibility options and alternative costs to properly evaluate the applicability and suitability of the proposed solution.

9.3 Future work

Potential areas for future work are presented below.

- **Decentralised battery systems and solar power production**.
  Modeling a microgrid similar to the one in this thesis where the power generation of the households and their energy storage in domestic batteries is considered.

- **Shorter timescales**.
  Constructing a model, which allows for simulation input data on shorter timescales, such as seconds or smaller.

- **Comparison of different energy management strategies**.
  Studying how the microgrid energy storage solution should be designed depending on what control strategy is used. For example, compare an energy management strategy similar to the one used in this thesis to another strategy, e.g. hysteresis band.

- **Optimisation**.
  Implementing a control strategy in the system, which is built on an optimisation algorithm.

- **Replace energy storage with more production**.
  Studying cost and operation in a system where the energy storage solutions are replaced with more production sources.

- **EE versus conversion losses**.
  Investigating how the trade-off between excess of energy and energy losses due to conversion processes should be valued.

- **Maximum power ratio, fuel cell and electrolyser**.
  Studying a similar microgrid system as in this thesis while allowing the sizes of fuel cell and electrolyser to vary in relation to each other.

- **Including demand response**.
  Modeling a microgrid similar to the one in this thesis where the flexibility of the consumers, demand response (DR), is considered.

# References

Areva (2014). *PEM Electrolysers.* [Brochure].

Behzadi, Mohammad Sadigh and Mohsen Niasati (2015). "Comparative performance analysis of a hybrid PV/FC/battery stand-alone system using different power management strategies and sizing approaches". In: *International journal of hydrogen energy* 40.1, pp. 538–548.

Berg, Helena (2015). "The electrochemical cell". In: *Batteries for Electric Vehicles: Materials and Electrochemistry*. Cambridge University Press, pp. 7–46. DOI: 10.1017/CBO9781316090978.004.

Bessarabov, Dmitri et al. (2016). *PEM electrolysis for hydrogen production: principles and applications*. CRC Press.

Bizon, Nicu, Mihai Oproescu, and Mircea Raceanu (2015). "Efficient energy control strategies for a standalone renewable/fuel cell hybrid power source". In: *Energy Conversion and Management* 90, pp. 93–110.

Bocklisch, Thilo (2015). "Hybrid energy storage systems for renewable energy applications". In: *Energy Procedia* 73, pp. 103–111.

Brka, Adel (2015). *Optimisation of stand-alone hydrogen-based renewable energy systems using intelligent techniques.*

Brka, Adel, Yasir M Al-Abdeli, and Ganesh Kothapalli (2015). "The interplay between renewables penetration, costing and emissions in the sizing of stand-alone hydrogen systems". In: *International Journal of Hydrogen Energy* 40.1, pp. 125–135.

Byrne, Raymond H et al. (2017). "Energy Management and Optimization Methods for Grid Energy Storage Systems". In: *IEEE Access.*

Cau, Giorgio et al. (2014). "Energy management strategy based on short-term generation scheduling for a renewable microgrid using a hydrogen storage system". In: *Energy Conversion and Management* 87, pp. 820–831.

Dell, Ronald M. and David A. J. Rand (2001). "How a battery operates". In: *Understanding Batteries*. Ed. by Ronald M. Dell and David A. J. Rand. The Royal Society of Chemistry, pp. 10–21. ISBN: 978-0-85404-605-8. DOI: 10.1039/9781847552228-00010.

Dong, Weiqiang, Yanjun Li, and Ji Xiang (2016). "Optimal Sizing of a Stand-Alone Hybrid Power System Based on Battery/Hydrogen with an Improved Ant Colony Optimization". In: *Energies* 9.10, p. 785.

Ecofys (2014). *Energy Storage Opportunities and Challenges (White Paper)*. Tech. rep. Utrecht: Ecofys.

Eichman, J, K Harrison, and Michael Peters (2014). *Novel electrolyzer applications: providing more than just hydrogen*. Tech. rep. National Renewable Energy Laboratory (NREL), Golden, CO.

Eichman, J, A Townsend, and M Melaina (2016). *Economic Assessment of Hydrogen Technologies Participating in California Electricity Markets*. Tech. rep. NREL (National Renewable Energy Laboratory (NREL), Golden, CO (United States)).

E.ON (2016). *ESS for LES Microgrid Project.* [Internal information].

E.ON Energidistribution (2018a). *Lokal energiproduktion - Ett nytt sätt att tänka kring energi.* URL: https://www.eon.se/om-e-on/innovation/lokala-energisystem/vi-pa-simris.html (visited on 02/13/2018).

– (2018b). *Lokala energisystem - direkt från Simris.* URL: https://www.eon.se/om-e-on/innovation/lokala-energisystem/direkt-fran-simris.html (visited on 01/22/2018).

– (2018c). *Tekniken bakom lokala energisystem.* URL: https://www.eon.se/om-e-on/innovation/lokala-energisystem/tekniken-bakom.html#/foerbrukning (visited on 02/13/2018).

Eriksson, ELV and E MacA Gray (2017). "Optimization and integration of hybrid renewable energy hydrogen fuel cell energy systems–A critical review". In: *Applied Energy* 202, pp. 348–364.

Etxeberria, Aitor et al. (2010). "Hybrid energy storage systems for renewable energy sources integration in microgrids: A review". In: *IPEC, 2010 Conference Proceedings.* IEEE, pp. 532–537.

European Commission (2017). *Interflex - Interactions between automated energy systems and flexibilities brought by energy market players.* URL: http://interflex-h2020.com (visited on 02/13/2018).

– (2018). *Paris Agreement.* URL: https://ec.europa.eu/clima/policies/international/negotiations/paris_en (visited on 02/13/2018).

Farrokhabadi, Mostafa et al. (2017). "Energy storage in microgrids". In: *IEEE power and energy magazine* 15.5, pp. 81–91.

Gou, Bei, Woonki Na, and Bill Diong (2016). *Fuel Cells: Dynamic Modeling and Control with Power Electronics Applications.* CRC press.

Gulin, Marko, Mario Vašak, and Mato Baotić (2015). "Analysis of microgrid power flow optimization with consideration of residual storages state". In: *Control Conference (ECC), 2015 European.* IEEE, pp. 3126–3131.

Han, Xuebing et al. (2014). "A comparative study of commercial lithium ion battery cycle life in electrical vehicle: Aging mechanism identification". In: *Journal of Power Sources* 251, pp. 38–54.

International Electrotechnical Commission, (IEC) (2011). *Electrical Energy Storage (White Paper).* Tech. rep. Geneva: IEC.

International Energy Agency (2015). *Energy and climate change.* World Energy Outlook special report.

– (2018). *World Energy Outlook 2017.* URL: https://www.iea.org/weo2017/ (visited on 02/13/2018).

International Energy Agency, (IEA) (2015). *Technology Roadmap Hydrogen and Fuel cells.* Tech. rep. Paris: IEA.

Ipsakis, Dimitris, Spyros Voutetakis, Panos Seferlis, Fotis Stergiopoulos, and Costas Elmasides (2009). "Power management strategies for a stand-alone power system using renewable energy sources and hydrogen storage". In: *international journal of hydrogen energy* 34.16, pp. 7081–7095.

Ipsakis, Dimitris, Spyros Voutetakis, Panos Seferlis, Fotis Stergiopoulos, Simira Papadopoulou, et al. (2008). "The effect of the hysteresis band on power management strategies in a stand-alone power system". In: *Energy* 33.10, pp. 1537–1550.

IVL Sweden Environmental Institute (2011). *Energy scenario for Sweden 2050 - based on renewable technologies and sources.*

Kurzweil, Peter (2015). "Lithium Battery Energy Storage: State of the Art Including Lithium–Air and Lithium–Sulfur Systems". In: *Electrochemical Energy Storage for Renewable Sources and Grid Balancing.* Elsevier, pp. 269–307.

Kwasinski, Alexis, Wayne Weaver, and Robert S. Balog (2016). "Energy storage". In: *Microgrids and other Local Area Power and Energy Systems.* Cambridge University Press, pp. 255–298. DOI: 10.1017/CBO9781139002998.007.

– (2016a). "Introduction". In: *Microgrids and other Local Area Power and Energy Systems.* Cambridge University Press, pp. 3–22. DOI: 10.1017/CBO9781139002998.002.

– (2016b). "Power generation sources". In: *Microgrids and other Local Area Power and Energy Systems.* Cambridge University Press, pp. 165–254. DOI: 10.1017/CBO9781139002998.006.

Li, Jianwei et al. (2016). "Design/test of a hybrid energy storage system for primary frequency control using a dynamic droop method in an isolated microgrid power system". In: *Applied Energy.*

Luna-Rubio, R et al. (2012). "Optimal sizing of renewable hybrids energy systems: A review of methodologies". In: *Solar Energy* 86.4, pp. 1077–1088.

Meng, Lexuan et al. (2016). "Flexible system integration and advanced hierarchical control architectures in the microgrid research laboratory of Aalborg University". In: *IEEE Transactions on Industry Applications* 52.2, pp. 1736–1749.

Miguel, N de et al. (2015). "Compressed hydrogen tanks for on-board application: thermal behaviour during cycling". In: *International Journal of Hydrogen Energy* 40.19, pp. 6449–6458.

Milligan, M et al. (2012). *Exploration of High- Penetration Renewable Electricity Futures (Vol. 4 of Renewable Electricity Futures Study).* Tech. rep. Golden, CO: National Renewable Energy Laboratory.

Minchala-Avila, Luis I et al. (2015). "A review of optimal control techniques applied to the energy management and control of microgrids". In: *Procedia Computer Science* 52, pp. 780–787.

Mittelsteadt, Cortney et al. (2015). "PEM Electrolyzers and PEM Regenerative Fuel Cells Industrial View". In: *Electrochemical Energy Storage for Renewable Sources and Grid Balancing.* Elsevier, pp. 159–181.

Nelson, DB, MH Nehrir, and C Wang (2006). "Unit sizing and cost analysis of stand-alone hybrid wind/PV/fuel cell power generation systems". In: *Renewable energy* 31.10, pp. 1641–1656.

Niakolas, Dimitris K et al. (2016). "Fuel cells are a commercially viable alternative for the production of "clean" energy". In: *Ambio* 45.1, pp. 32–37.

Olivares, Daniel E, Claudio A Cañizares, and Mehrdad Kazerani (2014). "A centralized energy management system for isolated microgrids". In: *IEEE Transactions on smart grid* 5.4, pp. 1864–1875.

Page, S (2015). *How to find out your MacBook battery cycle count.* URL: http://www.idownloadblog.com/2015/06/18/how-to-macbook-battery-cycle-count/ (visited on 01/11/2018).

Papaefthymiou, Georgios, Katharina Grave, and Ken Dragoon (2014). *Flexibility options in electricity systems.* Tech. rep. Berlin: Ecofys.

Pellow, Matthew A et al. (2015). "Hydrogen or batteries for grid storage? A net energy analysis". In: *Energy & Environmental Science* 8.7, pp. 1938–1952.

Petrollese, Mario (2015). "Optimal generation scheduling for renewable microgrids using hydrogen storage systems". PhD thesis. Universita degli Studi di Cagliari.

Petrollese, Mario et al. (2016). "Real-time integration of optimal generation scheduling with MPC for the energy management of a renewable hydrogen-based microgrid". In: *Applied Energy* 166, pp. 96–106.

PI, Hui Xu and MA Newton (2015). "High-Performance, Long-Lifetime Catalysts for Proton Exchange Membrane Electrolysis". In:

Planas, Estefania et al. (2015). "AC and DC technology in microgrids: A review". In: *Renewable and Sustainable Energy Reviews* 43, pp. 726–749.

PowerCellSwedenAB (2017). *Power Cell PS-100 Datasheet.* [Brochure].

Rayment, Chris and Scott Sherwin (2003). "Introduction to fuel cell technology". In: *Department of Aerospace and Mechanical Engineering, University of Notre Dame, Notre Dame, IN* 46556, pp. 11–12.

Riis, Trygve et al. (2006). "Hydrogen production and storage—R&D priorities and gaps". In: *International Energy Agency-Hydrogen Co-Ordination Group-Hydrogen Implementing Agreement.*

Roebuck, CM (2003). *Excel preliminary chemistry.* Pascal Press.

Rost, Ulrich, Jeffrey Roth, and Michael Brodmann (2015). *Modular Polymer Electrolyte Membrane Fuel Cell and Electrolyser Stack Design with Hydraulic Compression*. Universitätsbibliothek Dortmund.

Rudnick, Hugh and Luiz Barroso (2017). "Flexibility needed - challenges for future energy storage systems". In: *IEEE power and energy magazine* 15.5, pp. 12–19.

Salam, AA, A Mohamed, and MA Hannan (2008). "Technical challenges on microgrids". In: *ARPN Journal of engineering and applied sciences* 3.6, pp. 64–69.

Sammes, Nigel (2006). *Fuel cell technology: reaching towards commercialization*. Springer Science & Business Media.

Sauer, Dirk Uwe (2015). "Classification of Storage Systems". In: *Electrochemical Energy Storage for Renewable Sources and Grid Balancing*. Ed. by Patrick T. Moseley and Jürgen Garche. Elsevier, pp. 13–21. ISBN: 978-0-444-62616-5. DOI: 10.1016/B978-0-444-62616-5.00002-4.

Schäfer, Andreas et al. (2015). "Challenges of Power Systems". In: *Electrochemical Energy Storage for Renewable Sources and Grid Balancing*. Elsevier, pp. 23–32.

Schwaegerl, Christine and Liang Tao (2014). "The microgrids concept". In: *Microgrids: Architectures and control*, pp. 1–24.

Sioshansi, Fereidoon P (2011). *Smart grid: integrating renewable, distributed and efficient energy*. Academic Press.

Smolinka, Tom, Emile Tabu Ojong, and Jürgen Garche (2015). "Hydrogen Production from Renewable Energies—Electrolyzer Technologies". In: *Electrochemical Energy Storage for Renewable Sources and Grid Balancing*. Elsevier, pp. 103–128.

Steilen, Mike and Ludwig Jörissen (2015). "Hydrogen Conversion into Electricity and Thermal Energy by Fuel Cells: Use of H2-Systems and Batteries". In: *Electrochemical Energy Storage for Renewable Sources and Grid Balancing*. Elsevier, pp. 143–158.

Suzdalenko, Alexander and Ilya Galkin (2013). "Instantaneous, short-term and predictive long-term power balancing techniques in intelligent distribution grids". In: *Doctoral Conference on Computing, Electrical and Industrial Systems*. Springer, pp. 343–350.

Thurner, L. et al. (2017). *pandapower - an Open Source Python Tool for Convenient Modeling, Analysis and Optimization of Electric Power Systems*. preprint. URL: https://arxiv.org/abs/1709.06743 (visited on 01/18/2018).

Ton, Dan and Jim Reilly (2017). "Microgrid controller initiatives". In: *IEEE power and energy magazine* 15.4, pp. 24–40.

Ulbig, Andreas, Theodor S Borsche, and Göran Andersson (2014). "Impact of low rotational inertia on power system stability and operation". In: *IFAC Proceedings Volumes* 47.3, pp. 7290–7297.

Ulleberg, Øystein (2004). "The importance of control strategies in PV–hydrogen systems". In: *Solar Energy* 76.1, pp. 323–329.

Ulleberg, Øystein, Torgeir Nakken, and Arnaud Ete (2010). "The wind/hydrogen demonstration system at Utsira in Norway: Evaluation of system performance using operational data and updated hydrogen energy system modeling tools". In: *International Journal of Hydrogen Energy* 35.5, pp. 1841–1852.

U.S. Department of Energy, (DOE) (2006). *Hydrogen Fuel Cells*. [Brochure].

U.S. Energy Information Administration (2017). *International Energy Outlook 2017*. URL: https://www.eia.gov/outlooks/ieo/exec_summ.php (visited on 01/21/2018).

Uzunoglu, M, OC Onar, and MS Alam (2009). "Modeling, control and simulation of a PV/FC/UC based hybrid power generation system for stand-alone applications". In: *Renewable energy* 34.3, pp. 509–520.

Valverde, L, FJ Pino, et al. (2016). "Definition, analysis and experimental investigation of operation modes in hydrogen-renewable-based power plants incorporating hybrid energy storage". In: *Energy Conversion and Management* 113, pp. 290–311.

Valverde, L, F Rosa, et al. (2016). "Energy management strategies in hydrogen smart-grids: a laboratory experience". In: *International Journal of Hydrogen Energy* 41.31, pp. 13715–13725.

Wang, Caisheng, M Hashem Nehrir, and Steven R Shaw (2005). "Dynamic models and model validation for PEM fuel cells using electrical circuits". In: *IEEE transactions on energy conversion* 20.2, pp. 442–451.

Xu, Bolun et al. (2016). "Modeling of lithium-ion battery degradation for cell life assessment". In: *IEEE Transactions on Smart Grid*.

Xue-song, Zhou, Cui Li-qiang, and Ma You-jie (2011). "Research on control of micro grid". In: *Measuring Technology and Mechatronics Automation (ICMTMA), 2011 Third International Conference on*. Vol. 2. IEEE, pp. 1129–1132.

Yang, Hongxing et al. (2008). "Optimal sizing method for stand-alone hybrid solar–wind system with LPSP technology by using genetic algorithm". In: *Solar energy* 82.4, pp. 354–367.

Yusof, Mohd Fauzi Mohamad and Abu Zaharin Ahmad (2016). "Power energy management strategy of micro-grid system". In: *Automatic Control and Intelligent Systems (I2CACIS), IEEE International Conference on*. IEEE, pp. 107–112.

Zhang, Houcheng et al. (2012). "Efficiency calculation and configuration design of a PEM electrolyzer system for hydrogen production". In: *Int J Electrochem Sci* 7, pp. 4143–57.

Zhang, Yang et al. (2017). "Comparative study of hydrogen storage and battery storage in grid connected photovoltaic system: Storage sizing and rule-based operation". In: *Applied Energy* 201, pp. 397–411.

Zhou, Keliang, JA Ferreira, and SWH De Haan (2008). "Optimal energy management strategy and system sizing method for stand-alone photovoltaic-hydrogen systems". In: *International journal of hydrogen energy* 33.2, pp. 477–489.

Zhou, Wei et al. (2010). "Current status of research on optimum sizing of stand-alone hybrid solar–wind power generation systems". In: *Applied Energy* 87.2, pp. 380–389.

A Appendix: Energy management strategy
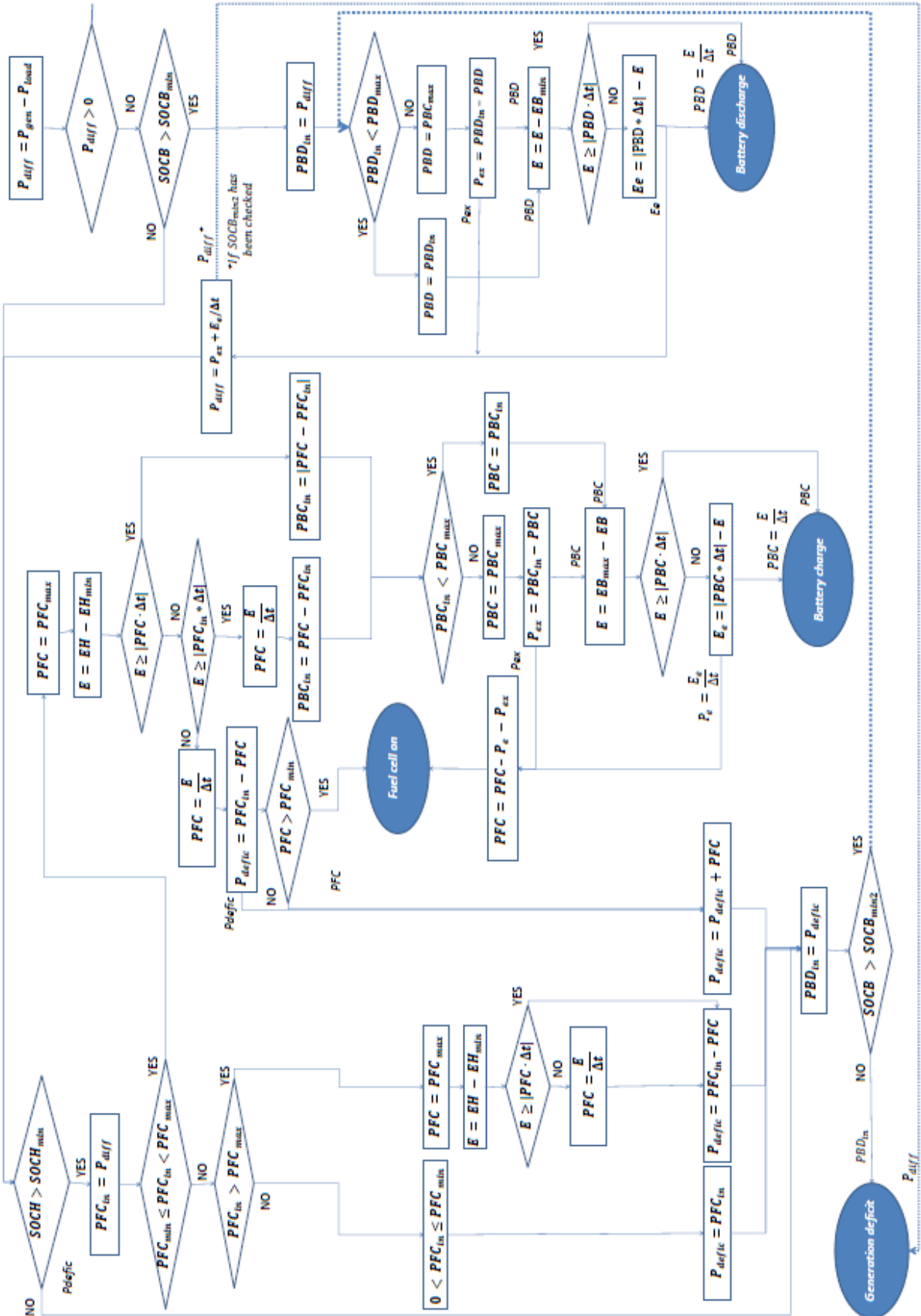
Figure 37: Management strategies dealing with negative power discrepancies.

Figure 38: Management strategies dealing with positive power discrepancies.

B   Appendix: Fuel cell

Figure 39: Graph displaying the fuel system cell efficiency as a function of power output.